

2021

The establishment and function of lung resident memory B cells after bacterial respiratory infection

<https://hdl.handle.net/2144/42223>

"Downloaded from OpenBU. Boston University's institutional repository."

BOSTON UNIVERSITY
SCHOOL OF MEDICINE

Dissertation

**THE ESTABLISHMENT AND FUNCTION OF LUNG RESIDENT MEMORY B
CELLS AFTER BACTERIAL RESPIRATORY INFECTION**

by

KIMBERLY ALYNN BARKER

B.S., Massachusetts Institute of Technology, 2013
M.P.H., Emory University, 2015

Submitted in partial fulfillment of the
requirements for the degree of
Doctor of Philosophy

2021

© 2021 by
KIMBERLY ALYNN BARKER
All rights reserved.

Approved by

First Reader

Joseph P. Mizgerd, Sc.D.
Professor of Medicine, Microbiology, and Biochemistry

Second Reader

Jeffrey L. Browning, Ph.D.
Research Professor of Microbiology

DEDICATION

To Mom, Dad, and Bree, who all inspired my love of learning from day one.

ACKNOWLEDGMENTS

Although the projects are individual, the pursuit of a Ph.D. requires a team, and I would like to acknowledge the many people that contributed to my achievement of this milestone. I must first thank Jay Mizgerd, who was not only an inspiring lab leader, but was first and foremost a mentor for both science and life. I am so appreciative of the opportunity I was given to guide a project from day one based on my own interests. Jay was a relentless advocate for me throughout graduate school and was unwavering in his support for whatever career path I wanted to take, for which I am extremely grateful. I would also like to give special thanks to my former department advisor, Dr. Greg Viglianti, and my colleague and friend Dr. Tina Lisk; without the compassion and advice of you both, I would not have completed these studies.

As a part of both the Pulmonary Center and the department of Microbiology, I was afforded an incredibly extensive and diverse network of mentors and peers. I'll begin my thanks with fellow Pulmonary Center members. Drs. Lee Quinton, Matt Jones, Katrina Traber, and P.J. Maglione were amazing secondary mentors whose help and feedback in lab meetings is forever appreciated. Dr. Antoine Guillon was instrumental to the success of many technical aspects of this work, and more importantly, has become a good friend and valued colleague. The Pneumonia Biology group is now so large it is impractical to list all its past and present members, but please know how important each of you has been to my grad school experience. Of course, Anukul, Carolina, and Emad, we made some unforgettable memories spending all those Saturdays together in the lab, and I can't wait to see where each of you goes next.

From the Microbiology department, I must first acknowledge the members of my committee: Drs. Hans Doms, Deborah Anderson, Tom Kepler, Jeffrey Browning and Lee Wetzler- I am immensely grateful for all your feedback and mentorship. Lee and Jeff, a special thanks for going above and beyond in your interest in my work and dedication to my success. I'd also like to thank some of my peers both within and outside of the department for the friendships required to get through grad school: Alex, Neelou, Whitney, Rachel, Fumi, Michelle, Tina and Gaby. I know I've found lifelong friends in you all.

Finally, I'd like to thank those who have played irreplaceable roles in my past and my personal life. Most people have a teacher who they remember as particularly inspiring; I think it likely that if you polled students from my high school, a majority would cite the same teacher as the one that they remember most fondly. Mr. Baker, I'm so appreciative of the skills and passion for learning that you helped instill in me back in high school, and I'll never forget how excited you were the day I got into college. Kailee, few people have the privilege of having a lifelong best friend. You teach me the values of patience and kindness every day and have made me a better person. Ben, I know how cliché it is to say that you make me feel like the luckiest girl in the world, but in this case that's true. You have been a source of unwavering love and support every day, and I look forward to the many more to come.

Mom and Dad, it is truly impossible to give enough thanks for all that you have done for me. There was never a day in my life that I thought any career was out of reach for me, which takes a special kind of support that I now see how lucky I was to have.

Bree, it's hard to argue that anyone has had a bigger impact on my life than you have.

Not many people are fortunate enough to have a free personal biology expert tutor who could also provide comfort when grad school left me in tears. It's such a gift to have an immediate family member to share a love of immunology with. You continue to inspire me through your dedication to mentorship and passion for science communication, and I hope to implement lessons I learn from you in these areas in my future career.

**THE ESTABLISHMENT AND FUNCTION OF LUNG RESIDENT MEMORY B
CELLS AFTER BACTERIAL RESPIRATORY INFECTION**

KIMBERLY ALYNN BARKER

Boston University School of Medicine, 2021

Major Professor: Joseph P. Mizgerd, Sc.D., Professor of Medicine, Microbiology, and
Biochemistry

ABSTRACT

Streptococcus pneumoniae, or pneumococcus, remains the most prevalent cause of bacterial pneumonia worldwide. The burden of pneumococcal disease peaks among children and the elderly, while young adults are well protected against disease from all pneumococcal serotypes. Whether memory B cells play a role in this naturally developing serotype-independent immunity has not been determined. Additionally, lung resident memory B cells (BRM cells) are elicited after influenza infections of mice, but their relevance to bacterial pathogens and to humans remains unknown, as do the signals required for their establishment. We sought to address these knowledge gaps.

We found that respiratory pneumococcal exposures in mice elicited lung BRM cells without concurrent tertiary lymphoid structure formation. Additionally, normal human lung tissue is enriched for B cells bearing a resident memory phenotype. Mice exposed to a low virulence pneumococcal strain were protected from a subsequent serotype-mismatched pneumococcal challenge. To address the role of B cells in this lung defense, we used a genetically engineered mouse strain allowing effective depletion of lung B cells bearing programmed death-ligand 2 (PD-L2, a memory B cell marker).

When pneumococcus-experienced mice were depleted of PD-L2⁺ B cells just before the

challenge infection, they experienced substantial defects in bacterial clearance compared to mice with lung B cells intact. These results provide the first evidence of a role for lung BRM cells in anti-bacterial immunity. Notably, this defense was pneumococcal serotype-independent, distinguishing it from the serotype-specific immunity elicited by current pneumococcal vaccines. Finally, we found that the establishment of lung BRM cells in mice requires CD4⁺ T cells and multiple respiratory pneumococcal exposures. A second pneumococcal infection, but not the first, induces lung chemokine (C-X-C motif) ligand 13 (CXCL13) production, establishment of local germinal center reactions, and accumulation of class-switched BRM cells in the lung.

In conclusion, herein we show that lung BRM cells are a common feature of antigen-experienced lungs and describe the kinetics of lung BRM cell establishment and the role these cells play in serotype-independent lung immunity against pneumococcal pneumonia.

TABLE OF CONTENTS

DEDICATION	iv
ACKNOWLEDGMENTS	v
ABSTRACT	viii
TABLE OF CONTENTS.....	x
LIST OF TABLES	xiv
LIST OF FIGURES	xv
LIST OF ABBREVIATIONS.....	xvii
CHAPTER ONE- INTRODUCTION.....	1
Pneumonia	1
Pneumococcal pneumonia	2
Immunity to <i>Streptococcus pneumoniae</i>	4
Innate mucosal responses.....	4
Innate-like B cell responses to pneumococcus	5
Pneumococcal innate immune evasion	7
Vaccine-elicited adaptive immunity to pneumococcus	8
Naturally acquired adaptive immunity to pneumococcus.....	10
Memory B Cells.....	14
The generation of B cell memory	15
MBC markers and subsets	19
MBC reactivation.....	21
Tissue Resident Memory B Cells	23

Lymphoid tissue BRM cells.....	24
Lung BRM cells.....	25
Research Objectives.....	28
CHAPTER TWO: MATERIALS AND METHODS	29
Mouse Strains	29
Bacterial Infections	29
Tissue Collection	30
Lung Digestion	31
Flow Cytometry	31
B and T Cell Depletion	34
ELISAs.....	35
Pneumococcal Opsonization.....	36
<i>Ex vivo</i> B Cell Stimulation and ELISpot	37
Whole Blood RNA-Seq	38
Microscopy	38
Statistical Analyses	39
CHAPTER THREE: LUNG RESIDENT MEMORY B CELLS PROTECT AGAINST BACTERIAL PNEUMONIA	41
Introduction.....	41
Results.....	44
Effects of resolved pneumococcal pneumonias on circulating cell transcriptomes .	44
MBCs in pneumococcus-experienced lungs without iBALT	46

Resident phenotype of lung MBCs elicited by pneumococcal exposures	51
Human lung BRM cells	54
Lung BRM cell isotypes and memory marker expression.....	56
Antibody secretion from lung BRM cells.....	58
Reliance of serotype-independent protection on B cell immunity.....	61
Pre-existing anti-pneumococcal antibodies	63
B1 B cells in the lung.....	65
Pneumonia protection by lung BRM cells	67
Discussion.....	72
CHAPTER FOUR: THE ESTABLISHMENT OF LUNG BRM CELLS AFTER	
PNEUMOCOCCAL PNEUMONIA	
Introduction.....	77
Results.....	81
CD4+ T cell dependence of lung BRM cell establishment	81
Kinetics of lung BRM cell recruitment after multiple pneumococcal exposures.....	83
Timing and requirements for lung class-switched MBC expansion.....	87
CXCL13 correlation with lung BRM cell recruitment	97
Discussion.....	101
CHAPTER FIVE: DISCUSSION.....	
An integrated model of serotype-independent anti-pneumococcal immunity in mice	
.....	106

A preliminary model of lung MBC recruitment following pneumococcal infections	111
Unresolved questions in the lung BRM cell field	115
MBCs and cross-reactivity	117
Conclusion	119
BIBLIOGRAPHY	120
CURRICULUM VITAE	141

LIST OF TABLES

Table 1. Observed contributions of various immune components to homotypic protection against secondary pneumococcal colonization or pneumonia in mice.	10
Table 2. Studies showing a presence of absence of heterotypic protection against pneumococcal pneumonia after prior colonization or direct lung infection.	12
Table 3. Observed contributions of various immune components to heterotypic protection against secondary pneumococcal colonization or pneumonia in mice.	13
Table 4. Characteristics of mouse MBC subsets as defined by expression of PD-L2, CD80, and CD73.....	20
Table 5. Antibodies used in flow cytometry analysis of mouse tissues.	33
Table 6. Antibodies used in flow cytometry analysis of human tissues.	34

LIST OF FIGURES

Figure 1. Pneumonia hospitalizations and deaths by age in the United States from 2007-2009.	2
Figure 2. Sequential waves of B cell memory emerge during a primary immune response.	12
Figure 3. Pneumococcal exposures provide lung protection without extensive changes to the blood transcriptome.	45
Figure 4. Pneumococcal exposures elicit B cell clusters in lungs without HEVs.	47
Figure 5. Flow cytometry gating schemes used to analyze mouse lung B cells.	49
Figure 6. Pneumococcal exposures elicit extravascular MBCs in the lung.	50
Figure 7. Lung B cells in experienced mice are resident.	53
Figure 8. Human lungs are enriched for B cells bearing a resident memory phenotype.	55
Figure 9. Experienced lungs are enriched in class-switched MBCs bearing multiple memory markers.	57
Figure 10. Lung BRM cells are poised to secrete antibody.	60
Figure 11. Experienced μ MT mice have intact lung CD4+ TRM cell responses but impaired serotype-independent lung defense.	62
Figure 12. Pre-existing heterotypic antibodies in the plasma are capable of contributing to serotype-independent anti-pneumococcal defense.	65
Figure 13. B1 B cells are not changed in the pleural fluid of experienced vs. naïve mice and do not infiltrate the lung upon Sp3 challenge.	66
Figure 14. Lung PD-L2+ MBCs are also established by pneumococcal experience in a genetically modified mouse model.	68
Figure 15. Lung MBCs are required for optimal serotype-independent anti-pneumococcal lung immunity.	70
Figure 16. Lung BRM cell establishment requires the presence of CD4+ T cells during initial infections.	83

Figure 17. Two pneumococcal infections are required to generate a robust lung BRM cell population.	86
Figure 18. The proportion of class-switched lung MBCs expands one week after a second Sp19 infection.	88
Figure 19. MBCs bearing multiple memory markers accumulate in the lungs starting one week after a second Sp19 infection.	90
Figure 20. Pre-GC and GC B cells are observed in mouse lungs following two Sp19 infections.	93
Figure 21. Continued influx of immune cells into the lung during and after the second Sp19 infection is required to generate lung GC reactions and class switching.	96
Figure 22. Lung CXCL13 levels and CXCR5+ B cells are elevated following a second Sp19 infection.	100
Figure 23. An integrated model of serotype-independent anti-pneumococcal immunity in mice.	110
Figure 24. A preliminary model of lung MBC recruitment following two pneumococcal infections.	114

LIST OF ABBREVIATIONS

7AAD	7-aminoactinomycin D
Adr	O-acetyltransferase
AID	Activation-induced cytidine deaminase
ANOVA	Analysis of variance
APC-	Allophycocyanin
APC	Antigen-presenting cell
ASC	Antibody-secreting cell
ATCC	American Type Culture Collection
Bach2	BTB domain and CNC homolog 2
BAL	Bronchoalveolar lavage
BALF	BAL fluid
Bcl-2	B cell lymphoma 2 protein
Bcl-6	B cell lymphoma 6 protein
BCR	B cell receptor
Blimp-1	B lymphocyte-induced maturation protein-1
BRM cell	Resident memory B cell
BSA	Bovine serum albumin
BUMC	Boston University Medical Center
°C	Degree(s) Celsius
CAP	Community-acquired pneumonia
CbpA	Choline-binding protein A

CCL.....	Chemokine (C-C motif) ligand
CD.....	Cluster of differentiation
CDC.....	Centers for Disease Control
CFU.....	Colony forming units
COVID-19.....	Coronavirus disease-19
CXCL.....	Chemokine (C-X-C motif) ligand
DAPI.....	4',6-diamidino-2-phenylindole
DC.....	Dendritic cell
DMSO.....	Dimethyl sulfoxide
DNA.....	Deoxyribonucleic acid
DP.....	Double positive
DT.....	Diphtheria toxin
EDTA.....	Ethylenediaminetetraacetic acid
ELISA.....	Enzyme-linked immunosorbent assay
ELISPOT.....	Enzyme-linked immunosorbent spot
EV.....	Extravascular
FACS.....	Fluorescence activated cell sorting
FBS.....	Fetal bovine serum
FDC.....	Follicular dendritic cell
FITC.....	Fluorescein isothiocyanate
GC.....	Germinal center
GM-CSF.....	Granulocyte/Macrophage Colony-Stimulating Factor

h.....	Hours
H & E	Hematoxylin and eosin
HEPES	2-[4-(2-hydroxyethyl)piperazin-1-yl]ethanesulfonic acid
HEV	High endothelial venule
HRP.....	Horseradish peroxidase
HSV.....	Herpes simplex virus
iBALT	Inducible bronchus-associated lymphoid tissue
Ig.....	Immunoglobulin
IL.....	Interleukin
IRF-4	Interferon regulatory factor-4
i.n.	Intranasal
i.p.	Intraperitoneal
i.t.	Intratracheal
IV	Intravascular
i.v.	Intravenous
kg.....	Kilogram
LLPC.....	Long-lived plasma cell
LoD	Limit of detection
LPS.....	Lipopolysaccharide
LRTI.....	Lower respiratory tract infection
MALT	Mucosa-associated lymphoid tissue
MBC.....	Memory B cell

mg	Milligram
MHC-II	Major histocompatibility complex class II
mL	Milliliter
mLN	Mediastinal lymph node
mM	Millimolar
Mtb	<i>Mycobacterium tuberculosis</i>
MZ	Marginal zone
NALT	Nasal-associated lymphoid tissue
nm	Nanometer
NP	4-hydroxy-3-nitrophenylacetyl
P value	Probability value
PBS	Phosphate buffered saline
PCho	Phosphorylcholine
pdgA	Peptidoglycan N-acetylglucosamine-deacetylase A
PD-L2	Programmed cell death-ligand 2
PFA	Paraformaldehyde
pg	Picogram
PIgR	Polymeric immunoglobulin receptor
PNAd	Peripheral node addressin
PZTD	PD-L2-ZsGreen-TdTomato-diphtheria toxin knock-in and inducible knockout
RCF	Relative centrifugal force
RNA	Ribonucleic acid

ROR α	Retinoic acid receptor-related orphan receptor alpha
RPM.....	Revolutions per minute
RPMI.....	Roswell Park Memorial Institute media
RSV.....	Respiratory syncytial virus
SARS.....	Severe acute respiratory syndrome
SD.....	Standard deviation
SLO.....	Secondary lymphoid organ
SP.....	Single positive
Sp.....	<i>Streptococcus pneumoniae</i>
TEM.....	Effector memory T cell
TFH.....	T follicular helper cells
TLR.....	Toll-like receptor
TMB.....	3,3',5,5'-tetramethylbenzidine
TN.....	Triple negative
TP.....	Triple positive
TRM cell.....	Resident memory T cell
μ g.....	Microgram
μ L.....	Microliter
US.....	United States

CHAPTER ONE- INTRODUCTION

Pneumonia

The constant environmental exposure of our airways combined with the delicate anatomical structures required for respiration confer a particular susceptibility to disease and damage to the human lung. Indeed, lower respiratory tract infections (LRTIs) were the 4th leading cause of morbidity globally in 2017, and are the only type of communicable disease to remain a top 30 cause of morbidity in high socio-demographic index countries for the past three decades (1). Two of the largest disease outbreaks in the last century, the 1918 influenza pandemic and ongoing coronavirus disease-19 (COVID-19) pandemic, were caused by respiratory pathogens, highlighting the devastating toll respiratory infections can take. Pneumonia, a type of LRTI, occurs when infection triggers immune cells and fluid to fill the alveoli, hindering the ability of the lung to carry out its primary function of exchanging gases between the airspaces and the blood. Pneumonia has been recognized as a common disease since the time of Hippocrates (2), especially among elderly individuals; a century ago, pneumonia was described in a medical textbook as "...the natural end of old people" (3). Despite the many advances of modern medicine, pneumonia remains extremely common, representing the leading cause of hospitalization among children (4) and most deadly cause of hospitalization among older adults in the United States (Fig. 1) (5).

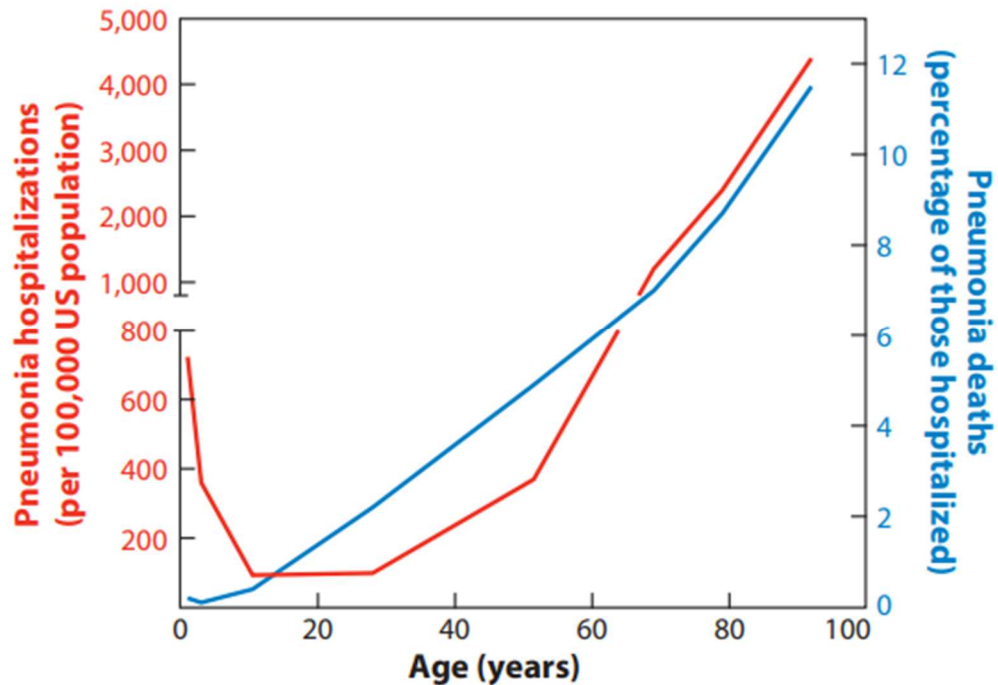


Figure 1. Pneumonia hospitalizations and deaths by age in the United States from 2007-2009. Reprinted with permission from: Quinton and Mizgerd, *Annu. Rev. Physiol.* 2015 (6).

Perhaps one reason for the frequent occurrence of pneumonia is the wide variety of pathogens that can lead to the condition. These include diverse bacteria, viruses, and fungi (7). Novel microbial causes of pneumonia, such as the severe acute respiratory syndrome (SARS)-associated coronaviruses, continue to emerge. This complex and often poorly defined etiology represents a major difficulty we face in defending against pneumonia.

Pneumococcal pneumonia

Streptococcus pneumoniae was first isolated in 1881, and the long history of research on this Gram-positive bacterium has yielded numerous scientific discoveries of

landmark importance, including Gram staining, bacterial transformation, and the acute phase response (8, 9). Pneumonia resulting from *S. pneumoniae* infection, referred to as pneumococcal pneumonia, is the most common bacterial etiology of community-acquired pneumonia (CAP), or pneumonia acquired during the normal activities of daily life outside of healthcare settings (10, 11). Infection with *S. pneumoniae* can lead to a variety of pathologies in addition to pneumonia, such as ear infection (otitis media), bacteremia, and meningitis (12). However, in the US, pneumococcal pneumonia is the leading cause of hospitalization due to pneumococcal infection and the most costly, accounting for 72% of medical costs related to pneumococcal disease (13). One of the most unique and challenging facets of *S. pneumoniae* is the large number of different serotypes known to exist, which recently increased to 100 (14). These serotypes are defined by different structural compositions of the polysaccharide capsule that encompasses the bacterial cell wall.

The natural reservoir of *S. pneumoniae* is the human nasopharynx, and colonization of children is especially common, with essentially all children being colonized multiple times by the age of 2 (15). The incidence of pneumococcal colonization decreases with age, although it is not uncommon in adults, of whom approximately 10% are colonized at any given time (16). Nasal colonization is a prerequisite for subsequent pneumococcal disease, including pneumonia (17).

Immunity to *Streptococcus pneumoniae*

Innate mucosal responses

Upon entering a new naive host, the pneumococcus faces some barriers to initial colonization, including the mucus layer and anti-microbial peptides such as lysozyme secreted by nasal epithelial cells (18). However, *S. pneumoniae* is well-adapted to these conditions (discussed below) and expresses many adhesion molecules that allow it to easily attach to the nasal epithelium and colonize the nose asymptotically. Progression into the lung, where the interaction between pneumococcus and host becomes pathogenic, occurs via aspiration but is limited by the physical action of the mucociliary clearance mechanism and bacteria-aggregating effect of surfactant proteins (19). If pneumococci are able to bypass these barriers, they must also contend with the highly phagocytic alveolar macrophages of the lung, which are activated after detection of the bacteria via pattern recognition receptors. Clearance by alveolar macrophage-mediated phagocytosis is sufficient to prevent severe infection by bacteria that reach the alveoli in most cases of pneumococcal aspiration (20). However, when bacteria persist, macrophages and epithelial cells in the lung can secrete chemokines such as interleukin (IL)-8, chemokine (C-X-C motif) ligand 5 (CXCL5), and granulocyte-macrophage colony-stimulating factor (GM-CSF), which call in neutrophils from the circulation to aid in bacterial killing (20, 21). The accompanying extravasation of plasma into the lung can bring in additional immune mediators such as complement, acute phase proteins, or circulating antibodies (discussed below) (22). This inflammatory reaction to pneumococci in the lungs is ironically what leads to many of the symptoms of

pneumococcal pneumonia, as the influx of fluid, immune cells and the cytotoxic products those immune cells produce can impair gas exchange and damage the host's own tissues.

Innate-like B cell responses to pneumococcus

A less-appreciated aspect of innate immunity to pneumococcal pneumonia involves particular subsets of B cells. B lymphocytes are typically considered a component of the adaptive immune system. However, the B cell lineage can be more broadly divided into conventional follicular or “B2” B cells and two more innate-like subsets: “B1” B cells and marginal zone (MZ) B cells. B1 and MZ B cells also contribute to innate immune responses against *S. pneumoniae*.

B1 B cells are a long-lived and self-replenishing subset that express an IgM⁺CD11b⁺B220^{lo}CD43⁺ surface marker phenotype when not activated (23). Most, but not all, B1 cells also express the inhibitory receptor CD5, which may be important for preventing autoimmune reactions by these frequently self-reactive cells (24). B1 cells develop largely in fetal tissues, are derived from B1-specific progenitors (25), and have a distinct anatomical localization compared to B2 or MZ B cells; although some are found in lymphoid tissues, many mature B1 cells migrate to the peritoneal and pleural cavities in response to macrophage-secreted CXCL13 and comprise the majority of B cells at these sites in mice (26).

In mice, B1 cells are capable of performing multiple effector functions important in responses to bacterial pathogens such as *S. pneumoniae*. Some B1 cells in the spleen and bone marrow constitutively secrete natural antibodies, which are made in the absence of prior antigenic stimulation; such antibodies are even observed in germ-free mice (27).

Natural antibodies are primarily of the IgM isotype and are well-suited for activation of the classical complement pathway to eliminate bound targets (23). These targets are usually evolutionarily conserved antigens such as phosphorylcholine (PCho), which is a unique part of the pneumococcal cell wall. Natural anti-PCho antibodies constitutively produced by CD5⁺ B1 cells provide a first line of defense against pneumococcal invasion of the blood (28, 29). In contrast, CD5⁻ B1 cells in the mouse peritoneum can respond in an antigen-specific manner to pneumococcal infection and produce protective capsular polysaccharide-specific IgM and IgG3 antibodies (29).

The existence of analogous B1 cells in humans has been controversial due to the lack of definitive distinguishing surface markers (30, 31). However, there is a clear role in bacterial immunity for human B1-like cells (CD19⁺CD20⁺CD43⁺CD27⁺CD70⁻) (32), which, along with traditional plasma cells, produce IgM, IgG, and IgA antibody against pneumococcal polysaccharide (33, 34).

MZ B cells (IgM^{hi}IgD^{lo}CD21^{hi}CD23⁻) develop from the same precursor cells as follicular B2 cells (25) and are named based on their enrichment in the splenic marginal zone surrounding the B cell follicles (35). At this site, MZ B cells are poised to respond to blood-borne antigens. Like B1 cells, MZ B cells respond to the pneumococcal polysaccharide in a T cell-independent manner to rapidly generate large amounts of serotype-specific IgM and some class-switched antibodies (35, 36). Although the pneumococcal polysaccharide-specific responses of B1 and MZ B cells are not technically innate, as they involve antigen-specific antibodies produced during infection, these responses occur much faster than classic T cell-dependent B cell immunity and aid

in defending against the potentially deadly invasion of pneumococci into the blood while a typical adaptive immune response develops.

Pneumococcal innate immune evasion

Although the above sections make clear that the immune system has many tools in its innate arsenal to prevent pneumococcal infection, *S. pneumoniae* also has a wide array of virulence factors that enable it to avoid these immune defenses. The most notable means of evading the immune system by *S. pneumoniae* is definitively the polysaccharide capsule. The negative charge of most pneumococcal capsules electrostatically prevents entrapment of the bacteria by mucus, which is also negatively charged (37). The steric hindrance of the capsule prevents efficient binding of complement, acute phase proteins, and antibody specific to internal bacterial structures (38). Even when such immune effectors manage to bind the bacteria, the capsule allows evasion of efficient opsonophagocytosis mechanisms by sterically hindering their interactions with corresponding receptors on phagocytes (38). In addition to capsule, bacterial enzymes are another main class of pneumococcal virulence factors enabling innate immune invasion. The enzymes PdgA and Adr, for example, modify the cell wall to confer resistance to degradation by mucosal antimicrobial peptides (39). The bacterial enzymatic toxin pneumolysin, along with other enzymes, causes epithelial cell damage and prevents effective mucociliary clearance (40). Pneumolysin can also lead to cell death of phagocytes, impairing efficient host bacterial clearance (41). Still other enzymes, pneumococcal surface endonucleases, enable bacterial escape from neutrophil extracellular traps (42). For nearly every aspect of innate immunity, the pneumococcus

contains one or more evasive mechanisms, highlighting the importance of the more potent, if slower, adaptive immune response.

Vaccine-elicited adaptive immunity to pneumococcus

In the 1918 flu pandemic, secondary bacterial pneumonia caused many of the millions of deaths worldwide (43), leading to recognition of the potential benefits of intentionally tipping the balance of the host-pathogen arms race to favor the immune response against pneumococcus. Multiple attempts to immunize with inactivated pneumococci were carried out during the 1918 pandemic, with varying efficacy (44). In 1945, the power of immunization with individual pneumococcal capsular polysaccharides for generating serotype-specific (homotypic) immunity was realized (45), leading to the eventual 1977 approval of a first pneumococcal polysaccharide-based vaccine (46).

The adaptive immune response to these polysaccharide vaccines is T cell-independent, because the repeating polysaccharide epitopes are able to cross-link the B cell receptor (BCR) and activate B cells in the absence of T cell help (47). However, because T cells generally respond only to protein antigens, these vaccines cannot generate the T cell help required for high affinity antibody production and memory B cell (MBC) responses (48). While polysaccharide vaccine-elicited plasma cells and resulting antibodies still provide protection against invasive pneumococcal disease in most adults (49, 50), children under 2 years old do not generate robust anti-polysaccharide immune responses (51). To provide protection against pneumococcal disease in this vulnerable population, a new vaccine approach where each polysaccharide capsule is conjugated to a protein carrier was approved in 2000. These pneumococcal conjugate vaccines are much

more effective in providing protection in young children and immunocompromised individuals due to their ability to elicit carrier protein-specific T cell help that promotes high affinity plasma cell responses and B cell memory (46, 48).

Today, a polysaccharide vaccine including the capsules of 23 pneumococcal serotypes and a conjugate vaccine including the capsules of 13 serotypes are used in the US (46). Interestingly, although these vaccines provide good protection against invasive diseases (bacteremia, meningitis, and pleural infection) caused by the included serotypes, neither type has high efficacy in preventing pneumococcal pneumonia (52). Other limitations of these vaccines include the technical difficulty in including more serotypes and the observation of serotype replacement, where disease caused by serotypes not included in the vaccines increased in prevalence as protection against vaccine serotypes became widespread (53, 54). Both the currently licensed vaccines are predicated on eliciting antibodies targeting the serotype-defining pneumococcal capsule, which have been known to provide serotype-specific protection since the successful use of passive anti-pneumococcal serum transfer early in the 20th century (55). The idea of serotype-specific immunity as the driving force of anti-pneumococcal protection has been so prevalent that the immunologist Charles Janeway Jr. wrote that, “from the point of view of the adaptive immune system, each serotype of *S. pneumoniae* represents a distinct organism” (56). Certainly, for the adaptive immunity elicited by current pneumococcal vaccines, this is true.

Naturally acquired adaptive immunity to pneumococcus

In contrast to vaccine-derived immunity, naturally acquired immunity refers to the immune responses that develop from natural exposures to a pathogen. Initially, naturally acquired protection against pneumococcal disease was also believed to largely derive from the development of serotype-specific antibodies following childhood colonization events (57-59). Indeed, pneumococcal colonization often results in systemic capsule-specific antibodies (16, 60). More recent studies have directly explored the contributions of colonization-elicited antibodies and other immune system components to protection against subsequent serotype-matched (homotypic) pneumococcal colonization or pneumonia in mice (Table 1). Generally, prior pneumococcal colonization elicits immunity to subsequent homotypic colonization that is dependent on CD4+ T cells and not antibodies. Protection against homotypic pneumonia, on the other hand, requires pre-existing antibodies and the long-lived plasma cells (LLPCs) that secrete them.

Immune Component	Protection vs. Colonization	Protection vs. Pneumonia
Antibodies	Not sufficient (61)	Required and sufficient (62, 63) Required (64) Sufficient (65)
CD4+ T Cells	Required (66)	Not required (62, 63) Required (64)
Memory B Cells		Not required (62)
Long-Lived Plasma Cells		Required (62)

Table 1. Observed contributions of various immune components to homotypic protection against secondary pneumococcal colonization or pneumonia in mice.

Although serotype-specific protection is commonly observed in humans and mice, epidemiological evidence indicates that naturally acquired immunity against pneumococcal colonization and disease may actually rely on serotype-independent (heterotypic) mechanisms (67). Pneumococcal disease incidence decreases in adults for all serotypes, regardless of how commonly a serotype colonizes children, indicating that anti-capsule antibodies are not the primary mechanism of natural immunity (58). This idea was supported by experiments in mice showing that prior colonization by a pneumococcal serotype protected equally well against subsequent homotypic and heterotypic colonization (68). Whether prior colonization protects against a future heterotypic pneumonia episode in mice has been less obvious. Two studies report no such protection (Table 2), and some authors have argued that pneumococcal exposures within the lung itself are required to provide definitive heterotypic protection against subsequent pneumonia (65). This idea is at odds with the fact that only a small minority of children exposed to pneumococcus experience a true pneumonia episode, while protection against pneumonia in young adults is common (67). The epidemiology therefore better aligns with three other studies in mice that did report colonization-elicited heterotypic protection against pneumococcal pneumonia (Table 2). Additionally, studies in humans have shown colonization-induced changes to lung immune components in the bronchoalveolar lavage fluid (BALF) (69, 70). Altogether, the epidemiologic and experimental evidence indicates that heterotypic naturally acquired protection against pneumococcal colonization and pneumonia in adults is elicited by the colonization events most individuals experience as children.

Exposure	Heterotypic Pneumonia Protection
Colonization with strain D39 (71)	No
Colonization with strain TIGR4 (62)	Yes
Colonization with a strain D39 pneumolysin mutant (72)	Yes
Colonization with a strain TIGR4 capsule mutant (73)	Yes
Colonization: with strain Sp23F (65)	No
Direct lung infection with strain Sp23F (65)	Yes
Direct lung infection with strain Sp19F (74)	Yes

Table 2. Studies showing a presence or absence of heterotypic protection against pneumococcal pneumonia after prior colonization or direct lung infection.

Many groups have investigated the immunological mechanisms behind this heterotypic naturally acquired protection. Table 3 describes the observed contributions of various immune components to protection conferred by prior exposure to live pneumococcus or pneumococcal proteins against subsequent heterotypic colonization or pneumonia.

Species	Immune Component	Protection vs. Colonization	Protection vs. Pneumonia
Mouse	Serotype cross-reactive antibodies	Not required (68, 75) Required (73)	Sufficient (62)
	CD4+ T cells	Required (68, 73, 75-77)	Required (65, 74)
Human	Serotype cross-reactive antibodies	No association with protection (78, 79)	Associated ¹ (78) Sufficient ² (80)

Table 3. Observed contributions of various immune components to heterotypic protection against secondary pneumococcal colonization or pneumonia in mice.

¹These authors observed an association between serum antibodies against pneumococcal proteins and lower incidence of respiratory tract infections (but not pneumococcal colonization) in children. ²These authors transferred pooled human serum immunoglobulin depleted of antibody against pneumococcal capsules into mice, which protected mice against pneumococcal lung infection.

There is strong evidence that CD4+ T cells generated by pneumococcal exposures are required for protection against subsequent heterotypic colonization and pneumonia. Most of these studies further show that it is specifically IL-17-producing CD4+ T cells that are important for this protection (65, 74-76). Most evidence indicates that serotype cross-reactive antibodies are dispensable for heterotypic protection against pneumococcal colonization in mice and are not associated with such protection in humans. However, these antibodies do appear to be important in both mice and humans for protection against heterotypic pneumococcal lung infection.

Altogether, the studies summarized above indicate a mechanism of naturally acquired immunity to pneumococcus that requires IL-17-producing CD4+ T cells for protection against colonization. These T cells also contribute to optimal heterotypic

protection against pneumonia. Serotype cross-reactive antibodies, on the other hand, appear to be dispensable for immunity to colonization but crucial for protection within the lung itself. Despite the proven importance of antibodies in this setting, nearly all studies have focused only on heterotypic protection conferred by pre-existing serum antibodies. Other potentially important sources of antibody, such as pre-existing antibodies in the lung airspaces or reactivated MBCs, have not been investigated in the context of natural heterotypic immunity to pneumococcal pneumonia.

Memory B Cells

Pathogens such as *Streptococcus pneumoniae* reproduce on time scales that are orders of magnitude greater than humans do and therefore can evolve over the course of hours to days vs. decades and centuries. The adaptive immune system is what allows the human species to compete with the multitude of rapidly changing pathogens around us. Typical B and T lymphocytes are set apart from the cells of the innate immune system in that each cell bears receptors that are highly specific for a single (usually) non-self antigen. These receptors are generated by a random recombination process of the adaptive receptor genetic loci. This process enables the production of lymphocytes with at least 10^{11} different potential specificities (56), such that the adaptive immune cell repertoire can essentially recognize any possible antigen, even those that don't exist naturally. The fundamental trade-off that accompanies this vast diversity in specificity is that T or B cells that recognize a given epitope are extremely rare in a naïve host. This problem is addressed by the concentration of lymphocytes in specialized secondary lymphoid organs (SLOs), where they can quickly be scanned for specificity to an

invading pathogen, as well as the huge proliferative capacity of lymphocytes once activated. The requirement for these initial recognition and proliferation steps in a primary adaptive immune response is why the response develops more slowly than an innate immune response, over weeks instead of hours to days. But evolution has also provided adaptive immunity with a key tool in the fight against frequently encountered pathogens: immunologic memory.

Memory T and B lymphocytes represent a small fraction of the cells initially activated in a primary response and remain in the host long after the infection is resolved. Memory cells specific to a pathogen are present at a higher frequency than the corresponding naïve cells were during the initial infection, and memory lymphocytes, although quiescent most of the time, are poised to carry out effector functions upon activation faster than naïve cells do. These factors enable secondary responses to a previously seen pathogen to occur much more rapidly than the primary response did. After recovery from some infections, the resulting immunologic memory is able to persist for the rest of a human lifetime. The power and longevity of immunological memory was recorded in 1846, when the measles virus had infected over 75% of residents on the Faroe islands. The last known occurrence of measles in this isolated part of the world had been in 1781, and none of the elderly residents in 1846 who were infected 65 years earlier became ill a second time due to their immunologic memory (81).

The generation of B cell memory

In a typical T cell-dependent primary immune response, B cells are usually activated in SLOs by recognition of intact antigen presented on the surface of CD169+

macrophages in the subcapsular sinus or follicular dendritic cells (FDCs) in the center of the B cell follicle (82). Either mode of recognition triggers BCR clustering, which results in signaling through the BCR (83) and changes to the B cell cytoskeleton allowing clathrin-mediated engulfment of the BCR and bound antigen (84). Like T cells, B cells do not achieve full activation upon BCR engagement alone, except in the case of highly multivalent antigens like the pneumococcal polysaccharide. A second signal can come in the form of toll-like receptor (TLR) signaling, which directs antigen-stimulated B cells to differentiate directly into plasma cells (85). Otherwise, the second signal is derived from helper T cells. After engulfing BCR-bound antigen, and in the absence of TLR engagement, the B cell can process and present peptides on MHC class II at its surface. BCR signaling in response to T cell-dependent antigens also enables B cells to move to the interface of the follicle and T cell zone (“the T-B border”) (84). This relocation and presentation of antigen allows for the first contact-dependent B cell:T cell interaction of the immune response: recognition of the peptide-bearing B cell by helper T cells of the same pathogen specificity that were previously activated by an antigen-presenting cell (APC). Recognition allows the T cell to provide help to the B cell in the form of surface co-stimulatory molecules (particularly CD40L) as well as cytokines (particularly IL-21 and IL-4), which then instruct the B cell to continue to proliferate and differentiate (86). It is also at this stage that the majority of isotype switching of the BCR constant region is initiated and completed based on cues from cytokines and T cell help (87). This initial T cell:B cell interaction drives differentiation of some B cells to become early extrafollicular plasmablasts that remain in the SLO and secrete large amounts of antibody

but are generally short-lived (88). Other of the B cells become extrafollicular MBCs, which are typically IgM⁺ but can express IgG or IgA BCRs (89). Finally a third group of B cells instead upregulate the transcription factor Bcl-6, migrate, and form a germinal center (GC) reaction within the follicle where they have the opportunity to mature their BCRs to better bind the relevant antigens (90). BCR affinity (and the proportional length of time that T cell help is received) plays a role in determining which of these three fates an individual naïve B cell follows. Cells with higher affinity BCRs are predisposed to become plasma cells, while lower affinity cells tend to differentiate into extrafollicular MBCs, and cells with intermediate affinity favor GC entry (91). This division of labor is efficient in that it leads to early production of relatively low affinity antibodies and memory cells as well as slower development of antibodies and cells with better specificity to the invading pathogen.

Within the GC, a cyclical microevolutionary process occurs, involving repeated rounds of mutation and selection. FDCs act as professional retainers of antigen within the GC, allowing ongoing antigen-driven selection. Newly arrived GC B cells bind this antigen on FDCs and present it to cognate TFH cells within the GC “light zone”; TFH cells provide help and instruct certain of the GC B cells to migrate into the GC “dark zone”, mutate their BCR, and proliferate (90). This somatic mutation process relies on high expression of the enzyme Activation-induced cytidine deaminase (AID), which catalyzes the deamination of cytosine bases within the BCR locus, followed by low fidelity DNA repair mechanisms (92). A minority of these mutation events result in BCRs with higher affinity for the antigen presented on the GC FDCs. The limited number

of GC TFH cells providing survival signals to the GC B cells acts as a selective force; GC B cells that mutated to express better affinity BCRs are able to have more frequent, prolonged, and stronger TFH interactions and thus preferentially receive positive selection in the form of T cell help (93, 94).

B cells exiting the GC go on to become plasma cells or GC-derived MBCs (86). Again, this fate decision appears to be influenced by BCR affinity and duration of B cell:TFH contact, with higher affinity favoring IRF-4 and Blimp-1 transcription factor upregulation and the plasma cell fate (88, 93). This affinity-based selection is likely based on a combination of stronger signals through higher affinity BCRs and the fact that higher affinity B cells acquire and process antigen from FDCs more efficiently (94, 95). In accordance with this, MBCs appear to emerge first from the GC reaction, having accumulated fewer somatic mutations than cells fated to become LLPCs (Fig. 2). Although high expression of the transcription factor Bach2 is required for GC B cells to become MBCs, there is not yet a known MBC-defining transcription factor (96).

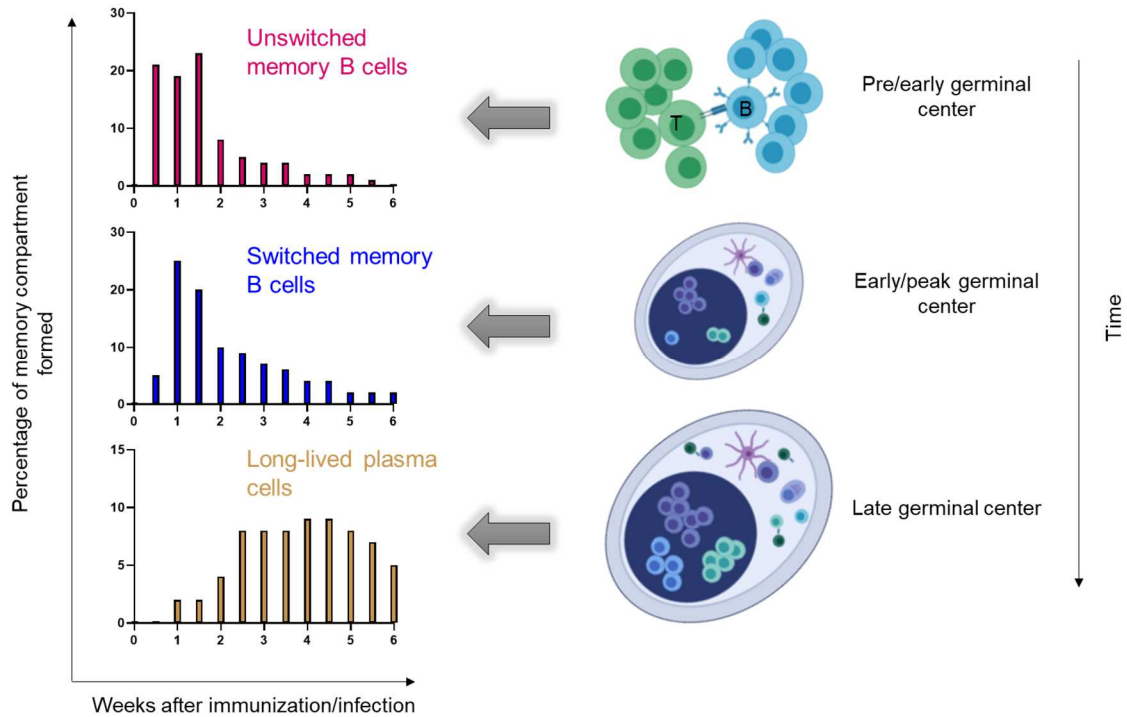


Figure 2. Sequential waves of B cell memory emerge during a primary immune response. Made using Biorender.com based on a figure in Weisel and Shlomchik, *Annu. Rev. Immunol.* 2017 (97).

MBC markers and subsets

Many initial studies of MBCs assumed these cells express only class-switched receptor isotypes (IgM-IgD-) (98). However, IgM+ MBCs have been definitively observed in humans and mice (99, 100). This, combined with the fact that isolation techniques involving the BCR can lead to undesirable B cell activation, necessitated the discovery of more nuanced marker combinations for practical MBC studies. Unlike many immunological principles that are characterized first in animal models, much of the initial knowledge regarding MBC markers was attained from human studies. This was in part due to the discovery in the 1990s of CD27 as a reliable surface marker of human MBCs (101, 102). A small population of ‘atypical’ human MBCs has recently been described.

These cells are CD27-, lack the usual expression of complement receptor 2 (CD21), and may be enriched for anergic or autoreactive cells (103-105). However, CD27 expression remains a reliable indicator of human MBCs. In mice, CD27 expression is not restricted to MBCs, necessitating use of either functional assays or an IgD-CD38+ surface marker phenotype to define these cells. The latter approach is unsatisfying, as murine naïve B cells also express high levels of CD38 (106). These challenges motivated a series of studies to define better mouse MBC markers; PD-L2, CD80, and CD73 were identified as three such surface markers that are expressed on memory, but not naïve, mouse B cells (107, 108). As shown in Table 4, MBCs expressing multiple of these markers are enriched for class-switched BCRs and have a higher BCR mutational load than MBCs not expressing them (109). While CD73 expression on MBCs did not seem to correlate with these phenotypes in initial studies, MBCs co-expressing CD73 with CD80 comprise an important subset of MBCs with mutated BCRs in various infection settings (110-112).

MBC Subset	Proportion Class-Switched	Relative Extent of BCR Mutation
Triple Low	Low	Lower
CD73 Single Positive	Low	Lower
PD-L2+CD80- (+/- CD73)	Intermediate	Intermediate
PD-L2+CD80+CD73-	High	Higher
Triple High	High	Higher

Table 4. Characteristics of mouse MBC subsets as defined by expression of PD-L2, CD80, and CD73.

MBC reactivation

Transcriptionally, memory and naïve B lymphocytes are very similar (113, 114). However, there are key differences in MBCs that confer the typical advantages of a memory response: faster and stronger activation. For example, cell-cycle regulatory genes are down-regulated in MBCs compared to naïve B cells, such that MBCs can enter cell division quickly upon stimulation (115). MBCs also have higher expression of anti-apoptotic molecules like Bcl-2, as well as proteins involved in homeostatic proliferation, like leukemia inhibitory factor receptor (113, 114). Unlike naïve B cells, MBCs constitutively express T cell co-stimulatory molecules (CD80/86), enabling them to quickly elicit T cell help (113, 116). Finally, changes to the intracellular signaling domains of class-switched BCRs confer IgG MBCs with enhanced sensitivity to low doses of antigen compared to B cells expressing IgM/IgD (117). This combination of subtle yet powerful changes allows MBCs to reactivate quickly and intensely to secondary challenge.

The splenic MZ and the lymph node subcapsular sinuses are well-established niches for MBCs in mice and humans, although they are not the only sites of MBC localization (discussed in the next section) (118, 119). These sites are enriched with CD169⁺ macrophages as well as follicular memory T cells, enabling easy presentation of antigen to and reactivation of MBCs upon reinfection (118). In these specialized sites, MBC reactivation leads these cells to two main fates; proliferation and differentiation into plasma cells or entry into a secondary GC where the BCR is further matured and more MBCs are generated. The signals controlling which of these fate paths is taken by a

reactivated MBC have not been fully elucidated, but certain surface markers have been shown to associate with each outcome in murine MBCs. MBCs concurrently expressing PD-L2 and CD80 differentiate into plasma cells upon restimulation and do not seed secondary GCs. MBCs expressing neither of these markers instead form secondary GC responses, while MBCs expressing either CD80 or PD-L2 alone have an intermediate response phenotype (120). Interestingly, while secondary GC formation has been readily observed in murine experimental systems involving adoptive transfer and reactivation of MBCs, recent work indicates that this outcome is relatively rare for MBCs responding to challenge in an immunized mouse (121).

The factors required for MBC reactivation are still an active area of research. Cognate antigen appears necessary for MBC reactivation *in vivo* (122). Once established, MBCs can survive independently of T cells, (123) but whether or not MBC reactivation is dependent on T cell help seems to be context-dependent. MBC responses to model antigens, such as hen egg lysozyme (118) and 4-hydroxy-3-nitrophenylacetyl (NP) (120), appear to require T cell help, but T cell-independent reactivation of MBCs specific to numerous viruses has been observed (124, 125). This T cell-independent activation required SLOs with unaltered lymphoid architecture (125). In contrast, activation of virus-specific MBCs in another study was T cell-dependent but could occur independently of SLOs (126). Therefore, it may be a combination of antigen structure and immune niche that dictate whether MBCs require T cell help to become plasma cells or not. The signals required for MBC responses to non-viral protein antigens remain unexplored.

The roles of transcription factors and cytokines in MBC reactivation are only just beginning to be described. IL-2 and IL-15 appear to not be involved (127), but a recent study implicated IL-9 as a necessary signal for NP-specific MBC differentiation into plasma cells (128). Development, maintenance, and reactivation of IgG2a/c+ MBCs is dependent on the transcription factor T-bet, and MBCs of these isotypes are responsive to interferon-gamma signaling (129). In contrast, IgA+ MBC development and function requires the transcription factor ROR α , and these MBCs are responsive to IL-17 and IL-22 (129). Similar transcription factor and cytokine requirements specific to other MBC isotypes have yet to be defined.

Tissue Resident Memory B Cells

Following infection resolution, immunology dogma indicates that the long-lived memory feature of adaptive immunity is conferred by memory T and B lymphocytes and LLPCs in the spleen, lymph nodes, bone marrow, mucosa-associated lymphoid tissue (MALT), and blood. In recent decades, however, these concepts of immune cell localization have expanded beyond the classic lymphoid organs; many non-lymphoid tissues are now recognized to have profound roles in adaptive immunity as well. One of the largest paradigm shifts in adaptive immune cell localization was the discovery of tissue resident memory T cells (TRM cells), which populate non-lymphoid tissues that have recovered from infection or inflammation (130). TRM cells bear an effector memory phenotype but do not recirculate through the blood and lymph like effector memory T cells do (131). Although TRM cells were initially observed in non-lymphoid tissues, lymphoid organs are now known to foster non-circulating lymphocytes as well

(132). Since their discovery, both CD4⁺ and CD8⁺ TRM cells have been described in multiple antigen-experienced tissues, infection settings, and species (133). TRM cells have even been well characterized in difficult-to-study human organs like the lung, where CD8⁺ TRM cells have been associated with better functional outcomes in viral infections (134, 135). While TRM cell studies have progressed at a rapid pace, research on analogous resident memory B cells (BRM cells) has a much shorter history. This discrepancy is likely due to the relative rarity of B cells within tissues compared to T cells (136) and the fact that one of the main B cell functions, antibody secretion, can be effective over a distance, making the benefits of a BRM cell population unclear.

Lymphoid tissue BRM cells

MBCs that do not re-enter the circulation have now been observed in several lymphoid tissues. As with T cells (137), there are MBCs that remain resident within draining lymph nodes (138, 139). BRM cells are also found in the bone marrow (140), and high T-bet expression was recently found to mark human and mouse MBCs that are preferentially retained as resident cells in the spleen and do not recirculate in the blood or lymphatics like T-bet^{hi}/T-bet^{lo} MBCs do (141). Oral immunization generates MBCs (primarily with IgA⁺ BCRs) localized within the Peyers' patches of the gut (142). Intra-tonsillar toxin immunizations elicit MBCs in human tonsils that preferentially localize to the tonsil that received the immunization, implying they may be resident there (143). RSV-specific MBCs with an atypical phenotype are found in the adenoids of human children; these MBCs produce antibodies with better virus neutralizing ability than antibodies derived from blood MBCs, suggesting they may comprise a distinct

compartment, though this was not formally tested (144). Although resident memory lymphocytes are typically considered in the context of non-lymphoid tissues, there are clearly many non-circulating MBCs that populate the immune tissues of the body where they may be poised for optimal reactivation and sentinel function.

Lung BRM cells

In contrast to the wide variety of non-lymphoid tissues and settings where TRM cells have been described, BRM cells have been observed rarely in healthy non-lymphoid tissues. Singular studies detected non-circulating MBCs in healthy human skin (145) and adipose tissue of mice (146). The majority of tissue BRM cell studies, however, have been in the context of the lung.

In 1987, Jones and Ada provided initial hints that influenza infection in mice may establish MBCs in the lung by showing a stimulation-dependent increase in antibody-secreting cells (ASCs) in influenza recovered lung cell suspensions (147). These authors further showed that the IgG, IgA, and IgM ASC precursors from these lungs were retained for 6 months post-infection, at which point they began to decline. Although this study was a pioneering effort in the field of immune memory localization and preceded the first descriptions of resident memory, the possible importance of these results was seemingly overlooked, and follow-up studies did not occur for over two decades. In 2008, the distribution of IgG and IgA MBCs to different sites in mice recovered from influenza pneumonia was characterized using modern variations on the technique implemented by Jones and Ada (148). Influenza-specific IgG and IgA MBCs were most frequent in the lung draining mediastinal lymph nodes (mLNs), the nasal-associated lymphoid tissue

(NALT), and the lung. The lung MBC numbers were maintained for at least 12 weeks post-infection, leading these authors to revitalize the notion that the lung is a site of MBC accumulation and retention after influenza infection, although retention was not formally tested. In 2012, these observations were extended by the work of Onodera et al (112). Novel phenotypic findings of this study included that many of the virus-specific lung MBCs express the markers CD73, PD-L2, and CD80, which are associated with MBCs poised for antibody secretion on reactivation (120), as well as the marker CD69, which is expressed on many TRM cells. Importantly, this study also provided the first evidence of a functional role for lung MBCs; lung influenza-specific MBCs confer better protection against influenza challenge when transferred to a naïve mouse than spleen influenza-specific MBCs do. Transfer of lung MBCs also correlated with higher virus-neutralizing antibody titers in the BALF after recipient challenge compared with spleen MBC transfer. These results indicated that the lung MBCs generated by flu infections in mice play an important part in respiratory anti-viral immunity and may be resident cells, although circulatory dynamics were not assessed. Adachi et al. (149) then showed that the influenza-specific lung MBCs in mice were protected from an intravascular B cell antibody stain, providing the first evidence these cells were in the lung tissue and not the vasculature. After these groups confirmed that influenza infections definitively elicit lung MBCs in mice, a 2018 study showed that this observation may extend to human lungs as well; healthy lungs of 3 human donors were enriched for total and influenza-specific MBCs compared to unmatched human blood samples (150). However, none of the above studies conclusively showed that the B cells observed within the lung never re-entered

the circulation. Definitive proof that lung MBCs generated by influenza infections of mice are resident and do not recirculate was provided in 2019 (139). These authors showed that if a mouse recovered from influenza was connected surgically via the circulatory system to a congenic partner mouse, the lung MBCs did not ever move into the partner mouse, indicating they did not enter the circulation at any point. This remained true regardless of whether the partner mouse was naïve, had recovered from influenza infection, or had ongoing LPS-induced lung inflammation.

The phenomenon of B cell memory residing within lungs recovered from influenza infections has now been well-documented and extensively reviewed (151, 152). However, the exact location of these MBCs within the lung tissue has surprisingly not been addressed. A consistent feature of influenza infections in mice is that they elicit inducible bronchus-associated lymphoid tissue (iBALT), a lung tertiary lymphoid structure typically defined to include B and T cell areas in close proximity, ongoing GC reactions, and high endothelial venules (HEVs) (153). These structures can be observed in mouse lungs recovered from influenza for as long as a month after infection resolution, and are capable of retaining MBCs (149, 154). Disruption of influenza-induced iBALT in mice impaired secondary antibody responses to a challenge infection, leading to speculation that iBALT is a likely site of localization for lung BRM cells (155, 156). In support of this idea, transfer of influenza-specific lung MBCs only provided protection in naïve recipients if iBALT was pre-formed in the recipient lungs prior to transfer (112). Additionally, the one study that visualized MBC-containing lungs after influenza

infection observed large clusters of B and T cells with ongoing GC reactions, although the cells within the iBALT were not nearly as organized as is observed in SLOs (149).

Therefore, at least some of the lung BRM cells generated after influenza appear to localize to iBALT structures. However, iBALT is not typically seen in the lungs of healthy humans, nor is it elicited by all respiratory infections (157). Pneumococcal infections of mice, for example, do not lead to iBALT structures detectable on hematoxylin and eosin (H & E) staining (74). This leads to the question of whether lung BRM cells are a feature unique to influenza infections or can be found in iBALT-free lungs that have been exposed to other, non-viral pathogens. Whether and how the kinetics of and signals for BRM cell establishment in the lungs would differ between influenza and other infection settings is also unclear.

Research Objectives

The research described in this dissertation aims to address three main areas of investigation described in the above introduction that have not yet been elucidated by the scientific community. These are: 1) the contribution of MBCs to naturally acquired serotype-independent pneumococcal immunity; 2) the extent to which lung BRM cells are formed by bacterial respiratory infections and are maintained in iBALT-free lungs; and 3) the kinetics and signals required during BRM cell establishment outside the setting of influenza infections.

CHAPTER TWO: MATERIALS AND METHODS

Mouse Strains

All animal protocols were approved by the Boston University Institutional Animal Care and Use Committee. C57BL/6J mice were purchased from Jackson Laboratories (Bar Harbor, Maine). *Ighm^{tm1cgn}* (μ MT) B cell-deficient mice (158) on a C57BL/6 background were purchased from Jackson Laboratories and maintained by breeding homozygous animals. Homozygous PZTD (PD-L2+ indicator knock-in and inducible knockout) mice with CD19-Cre transgenes were previously described (159). Mouse experiments were initiated when mice were 6-12 weeks of age and included both male and female animals. Mice were maintained in specific pathogen-free conditions on a 12 h light-dark cycle with *ad libitum* access to food and water.

Bacterial Infections

Anti-pneumococcal immunity was generated as previously described (74) by giving mice two exposures to *S. pneumoniae* serotype 19F (Sp19F EF3030, kindly provided by Dr. Marc Lipsitch) one week apart before allowing mice to recover for at least four weeks. Sp19F exposures were given either intratracheally (i.t.) or intranasally (i.n., only for Fig. 5I). Mice were anesthetized via i.p. injection of ketamine (75 mg/kg for i.t. or 50 mg/kg for i.n.) and xylazine (5 mg/kg). For i.t. exposures, a small incision was made to expose the trachea, and a 24-gauge catheter (Becton Dickinson 381112) was inserted into the trachea and down into the left bronchus. A 50 μ L volume containing 1×10^6 bacterial CFU was instilled in the left lung lobe of each mouse. For i.n. exposures, 50 μ L of bacterial suspension (25 μ L per nare) containing 1×10^6 bacterial CFU was

instilled into each mouse until it was inhaled completely. Challenge infections after the development of immunity were given by i.t. instillation of $0.5-1 \times 10^6$ *S. pneumoniae* serotype 3 (6303), which was purchased from the American Type Culture Collection (ATCC). Sp3 bacterial burdens in homogenized whole lungs were assessed by euthanizing mice at specified time points and counting serial dilutions of bacterial CFU.

Tissue Collection

Various samples were collected from mice after euthanasia by isoflurane overdose. Heparin-coated syringes were used for collection of blood from the inferior vena cava, and blood plasma was separated from erythrocytes by centrifugation at 1500 rcf for 15 minutes at 4°C. Pleural fluid was collected by washing the pleural space with 3 mL of PBS. For BALF protein samples, the trachea was cannulated with an 18-gauge angiocatheter (Becton Dickinson 381444), and the lungs were lavaged twice with 0.5 mL of PBS. For collection of lung protein, harvested lungs were homogenized in a bullet blender (Next Advance) in water containing protease inhibitor (Roche). Samples were centrifuged at 4°C and 10,000 rcf for 20 minutes, and supernatants were stored at -80°C.

For human samples, pathologist-determined normal lung tissue from 7 patients undergoing surgical lung cancer resection was collected under protocols approved by the Boston University institutional review committees. The tissues were immediately immersed in RPMI Medium and transported to the laboratory on ice. Informed consent was obtained from all subjects.

Lung Digestion

For experiments requiring mouse lung single-cell suspensions, isolated lung lobes were minced with a razor blade then digested by shaking at 250 rpm and 37°C for 1 hour in digestion buffer containing type 2 collagenase (1 mg/mL, Worthington Biochemical), DNase I (150 µg/mL, Sigma), and CaCl₂ (2.5 mM) in PBS. Digested cells were passed through a 70 micron filter, and red blood cells were lysed in cell lysis buffer (Sigma). Single cell suspensions were then counted on a Luna Dual Fluorescence Cell Counter (Logos Biosystems) and used for flow cytometry and *ex vivo* stimulation assays. For human lung samples, the tissue was similarly processed into single cell suspensions by mincing and digestion under the same conditions as above but with a buffer containing: 0.2 µg/mL type A collagenase (Worthington Biochemical), 40 µg/mL DNase I (Sigma), 1 mM CaCl₂, 50 µL/mL heat-inactivated FCS (Sigma), and 10 µL/mL HEPES (Thermo Fisher Scientific) in HBSS. Digested human lung tissue was passed through a cell strainer as above, then red blood cells were lysed using BD PharmLyse buffer according to the manufacturer's instructions. Single cell suspensions were counted as above and analyzed via flow cytometry.

Flow Cytometry

To distinguish circulating (IV) from lung tissue (EV) cells, mice were injected i.v. with 2 µg of the indicated fluorescent anti-CD45 antibody 3 minutes prior to sacrifice and lung harvest. Single cell lung suspensions were prepared as above, with left and right lobes digested separately. Single cell spleen suspensions were obtained by filtering mechanically disrupted organs through 70 micron filters. All staining was performed with

specified fluorescent antibodies (see Table 1) in FACS buffer (PBS containing 0.5% FBS and 2 mM EDTA) on ice in the dark for 30 minutes. After staining, all samples were resuspended in FACS buffer containing 7-AAD (BD Biosciences) live/dead stain at a 1:100 dilution. Stained cells were assessed on LSR-II (BD Biosciences) or Cytex Aurora (Cytex Biosciences) flow cytometry analyzers. Controls in each experiment included unstained cells, single-stain UltraComp eBeads (Thermo Fisher Scientific) used for automatic compensation, and fluorescence minus one controls for each stain that preliminary experiments determined did not result in easily distinguished populations. The data were analyzed using FlowJo v10 software (BD Biosciences).

Marker	Fluorophore/Conjugate	Clone	Vendor	Product Number
IgA	Biotin	RMA-1	Biologend	407003
B220	APC Fire 750	RA3-6B2	Biologend	103259
B220	PerCpCy5.5	RA3-6B2	Biologend	103235
CD11a	APC	M17/4	Biologend	101119
CD11a	PECy7	M17/4	Biologend	101121
CD19	BUV395	1D3	BD Biosciences	563557
CD19	BV605	6D5	Biologend	115539
CD19	BV421	6D5	Biologend	115537
CD20	APC	SA275A11	Biologend	150411
CD38	PerCPef710	90	Thermo Fisher	46-0381-80
CD4	APC	GK1.5	Biologend	100411
CD43	BV750	S7	BD Biosciences	747277
CD43	APC	S11	Biologend	143207
CD44	BV421	IM7	BD Biosciences	563970
CD45	FITC	30-F11	Biologend	103108
CD45	AF532	30-F11	Thermo Fisher	58-0451-82
CD45	PerCpCy5.5	30-F11	Biologend	103131
CD45	BUV737	30-F11	BD Biosciences	748371
CD45.2	BUV737	104	BD Biosciences	612778
CD62L	PECy7	MEL-14	Biologend	104418
CD69	PE	H1.2F3	Biologend	104508
CD73	APC	TY/11.8	Biologend	127209
CD73	PE-Vio 770	TY/11.8	Miltenyi	130-103-055
CD80	BV421	16-10A1	BD Biosciences	562611
CXCR5	PE-eFluor 610	SPRCL5	Thermo Fisher	61-7185-82
GL7	Biotin	GL7	Biologend	144616
IgD	PerCPef710	11-26c	Thermo Fisher	46-5993-82
IgD	AF488	11-26c	Biologend	405717
IgG1	FITC	RMG1-1	Biologend	406606
IgG2b	FITC	RMG2b-1	Biologend	406705
IgG2c	FITC	polyclonal	Southern Biotech	1079-02
IgG3	Biotin	RMG3-1	Biologend	406803
IgM	PECy7	RMM-1	Biologend	406514
IgM	eF450	eB121-15F9	Thermo Fisher	48-5890-82
PD-L2	APC	TY25	Biologend	107210
PD-L2	PE	TY25	Biologend	107205

Table 5. Antibodies used in flow cytometry analysis of mouse tissues.

Marker	Fluorophore/Conjugate	Clone	Vendor	Product Number
B220	BUV737	RA 3-6B2	BD Biosciences	564449
CD19	FITC	HIB19	Biolegend	302206
CD27	BV421	M-T271	BD Biosciences	562513
CD38	APCCy7	HB-7	Biolegend	356616
CD4	PECy7	RPA-T4	BD Biosciences	560649
CD69	PE	FN50	Biolegend	310906
CD83	APC	HB15e	Biolegend	305311
IgD	PerCPCy5.5	1A6-2	BD Biosciences	561315
IgM	BV510	G20-127	BD Biosciences	563113

Table 6. Antibodies used in flow cytometry analysis of human tissues.

B and T Cell Depletion

For circulating B cell depletion studies, mice were treated once with an anti-CD20 monoclonal antibody (clone 5D2, Genentech) or a rat IgG2a isotype control antibody (BioXCell) i.p. (100 µg) and i.n. (100 µg). B cell depletion was assessed via flow cytometry either 4 days or two weeks after antibody treatment. In experiments to assess effects of anti-CD20 depletion on lung immunity to pneumococcus, mice were infected i.t. with Sp3 four days after treatment with anti-CD20 or the isotype control.

For depletion of PD-L2⁺ B cells, experienced PZTD mice were treated once with i.t. (50 ng into the left lung lobe) and i.p. (50 ng) diphtheria toxin (Sigma, d0564) in sterile saline. Vehicle-treated mice were given i.t. and i.p. sterile saline.

For CD4⁺ depletion studies, mice were treated with an anti-CD4⁺ monoclonal antibody (clone GK1.5) or a rat IgG2b isotype control antibody (both from BioXCell). Antibodies were diluted in sterile saline and administered i.p. (500 µg) and i.n. (100 µg). For depletion studies in µMT mice, antibodies were administered 72 and 24 hours prior

to Sp3 challenge. For depletion studies during the initial pneumococcal exposures, antibodies were administered as indicated in Fig. 16A.

For studies involving inhibition of leukocyte egress from tissues, mice were treated i.p. with 1 mg/kg body weight of FTY720 (Sigma, SML0700) every other day beginning 7 days following the first pneumococcal infection.

ELISAs

Pneumococcal-specific antibodies were measured in plasma, *ex vivo* culture supernatants, and BALF using a whole bacterial cell ELISA protocol based on the method described in (160). The indicated pneumococcal strain used as a capture antigen was grown overnight on blood agar plates and was then suspended in sterile PBS such that 1×10^7 CFU was added in 50 μ L to coat each well of a 96-well plate. The acapsular pneumococcal strain used in the culture supernatant and BALF experiments was generated by Dr. Stephen Pelton at Boston University Medical Center and was derived from a serotype 3 parent strain. Plates were coated overnight at 4°C, then washed and blocked with 100 μ L/well 1% bovine serum albumin in PBS for 2 hours at room temperature. Plates were again washed then incubated at room temperature for 2 hours with 50 μ L of the indicated sample per well. Plasma samples were diluted as indicated. *Ex vivo* culture supernatants were not diluted. BALF samples were diluted 1:2. After washing, 100 μ L per well of one of the following HRP-conjugated anti-mouse antibodies was added and incubated at room temperature for 2 hours: anti-total IgG (1:2000, R&D Systems, HAF007), anti-IgG3 (1:10,000, Abcam, ab97260), anti-IgG1 (1:10,000, Abcam, ab97240), anti-IgG2b (1:10,000, Abcam, RRID: AB_10695945), anti-IgG2c (1:10,000,

Abcam, ab97255), anti-IgA (1:2000, Thermo Fisher Scientific, RRID: AB_2533951), anti-IgM (1:2000, Thermo Fisher Scientific, RRID: AB_2533954). The plate was then washed and developed with 3,3',5,5'-tetramethylbenzidine (TMB) substrate (R&D Systems). The reaction was stopped with 2N sulfuric acid stop solution (R&D Systems). The optical density of each well at 450 nm was determined using a microplate reader (BioTek Synergy LX Multi-Mode).

IL-17 was measured in lung homogenates of μ MT mice using a DuoSet IL-17 ELISA kit (R&D Systems, DY421) performed according to the manufacturer's instructions. CXCL13 and CXCL12 were measured in lung homogenates using DuoSet ELISA kits (R&D Systems; DY470 and DY460, respectively) according to the manufacturer's instructions.

Pneumococcal Opsonization

For opsonization with plasma, Sp3 was added to 500 μ L of pooled plasma from mice that received i.n. Sp19 or saline 4-8 weeks prior until the mixture reached an optical density of 0.3. For opsonization with BALF, 25 μ L of a 1:4 dilution of Sp3 at an optical density of 0.3 was mixed with approximately 300 μ L of pooled BALF from mice that received i.n. Sp19 or saline 4-8 weeks prior. For both experiments, the mixture was rotated for 1 hour at 4°C, then bacteria were spun down at 9600 rpm for 9 minutes. Bacterial pellets were resuspended in 500 μ L of sterile saline, then 50 μ L was instilled i.n. into each recipient mouse. Recipient mice were healthy naïve mice that had never been exposed to pneumococcus or saline previously. Lung Sp3 CFU were determined 24 hours later.

***Ex vivo* B Cell Stimulation and ELISpot**

Mice were given an i.v. injection of 2 μ g PE anti-CD45 (Biolegend, RRID: AB_312971) 3 minutes before sacrifice and harvest of lung left lobes and spleens. Single cell suspensions of lung and spleen tissue were procured as described above, including red blood cell lysis. Cells in lung tissue that were not protected from the i.v. stain (i.e., were bound to PE anti-CD45) were then selected out using an EasySep Mouse PE Positive Selection Kit (StemCell Technologies, 17666) according to the manufacturer's instructions. Following selection of lung cells, all cells were resuspended at 4×10^6 /mL in CTL-Test B Medium (ImmunoSpot, Cellular Technology Ltd.) containing Resiquimod (R848) and IL-2 (ImmunoSpot, CTL-mBPOLYS-200) and 1% L-glutamine (Thermo Fischer Scientific) for stimulated samples or CTL-Test B Medium with 1% L-glutamine alone for unstimulated controls. Cells were incubated on 12-well plates (1 well per tissue sample) for 4-5 days at 5% CO₂ and 37°C. Following culture, supernatants of each well were collected and stored at -80°C for pneumococcal-specific antibody analysis. Cells were collected and used for total IgG ELISpot assays using the Immunospot Mouse IgG Single-Color ELISpot kit following the manufacturer's instructions. Developed ELISpot plates were visualized and counted on a BioSpot S5 Macro Analyzer using the Immunospot software package (Cellular Technology Ltd.). Prior to the automated counting, a quality control step was done to remove fibers and edge artifacts from the wells.

Whole Blood RNA-Seq

Facial vein blood from 10 naïve and 10 experienced mice that had been rested for 6 weeks was collected into anticoagulant-coated tubes (BD 365974). RNA was extracted from the whole blood using the Mouse RiboPure-Blood RNA Isolation Kit (Thermo Fisher Scientific, AM1951) according to the manufacturer's instructions. RNA was purified and a cDNA library was generated using a TruSeq Stranded Total RNA Library Prep Globin (Illumina, 20020612). Single-end 50 base pair read length sequencing was performed on an Illumina HiSeq 2500. Libraries were constructed, quantified, and sequenced by the Tufts University Core Facility in Genomics (<http://tucf-genomics.tufts.edu/>). Illumina fastq files were quality-trimmed using FastQC and Trimmomatic 0.36 (161) and were then aligned to the GRCm38.p5 build of the mouse genome (<https://www.gencodegenes.org/>) using STAR 2.5.3a (162). Only uniquely aligned reads, which accounted for 47%–56% of all reads from the sample set were used for downstream analysis. The relatively low proportion of uniquely aligned reads was due to high amounts of sequenced non-coding RNA species such as mt-Rnr2 and Rn7sk. Indexed bam files were then converted to raw gene counts using HTSeq (163) and the GENCODE M15 gene annotation reference. The Bioconductor package DESeq2 (164) was used for statistical evaluations of expression differences between naïve and experienced mice.

Microscopy

Lungs of euthanized experienced and naive mice were prepared for immunofluorescence by i.t. instillation of OCT (Tissue-Tek) to inflate the lungs, which

were then embedded and flash frozen in OCT. Frozen blocks were cut into 8 micron sections and were then stained with the following primary antibodies: rabbit anti-CD4 (1:500, Abcam, ab183685); rat anti-B220 (1:1000, BD Pharmingen, 553084), followed by staining with Alexa 488 donkey anti-rabbit secondary antibody (1:1000, Jackson ImmunoResearch, 711-546-152), Alexa 594 donkey anti-rat secondary antibody (1:1000, Jackson ImmunoResearch, 712-586-153), and DAPI. Slides were imaged at room temperature with a Leica DM4 microscope and Leica DFC 7000T camera, and were acquired with Leica LAS X software. Images were captured using a 20x objective with a numerical aperture of 0.55 or a 40x objective with a numerical aperture of 0.8.

For confocal imaging of HEV markers, 10 micron thick frozen sections of murine lungs or mediastinal lymph nodes prepared as above were used. Staining and imaging were performed as previously described (165, 166). The primary antibodies used were rat anti-PNAd (1:1000, Santa Cruz Biotechnology, sc-19602) and rabbit anti-CD34 (1:200, Abcam, ab81289), with a DAPI counterstain. Images were captured with Fluoview acquisition software on an Olympus Fluoview 10i scanning laser confocal microscope using a 10x objective, numerical aperture 0.4. Photomultiplier tube gain and laser power settings were such that no signal was visible on isotype control sections.

All images were processed in ImageJ/FIJI using identical look-up table settings for all images of the same magnification.

Statistical Analyses

Statistical analyses were performed using GraphPad Prism 8.0. Each graph represents at least two independent experiments. Unless otherwise indicated, each

individual point on a graph corresponds to an individual animal/sample. Plots displaying data as individual points and summary data depicted as violin plots are shown with medians indicated. Other summarized data are shown as means with standard deviations. Mann-Whitney U tests were used to assess comparisons of two groups, while three or more groups were compared using either a Kruskal-Wallis test with Dunn's multiple comparisons test or a two-way ANOVA with a Holm-Sidak multiple comparisons test, as indicated. Where multiple comparisons tests were used, all possible comparisons were made unless otherwise indicated in the figure legend. The FDR was calculated to control for multiple comparisons in RNA-seq data. Two-sided P values were calculated in all cases. Values of P or FDR $q < 0.05$ were considered to indicate statistically significant differences.

CHAPTER THREE: LUNG RESIDENT MEMORY B CELLS PROTECT AGAINST BACTERIAL PNEUMONIA

Portions of the data and text in this chapter have been submitted as a manuscript to the Journal of Clinical Investigation.

Introduction

Humans evolved alongside a vast array of microbial organisms and environmental antigens. Consequently, our immune system is highly adaptable, undergoing long-term systemic and mucosal remodeling following exposure to commonly encountered external stimuli (167). Traditional specific pathogen-free laboratory mice immunologically resemble infant humans and lack immune features observed in healthy adults, including resident lymphocytes in non-lymphoid tissues, but gain these more human-like immune features upon pathogen exposures (136, 167).

Tissue resident immune cells comprise a group of non-circulating leukocytes that act as a front-line barrier of defense, especially at mucosal sites of constant environmental antigen exposure such as the lung. Although multiple immune cell types, including innate immune cells, may be resident, the long-term protective potential of adaptive memory cells makes resident memory lymphocytes particularly intriguing. TRM cells populate mucosal surfaces in response to various bacterial and viral pathogens and provide rapid local protection against reinfection (168). In the lung, TRM cells are maintained in niches independent of organized iBALT (169). Although TRM cells have

been extensively studied over the last two decades, it remains uncertain whether complementary BRM cells are a common feature at mucosal sites.

MBCs located in mucosal tissues play important roles in mice and humans, but generally are found in organized lymphoid structures such as the gut-associated lymphoid tissue (170) and human tonsils/adenoids (171). In the female mouse reproductive tract, HSV immunization generates local TRM cells without concurrent BRM cell formation, indicating that the presence of mucosal TRM cells does not always correlate with establishment of a BRM cell pool (172). Lung BRM cells are elicited by influenza infections in mice (112, 139). These B cells do not recirculate (139) and provide enhanced protection when adoptively transferred compared to splenic flu-specific MBCs (112). However, the detailed location of these BRM cells in the lung has not been described. Notably, influenza generates long-lasting iBALT in mice (155). Like other organized lymphoid structures, iBALT has been shown to support MBCs but is not a typical feature of healthy adult human lungs (153, 157). Lungs of rhesus monkeys recovered from asymptomatic H1N1 infection are enriched for TRM cells but not for BRM cells, a finding attributed to the likely lack of iBALT from such low virulence infections (173). Thus, whether lung BRM cells are unique to iBALT-containing mouse lungs after influenza or are a common feature of the lung adaptive immune cell landscape remains to be determined.

Both viral and bacterial lung infections impart a large burden of disease globally and in the US, especially among children and the elderly, for whom pneumonia leads to more deaths than any other infectious disease (5, 6). *Streptococcus pneumoniae*

(pneumococcus), comprised of at least 100 serotypes defined by polysaccharide capsule, represents the most common bacterial cause of CAP (10). Essentially all children, even those given pneumococcal vaccination, are colonized or infected multiple times with pneumococcus before the age of 2 (174). These natural exposures generate serotype-independent (heterotypic) immune protection (175). Heterotypic antibodies, LLPCs, and lung TRM cells contribute to naturally acquired immunity to pneumococcus (67), but a role for MBCs has yet to be investigated. Given that virus-elicited MBCs can harbor cross-reactive specificities against mutated viral strains (149, 176), we hypothesized that MBCs may play a similar role in immunity against multiple pneumococcal serotypes. Therefore, we undertook this study to address the fundamental gaps in knowledge regarding the existence of lung BRM cells outside the setting of flu-recovered mouse lungs and the contribution of these cells to anti-bacterial lung immunity.

Results

Effects of resolved pneumococcal pneumonias on circulating cell transcriptomes

The resolution of pneumococcal pneumonias in mice provides serotype-independent lung protection against subsequent pneumonia conferred in part by CD4⁺ TRM cells and remodeled alveolar macrophages (74, 177, 178). We suspected that additional immune changes elicited by pneumococcal exposures remained to be identified. The remodeled immunity in specific pathogen free mice exposed to pathogen-rich pet store mice was defined by a profound change in circulating blood leukocytes, evident in their transcriptomes (167). To investigate whether respiratory infections with *S. pneumoniae* elicited similar systemic changes, we infected mice in the left lung lobe with pneumococcal serotype 19F (Sp19F) twice at a one-week interval (Fig. 3A). Such infections are self-limiting, and animals fully recover without the aid of antibiotics or supportive treatment (177). Control mice were concurrently given saline instillations. Infected and control mice were rested for at least 4 weeks. Previously infected mice were referred to as “experienced,” while control mice were referred to as “naïve.” As described above, experienced mice contain serotype-independent (heterotypic) immune protection, as evidenced by their ability to clear a serotype mismatched challenge infection with pneumococcal serotype 3 (Sp3), which grows uncontrollably in naïve mice (Fig. 3B). However, unlike the radically transformed blood transcriptomes of so-called “dirty” mice compared to naïve laboratory mice (167), the whole blood transcriptomes of uninfected experienced and naïve mice in our model were essentially identical (Fig. 3C-3D). Only four genes were differentially expressed (FDR<0.05) at the mRNA level between naïve

and experienced mice (*Lpp*, *Pmaip1*, *Nt5c*, and *Arfgap2*), none of which exhibited a fold change greater than 1.36 (0.76, 1.36, 1.22, and 1.23, respectively). Thus, while prior studies revealed new cells and altered resident cell phenotypes in the lungs of mice recovered from such Sp19F infections (74, 177, 178), the circulating cell transcriptomes were unchanged.

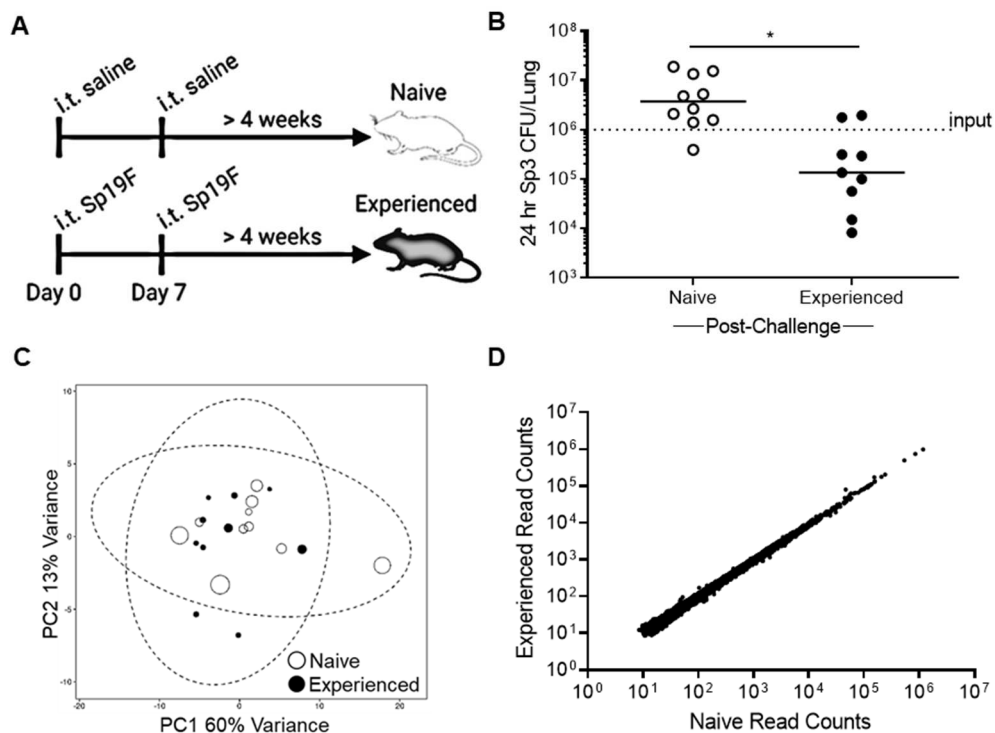


Figure 3. Pneumococcal exposures provide lung protection without extensive changes to the blood transcriptome. (A) C57BL/6 mice were exposed to i.t. pneumococcus (Sp19F) or saline in the left lung lobe twice at a one week interval then allowed to recover for at least four weeks, at which point they were referred to as experienced and naïve mice, respectively. (B) Experienced and naïve mice were challenged with i.t. pneumococcus (Sp3) for 24 hours before lung bacterial burdens were assessed (Mann-Whitney test, $P=0.0006$). (C and D) Principal component analysis (C) and read counts (D) from RNA sequencing of whole blood collected from the same naïve and experienced mice as in (B) prior to Sp3 challenge. Point size in (C) is proportional to the 24 hour lung Sp3 CFU of each mouse in (B). Each point in (D) represents one gene.

MBCs in pneumococcus-experienced lungs without iBALT

The lack of systemic transcriptomic differences between naïve and experienced mice led us to focus on unexplored cell types in the lung itself that may be contributing to improved immunity in experienced mice. Depleting CD4⁺ TRM cells before the Sp3 challenge only partially abrogates lung protection in experienced mice (74). Based on these findings and the recent descriptions of lung BRM cells in mice recovered from influenza (112, 139, 149), we hypothesized that MBCs may be found in pneumococcus-experienced lungs. At 4 weeks after the last Sp19F exposure, the lungs of experienced and naïve mice are histologically normal, and do not contain visible iBALT structures by H & E staining (74). However, immunofluorescence analysis revealed B220⁺ cells in small clusters around bronchovascular bundles in experienced (Fig. 4A-E), but not naïve (Fig. 4F), mice. Organized aggregates consisting of B and T cell zones were not observed, although individual CD4⁺ cells were apparent in or near B cell clusters to varying degrees (Fig 4B,D,E, white arrows). We also stained lung sections of experienced mice for CD34 and peripheral node addressin (PNAd), which co-stain HEVs found in well-organized lymphoid structures such as lymph nodes (Fig. 4G) or lung iBALT (153). Although the lung sections stained brightly for the vascular endothelial marker CD34, we did not observe PNAd staining, indicating HEVs were not present in these lung sections (Fig. 4H-J).

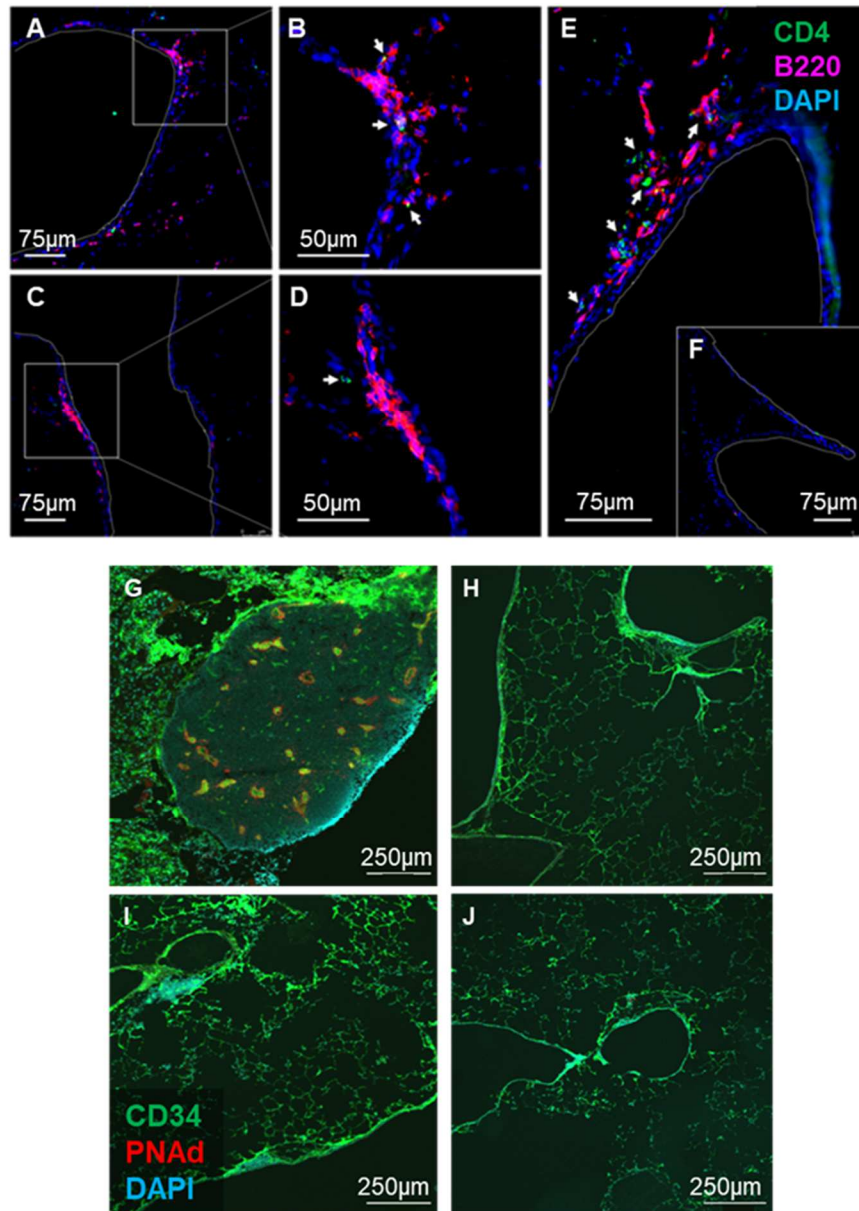


Figure 4. Pneumococcal exposures elicit B cell clusters in lungs without HEVs. (A to F) Immunofluorescence of representative experienced (20x: A,C,E; 40x: B,D) and naïve (20x: F) lungs [B220 (red), CD4 (green, indicated by white arrows), nuclei (DAPI; blue)]. (G to J) Frozen sections of an experienced mouse mediastinal lymph node positive control (G) or of lungs from three experienced mice (H-J) were stained for nuclei (DAPI, blue), the blood vessel marker CD34 (green), and peripheral node addressin (PNAAd, red) and visualized via confocal microscopy.

To phenotype these lung B cells, we used flow cytometry with an i.v. anti-CD45 stain to distinguish circulating from lung leukocytes (gating schemes for all flow cytometry experiments in Fig. 5). A population of CD19⁺ cells protected from the i.v. stain, defined as extravascular (EV) B cells, was observed in the lungs of experienced but not naïve mice (Fig. 6A). The EV B cells in experienced mice were predominantly IgD⁻, while the intravascular (IV) B cells positive for the i.v. stain in the same mice were largely IgD⁺ (Fig. 6B-C). Additionally, the EV lung IgD⁻ B cells, but not the EV IgD⁺ B cells, were significantly increased by experience, and there was no effect of experience on the IV B cells in these lung digests (Fig. 6D). These data suggest that the lung EV B cell compartment after pneumococcal exposures is enriched for non-naïve B cells, which we hypothesized were comprised largely of memory cells. Consistent with this hypothesis, the number of IgD⁻ EV B cells in experienced lungs remained constant for as long as 12 weeks after the last Sp19 infection before declining by 6 months post-exposure, when the significant difference in lung B cell numbers between experienced and naïve mice was lost (Fig. 6E). Moreover, all the EV IgD⁻ B cells in experienced mice were CD38⁺, an MBC phenotype in mice (Fig. 6F) (106). Altogether, these results indicate that repeated pneumococcal exposures in mice elicit MBCs within the lung tissue that are maintained independently of iBALT.

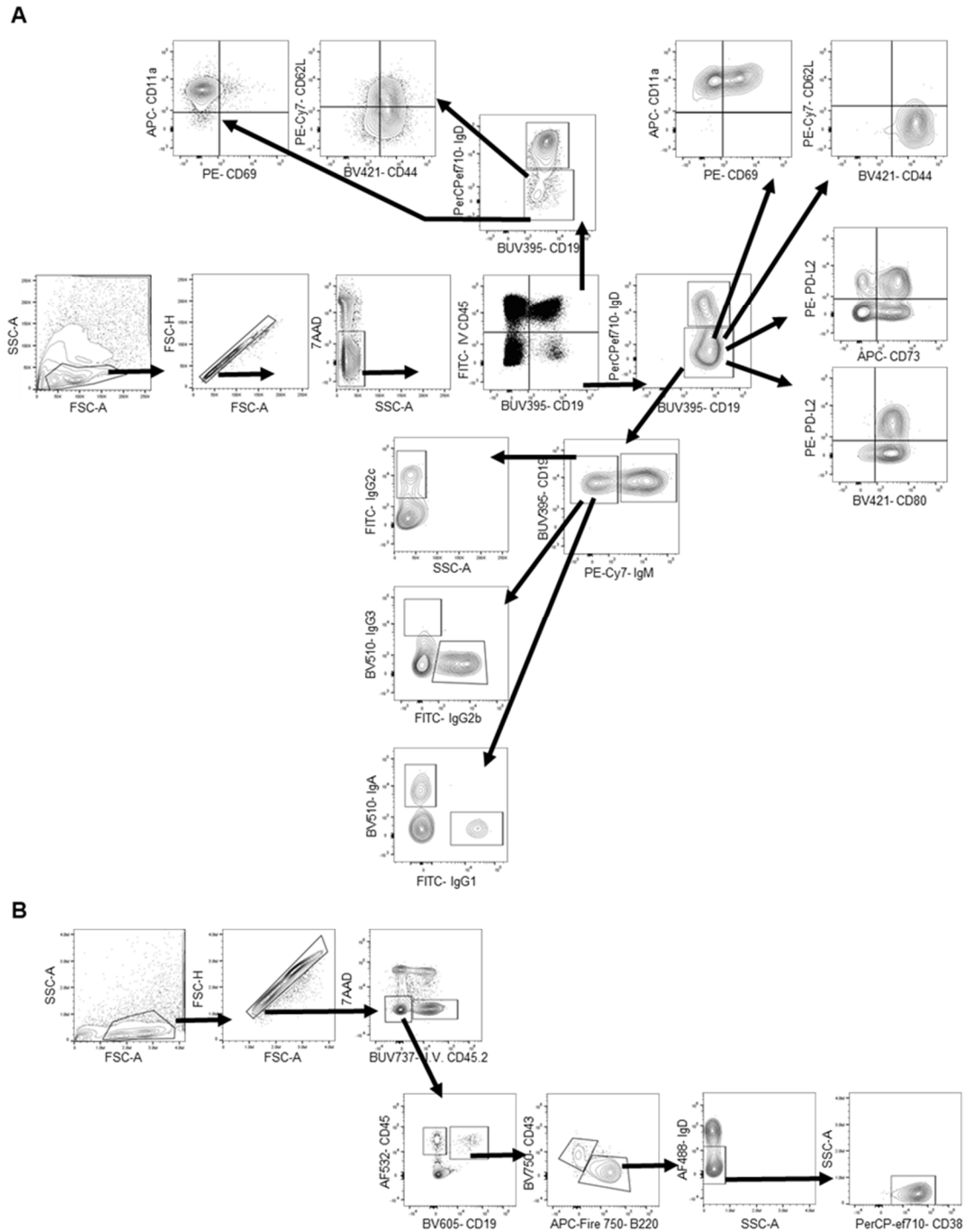


Figure 5. Flow cytometry gating schemes used to analyze mouse lung B cells. (A) Gating used for all flow cytometry data except that noted for **(B)**, collected on the BD LSR II. **(B)** Gating used in a subset of mice from Fig. 6 D-E and all mice in Fig. 6F, collected on the Cytex Aurora spectral cytometer.

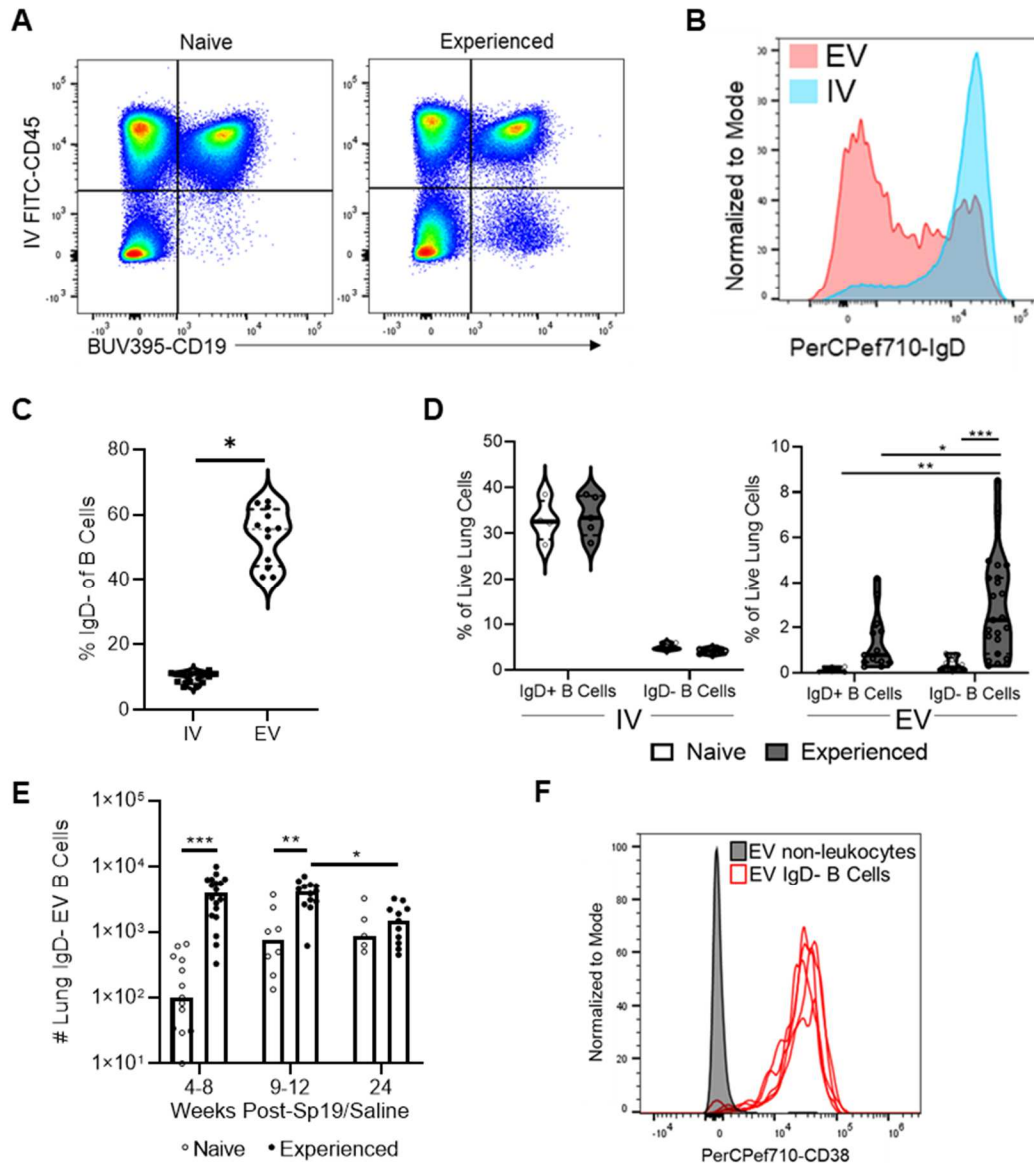


Figure 6. Pneumococcal exposures elicit extravascular MBCs in the lung. (A) Representative gating of i.v. CD45⁺ CD19⁺ cells (“IV B cells”) and i.v. CD45⁻ CD19⁺ cells (“EV B cells”) in lungs of naïve and experienced mice at least 4 weeks after pneumococcal exposure. (B) Representative IgD expression on IV and EV B cells in experienced lungs. (C) The percent of IV and EV B cells that are IgD⁻ in experienced lungs (Mann-Whitney test, $P < 0.0001$). (D) Percentages of IgD⁺ and IgD⁻ B cells of live lung cells in the IV and EV compartments of naïve and experienced mice analyzed between 4 and 12 weeks after the previous Sp19 exposure (2-way ANOVA, $*P = 0.029$, $**P = 0.0006$, $***P < 0.0001$). (E) The number of IgD⁻ EV B cells in naïve and experienced lungs at the indicated times after lung exposure (2-way ANOVA, $*P = 0.01$, $**P = 0.0054$, $***P < 0.0001$). (F) CD38 expression determined via flow cytometry on EV

IgD⁻ B cells (each red curve from one of five separate mice) and on EV CD45⁻ cells (shaded curve, representative).

Resident phenotype of lung MBCs elicited by pneumococcal exposures

The lack of i.v. CD45 staining of the lung B cells in experienced mice indicated that these cells were excluded from circulation at the time of assay. We hypothesized that the lung MBCs represent a resident immune cell pool, and considered whether they bore surface markers similar to lung TRM cells (CD69⁺CD11a^{bright}CD62L^{lo}CD44⁺) (74). Consistent with prior reports on lung BRM cells (112, 139), many of the EV B cells in experienced mice expressed the lymphocyte residence marker CD69 and the integrin CD11a (Fig. 7A, left panel). Compared to IV B cells, EV B cells had lower expression of the lymphoid organ homing molecule CD62L and higher expression of the glycoprotein CD44 (Fig. 7A, right panel). The similarity in surface marker profiles between the MBCs in pneumococcus-experienced lungs and lung TRM cells reported in many experimental systems indicates that the MBCs observed here are likely to be resident cells and that there may be a common lymphocyte residency signature.

Since we were modeling lobar pneumonias, and prior studies revealed immunological changes in the lung occur locally (74, 139, 178), we examined the lobe specificity of the lung B cell phenotypes. The initial Sp19F exposures were restricted to the left lung lobe. EV B cells in the left lobes of experienced mice contained significantly greater CD69⁺ fractions (Fig. 7B) and had significantly higher expression of CD11a (Fig. 7C) compared to the EV B cells from all other groups. The increase in IgD⁻ EV B cells due to experience was also restricted to the previously infected left lobe, with no such

increase in the contralateral right lobes that did not have prior infections (Fig. 7D). Thus, prior experience with pneumococcal infection changed only the EV B cells of the involved lobe.

The phenotype of these B cells suggested they were BRM cells. In parabiosis experiments, cells that fail to relocate to the relevant organ in the parabiont via anastomosed circulatory systems are designated as tissue-resident rather than tissue-homing cells (139). The restriction of B cell phenotypes to the involved lobe and not the contralateral lobes (Figs. 7B-D) matches the parabiosis logic for concluding that these cells are lung resident rather than lung homing. However, we recognized an alternative hypothesis may be that these B cells are not resident, but instead are circulating B cells that home only to previously infected tissue. We therefore wanted to test whether the EV lung MBCs stably remained in the lung compartment. To do so, we leveraged the fact that murine IgG2a anti-CD20 antibodies deplete CD20⁺ B cells in a circulation-dependent manner (179). Both IV and EV lung B cells expressed CD20 (Fig. 7E, IgG-treated mice). An anti-CD20 antibody administered i.n. and i.p. reached the EV lung B cells and remained bound, as shown by blocking of binding of a directly labeled APC-CD20 antibody to EV lung B cells in mice treated two weeks prior with anti-CD20 (Fig. 7E). The anti-CD20 antibody effectively depleted IV B cells but had no effect on EV B cells, observed at both 4 days and 2 weeks after anti-CD20 administration (Fig. 7F-G). Because anti-CD20 bound but did not deplete the EV lung B cells, we conclude that these cells do not re-enter the circulation throughout the 2 week time period examined. Thus,

the lung MBCs elicited by bacterial pneumonia are lung resident rather than lung homing cells.

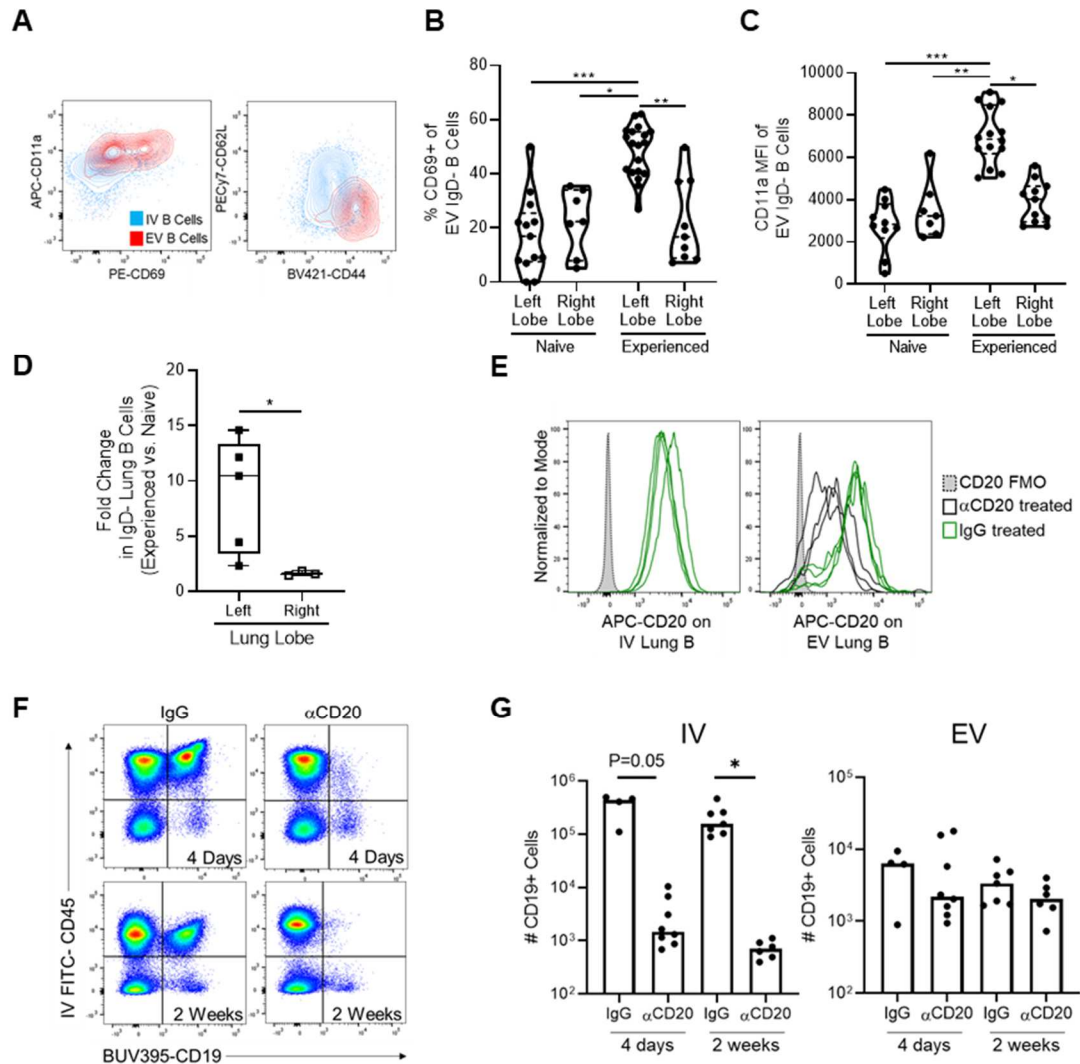


Figure 7. Lung B cells in experienced mice are resident. (A) Representative flow cytometry plots showing expression of CD69, CD11a, CD62L, and CD44 on IV and EV IgD- lung B cells in experienced mice. (B) Percent CD69+ of EV IgD- B cells in the exposed left lung lobe and control right lung lobes of naïve and experienced mice (1-way ANOVA, * $P=0.0054$, ** $P=0.0021$, *** $P<0.0001$). (C) The median fluorescence intensity (MFI) of CD11a on EV IgD- B cells in the exposed left lung lobe and control right lung lobes of naïve and experienced mice (1-way ANOVA, * $P=0.0047$, ** $P=0.0017$, *** $P<0.0001$). (D) The fold change in EV IgD- lung B cells between saline and experienced mice in the exposed left lung lobe and unexposed control right lobes. Each

dot represents the average fold change in one experiment containing ≥ 3 naïve and 3 experienced mice (Mann-Whitney test, $P=0.036$). **(E)** Binding of a fluorescent anti-CD20 antibody to lung B cells from mice treated two weeks previously with isotype control IgG or anti-CD20 (5D2 clone). **(F and G)** Representative flow cytometry plots **(F)** and quantified CD19+ cells **(G)** in lung compartments 4 days or 2 weeks after anti-CD20 or IgG treatment of experienced mice (Kruskal-Wallis test, $*P=0.002$).

Human lung BRM cells

Since pneumococcus and influenza are both common causes of lung infection in humans (10) and both lead to deposition of lung BRM cells in mice (Figs. 4-7 and (139)), we hypothesized that human lungs may contain BRM cells. Disease-free samples from lung tissue wedge resections or lobectomies were assessed via flow cytometry (Fig. 8A). Consistent with a prior report (136), significantly more CD4+ T cells than B cells were observed in the human lungs (Fig. 8B). Of the CD19+ cells in these lungs, the majority (~65%) were positive for the human MBC marker CD27, and the remaining cells were mostly IgD+ (Fig. 8C). Most of the MBCs (CD19+CD27+) as well as the CD4+ T cells in these lung samples were CD69+, whereas most naïve B cells (CD19+IgD+) in the same lungs were not (Fig. 8D). The percentages of lung CD4+ T cells that were CD69+ in our samples matched well to lung T cell data from studies of humans with no known lung disease (136, 180), suggesting our samples fairly represented human lung immunology. The majority of MBCs in these lungs were class-switched, with only ~17% expressing IgM (Fig. 8E). The CD69+ MBCs were negative for CD38 (Fig. 8F), indicating they were not GC or plasma cells (181). In addition to being a residence marker, CD69 is expressed by activated B cells, but almost all the human CD69+ MBCs

were negative for CD83 (Fig. 8F), another marker of B cell activation (182). Therefore, it is likely that CD69 is a marker of resident, as opposed to recently activated, cells in this context. These data provide evidence that human lungs contain class-switched BRM cells.

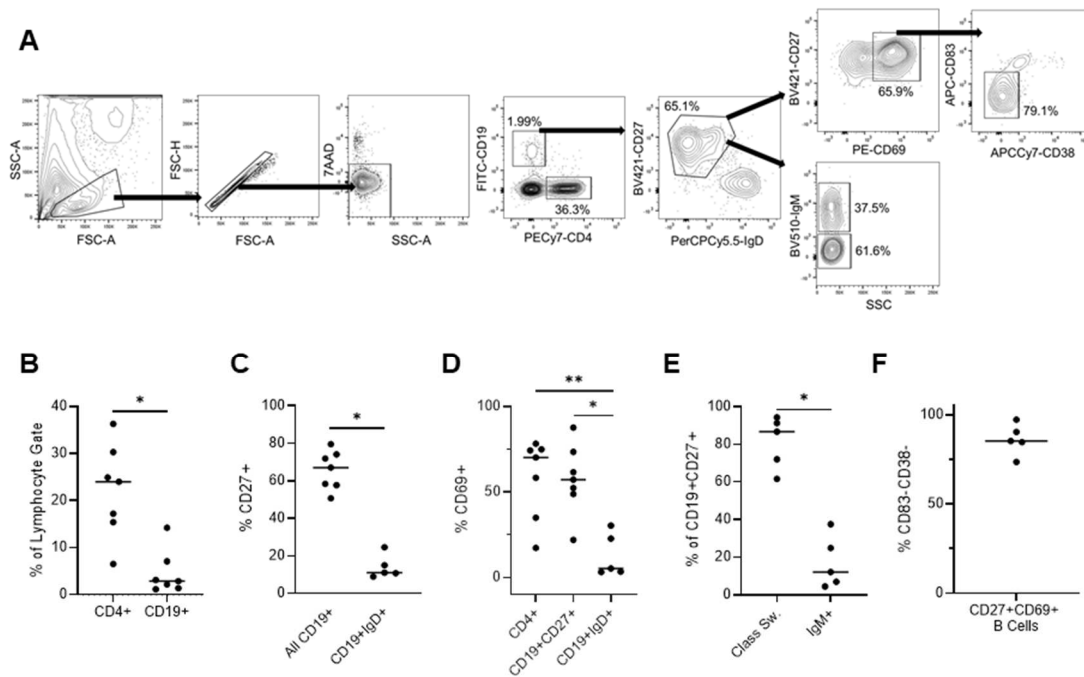


Figure 8. Human lungs are enriched for B cells bearing a resident memory phenotype. (A) Pathologist-determined normal tissue from wedge resection or biopsy samples from humans with lung cancer were collagenase digested and analyzed via flow cytometry using the gating scheme shown. (B to F) Various cell surface phenotypes of B and T cells in the human lung digests. (B) The percent of CD4+ and CD19+ cells among live, single cells (Mann-Whitney test, *P=0.0023). (C) The percent of CD27+ cells among all CD19+ cells and among naïve (CD19+IgD+) B cells (Mann-Whitney test, *P=0.0025). (D) The percent of CD69+ cells among CD4+ cells, memory B cells (CD19+CD27+), and naïve B cells (Kruskal-Wallis test, *P=0.021, **P=0.049). (E) The percent of memory B cells that are class-switched and the percent that are IgM+ (Mann-Whitney test, *P=0.0079). (F) The percent of resident memory B cells (CD27+CD69+CD19+) that are negative for the B cell activation marker CD83 and for CD38.

Lung BRM cell isotypes and memory marker expression

After observing that pneumococcal exposures elicit lung BRM cells, we wanted to more deeply explore the phenotypic and functional aspects of these cells. Although the EV lung B cell compartment included naïve B cells (IgD+IgM+), a larger fraction was IgM+IgD- than in the spleen or the blood (Fig. 9A). Additionally, and in contrast to the spleen and blood compartments, an appreciable proportion of class-switched B cells was observed in the lung EV tissue, highlighting the enrichment of switched memory cells at this site (Fig. 9A). Of the class-switched EV lung B cells, the majority were of an IgG isotype, with a small fraction of IgA+ B cells (Fig. 9B).

In mice, the markers PD-L2, CD73, and CD80 distinguish functional MBC phenotypes (109). In lung B cells of experienced mice, the expression of all three markers was restricted, as expected, to IgD- cells, and the EV compartment was heavily enriched with B cells bearing these markers compared to IV B cells in the same mice (Fig. 9C). Importantly, the EV B cells in experienced lungs predominantly expressed more than one of these markers (Fig. 9D-E). Co-expression of at least two of these three memory markers distinguishes MBCs likely to differentiate into ASCs upon reactivation (109).

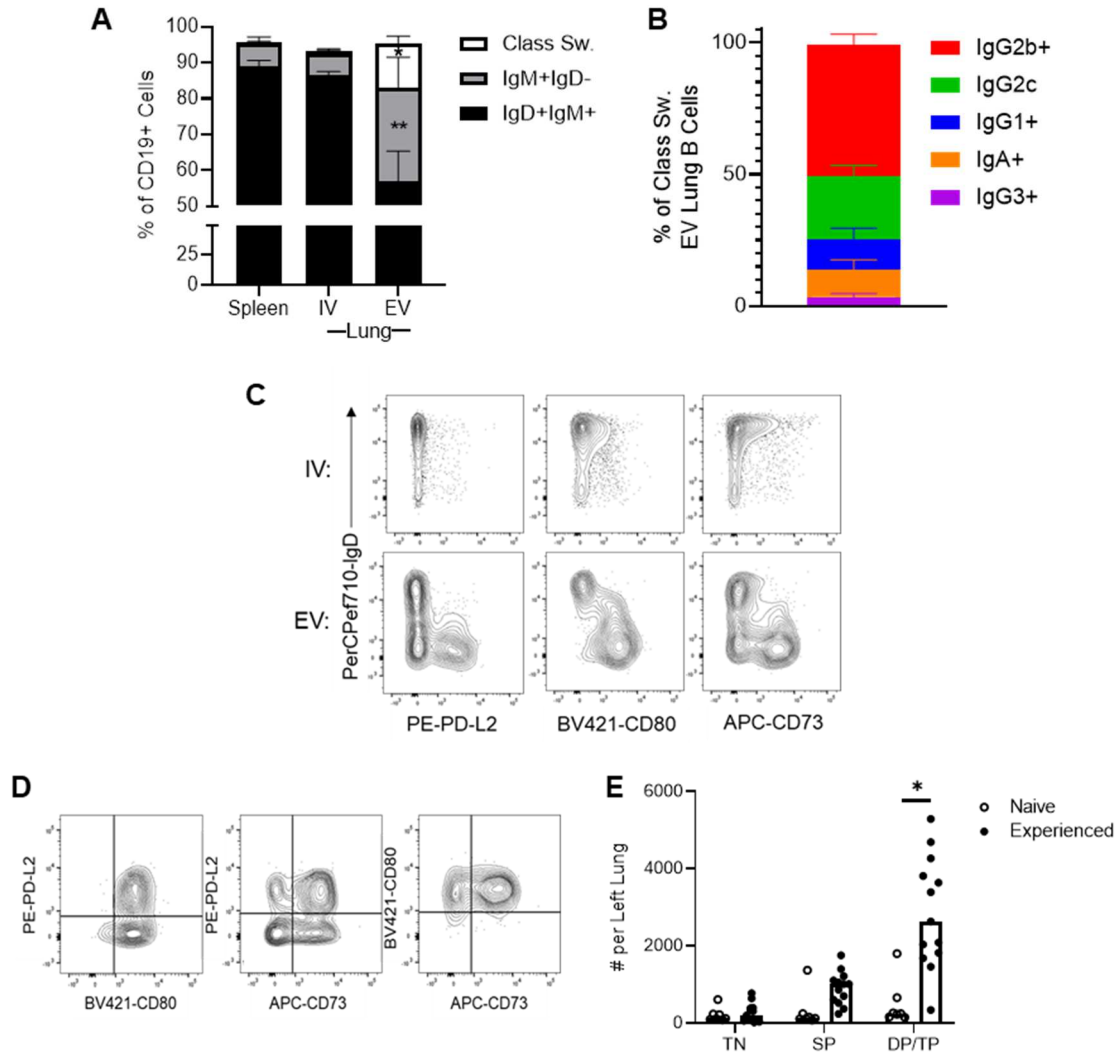


Figure 9. Experienced lungs are enriched in class-switched MBCs bearing multiple memory markers. (A) Distribution of naïve, IgM+IgD-, and class-switched B cells in experienced lungs and spleens (2-way ANOVA comparing isotypes across compartments, N=3 for spleen, 5 for lung; *P<0.0022 vs. spleen, 0.0009 vs. IV lung; **P<0.0001 vs. either compartment). (B) Experienced EV lung IgM-IgD- B cell isotypes. N=5. (C-E) Representative flow plots from experienced lungs showing MBC marker expression on IgD- EV B cells (C) and co-expression (D) as quantified in (E), where numbers of triple negative (TN), single positive (SP), or double or triple positive (DP/TP) B cells are shown (2-way ANOVA comparing each marker category between naïve and experienced mice, *P<0.0001).

Antibody secretion from lung BRM cells

To test whether the lungs of experienced mice contained more MBCs that could be reactivated into ASCs, we stimulated total splenic B cells and EV lung B cells from naïve or experienced mice. After 4 days of *ex vivo* culture followed by IgG ELISpot analysis, spots representing reactivated MBCs were detected more frequently in wells containing stimulated cells from experienced mouse lungs compared to unstimulated cells from experienced mice or stimulated cells from naïve mice (Fig. 10A-B). Although stimulation also elicited ASC differentiation in spleen cells, there was not a significant difference in the number of spleen IgG ASCs between naïve and experienced mice (Fig. 10B). Supernatants from *ex vivo* cultures of stimulated experienced, but not stimulated naïve, mouse lung cells contained IgG and IgM antibodies that bound to an acapsular pneumococcal isolate, indicating they were specific to serotype-independent pneumococcal antigens. Again, stimulated spleen cells from both naïve and experienced mice were able to produce pneumococcus-reactive IgG and IgM, with no significant differences between the groups (Fig. 10C). These results show that the spleens of naïve mice contain B cells that can be stimulated to secrete antibody against pneumococcal antigens, and there is no significant enrichment of such B cells after lung exposure to pneumococcus. These splenic B cells in naïve and experienced mice are likely comprised of innate-like marginal zone or B1 B cells surviving culture only with stimulation and able to produce pneumococcus-binding antibodies (183). In the lung, however, prior pneumococcal exposure is required to generate pneumococcus-specific MBCs. To see whether local antibody secretion in the lung occurred following pneumococcal challenge

in vivo, we analyzed the BALF of experienced mice at baseline and 96 hours after Sp3 challenge. The BALF of experienced mice post-challenge contained significantly more IgA, IgG, and IgM antibodies able to bind an acapsular pneumococcal strain (Fig. 10D). These findings provide evidence that BRM cells in the experienced lung are reactivated by a heterotypic pneumococcal challenge to locally secrete serotype cross-reactive antibodies. Thus, the lungs of mice previously exposed to pneumococcus are enriched with pneumococcus-specific lung BRM cells that are poised to rapidly secrete antibody upon stimulation.

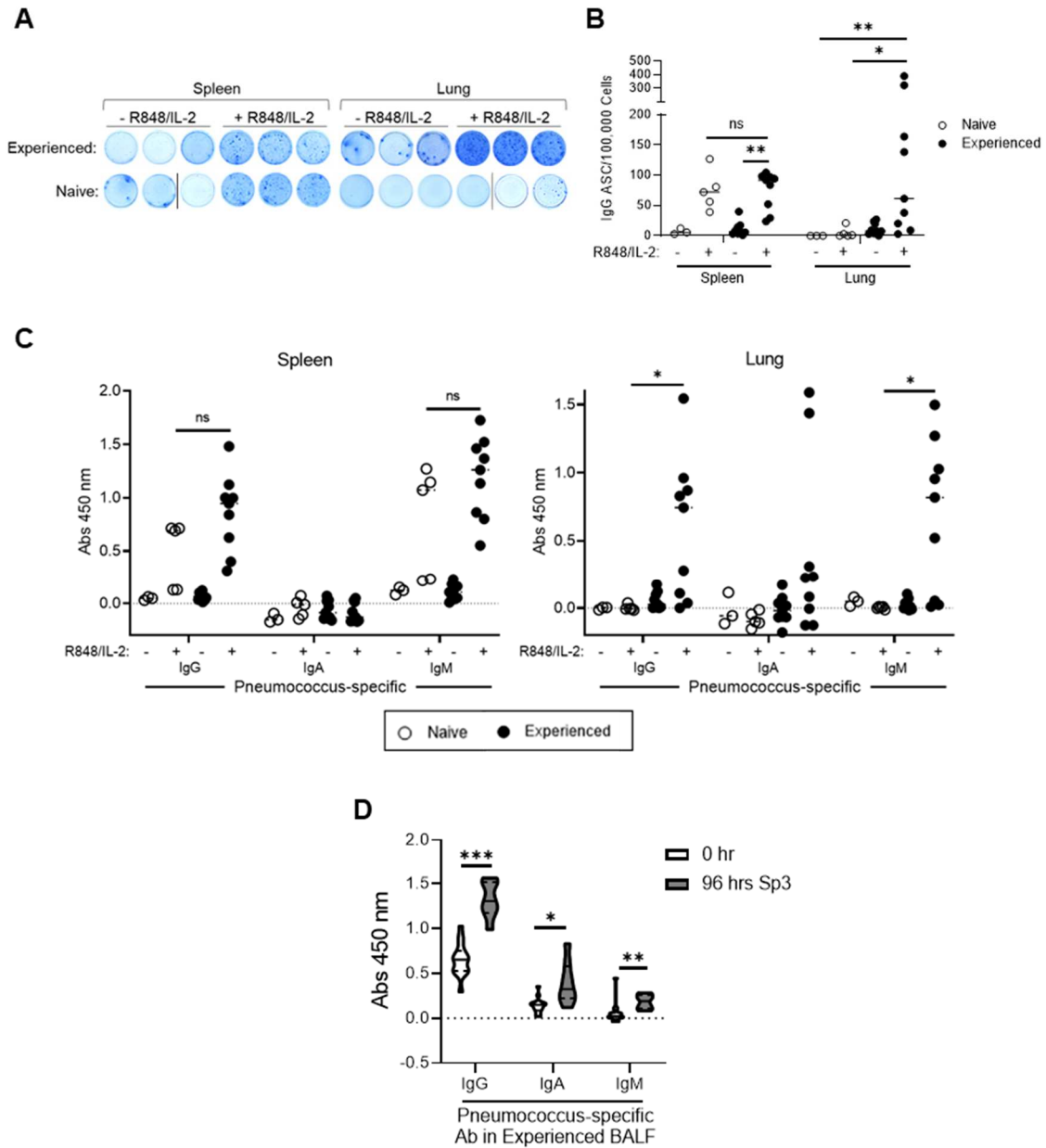


Figure 10. Lung BRM cells are poised to secrete antibody. (A-B) Total IgG ELISPOT image (A) and counts (B) of spleen and EV lung B cells after *ex vivo* culture (Kruskal-Wallis test for each organ, * $P=0.028$, ** $P=0.0035$ for spleen, 0.006 for lung). Vertical lines in (A) separate images within a group obtained from different plates. (C) Pneumococcus-specific antibody levels in *ex vivo* culture supernatants from (A-B) (Kruskal-Wallis test for each isotype within each organ, * $P=0.0039$ for IgG, 0.0064 for IgM). (D) Pneumococcus-specific antibody in experienced BALF at baseline or after Sp3 infection (Mann-Whitney test for each isotype, $N=15$ for baseline, 8 for 96 hours, * $P=0.0018$, ** $P=0.0007$, *** $P<0.0001$). ns, not significant.

Reliance of serotype-independent protection on B cell immunity

The above data led us to hypothesize that B cells in the lung may contribute to serotype-independent pneumococcal immunity. Recovery from pneumococcal infections later protects mice from a serotype mismatched challenge with Sp3 (Fig. 3 and (74)). We found that this protection is partially dependent on B cell-mediated immunity, as evidenced by the increased bacterial burdens (Fig. 11A) and morbidity (Fig. 11B) in experienced B cell deficient (μ MT) mice compared to experienced C57BL/6 (B6) mice after Sp3 infection. Notably, although μ MT mice in our model develop a slightly diminished lung TRM cell pool compared to B6 mice (Fig. 11C-D), experienced μ MT mice still generate as much lung CD4⁺ T cell-derived IL-17A after Sp3 challenge as experienced B6 mice do (Fig. 11E-F and (74)). Therefore, the less robust protection of experienced μ MT mice is not due to a failure to generate effective lung T cell memory, as has been observed in other infection settings (184).

Although experienced μ MT mice lacking all mature B cells have diminished protection, which B cells contribute to this are unknown. Since the anti-CD20 antibody effectively depletes circulating B cells but not lung BRM cells (Fig. 7), we tested whether anti-CD20 treatment affected lung defense in experienced mice. Depletion of all circulating B cells in experienced B6 mice via four days of anti-CD20 treatment had no effect on 24-hour clearance of Sp3 (Fig. 11G). These data suggest that aspects of B cell immunity, but not circulating B cells, contribute to lung defense in experienced mice.

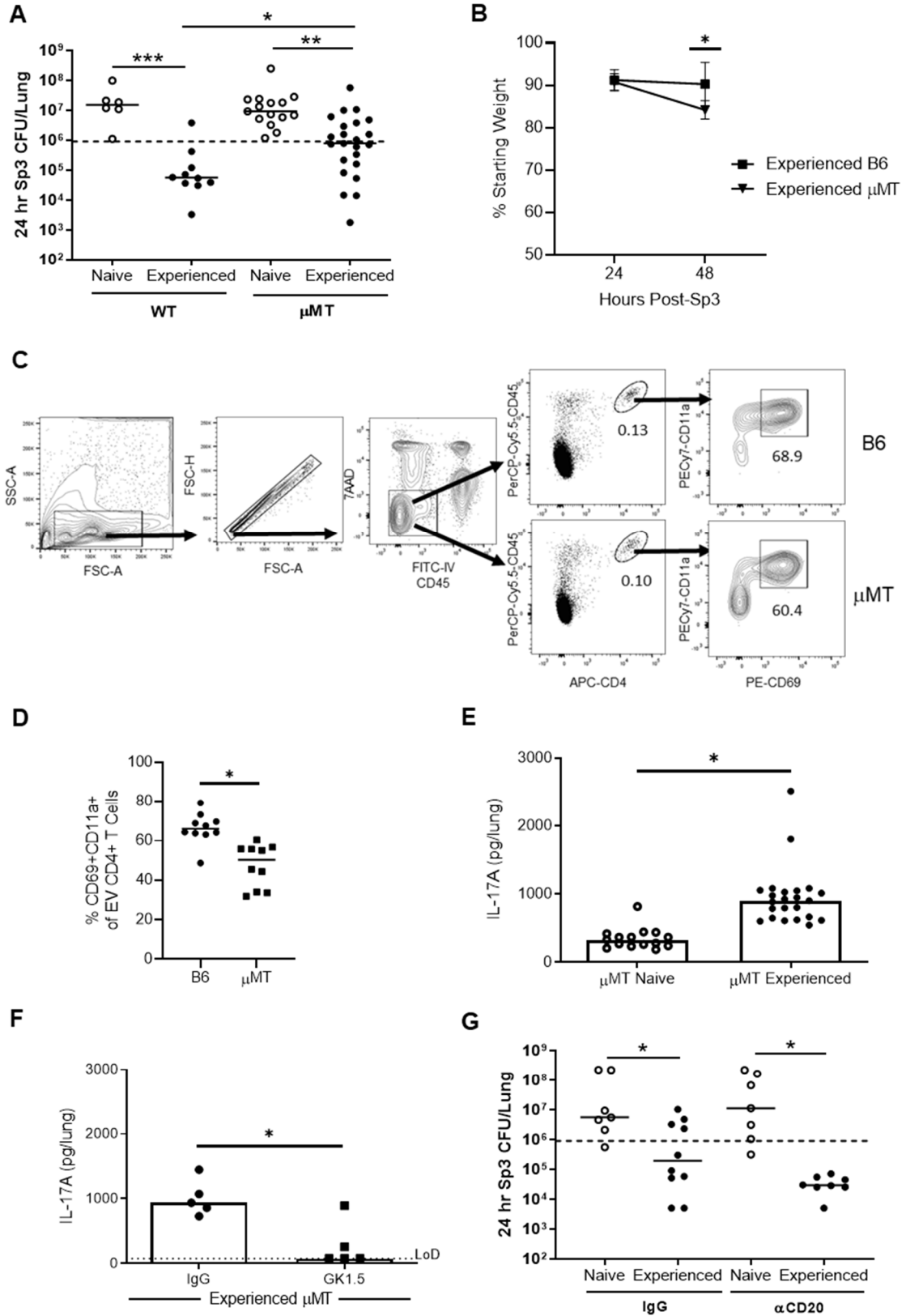


Figure 11. Experienced μ MT mice have intact lung CD4⁺ TRM cell responses but impaired serotype-independent lung defense. (A) 24-hour lung Sp3 burdens in naïve and experienced B6 or μ MT mice (2-way ANOVA, *P=0.013, **P=0.0004, ***P<0.0001). (B) Weight loss after Sp3 challenge in experienced B6 and μ MT mice (2-way ANOVA comparing mouse strains within each time point, N=16 B6 and 9 μ MT, *P=0.0004). (C) Flow cytometry gating scheme used to assess lungs of experienced B6 and μ MT mice for EV T cells bearing a resident memory phenotype (CD69+CD11a^{hi}). (D) Results obtained from gating in (C), showing the percent of EV lung CD4⁺ T cells that were CD69+CD11a^{hi} in lungs of experienced B6 and μ MT mice (Mann-Whitney test, *P=0.0002). (E) IL-17A levels determined by ELISA in whole lung homogenates of naïve and experienced μ MT mice after 24 hours of Sp3 pneumonia (Mann-Whitney test, *P<0.0001). (F) IL-17A levels determined by ELISA in whole-lung homogenates of experienced μ MT mice treated with either an IgG isotype control or a CD4⁺ T cell depleting antibody (GK1.5) prior to 24 hours of Sp3 challenge (Mann-Whitney test, *P=0.032). (G) 24-hour lung Sp3 burdens in naïve and experienced B6 mice treated four days prior with isotype control or anti-CD20 (2-way ANOVA, *P=0.0024 for IgG, 0.0027 for anti-CD20).

Pre-existing anti-pneumococcal antibodies

The finding that μ MT mice have diminished protection in our model while anti-CD20-treated mice remain protected could be due to contributions of pre-formed anti-pneumococcal antibodies secreted by long-lived plasma cells. μ MT mice lack both pre-existing antibodies and MBCs (158), and plasma cells do not express CD20 and are therefore not depleted by anti-CD20 treatment (185). Given that serotype-independent pneumococcal protection in experienced mice is limited to the exposed lung lobe and is not seen in the contralateral lobe, systemic factors such as antibodies that should be able to distribute equally to both lung lobes are not sufficient for protection (74). However, this does not exclude the possibility that such antibodies contribute to lung defenses. Consistent with prior studies (62), lung exposure to pneumococcus resulted in plasma antibodies in experienced mice that could bind to a previously unseen pneumococcal

serotype (Fig. 12A), indicating a systemic heterotypic response to these lung infections. The BALF of experienced mice also contained heterotypic anti-pneumococcal antibodies (Fig. 12B), although the distribution of isotypes observed was markedly different than that in the plasma of the same mice.

To determine whether these antibodies have the capacity to contribute to protection, we incubated Sp3 with plasma or BALF from uninfected experienced or naïve mice before instilling the pre-opsonized bacteria into the lungs of naïve recipients. Pre-opsonization of Sp3 with BALF of experienced versus naïve mice resulted in no difference in the lung bacterial burden of recipient mice (Fig. 12C). This finding may be a reflection of the extremely low titers of serotype cross-reactive BALF antibodies observed in our model compared to other settings where specific BALF antibody titers can be much higher, on the order of 1:100 or even 1:1000 (186, 187). In contrast, mice receiving bacteria pre-opsonized with experienced plasma were able to control bacterial growth compared to recipients of bacteria pre-opsonized with naïve plasma (Fig. 12D), indicating that circulating antibodies have some ability to protect against Sp3 challenge. However, neither recipient group was able to clear the Sp3 compared to input levels, confirming that pre-existing antibodies are not sufficient to confer the full protection observed in our model. Contributions from other immune components, including memory T (74) and possibly memory B cells in the lungs, are required for optimal serotype-independent lung protection.

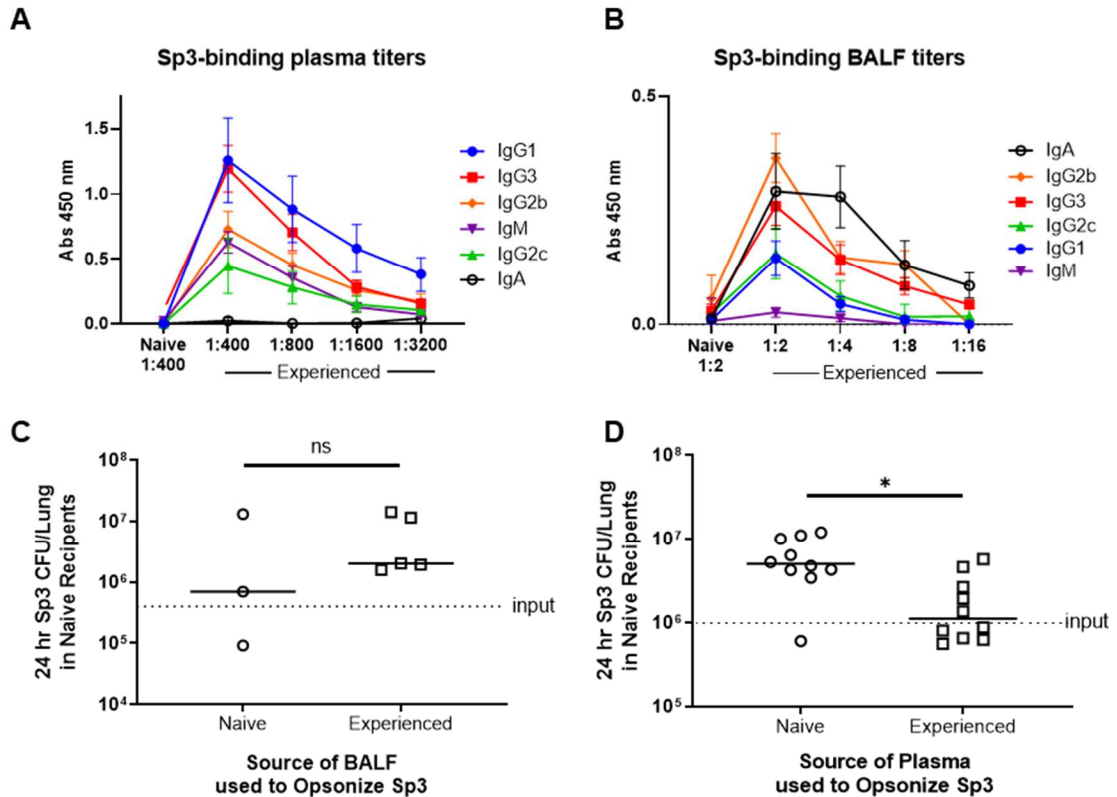


Figure 12. Pre-existing heterotypic antibodies in the plasma are capable of contributing to serotype-independent anti-pneumococcal defense. (A-B) Plasma (A) or BALF (B) collected from uninfected naïve and experienced mice was assessed for titers of Sp3-reactive antibodies of the indicated isotypes via whole-cell pneumococcal ELISA. N=3 for naïve mice and 6 or more for experienced mice. (C-D) BALF (C) or Plasma (D) of experienced or naïve mice was used to pre-opsonize Sp3 prior to bacterial instillation in naïve mice and determination of 24 h lung CFU (Mann-Whitney test, *P=0.01).

B1 B cells in the lung

B1 B cells, which are known to contribute to immunity against pneumococcus in mice (29), are also not thoroughly depleted by anti-CD20 treatment (179). Additionally, the pleural fluid is rich in B1 B cells, which can migrate to the lung in response to a primary pneumococcal exposure (183). We considered whether a lack of pleural fluid B1 cells may contribute to the diminished protection in μ MT mice. However, in B6 mice,

there are no substantial differences in pleural fluid total B cells (Fig. 13A) or B1 B cells (Fig. 13B) after pneumococcal experience, and we observe no change in the experienced lung B1 B cell proportion upon Sp3 infection. These findings indicate it is unlikely that pleural B1 B cells are an important component of serotype-independent pneumococcal immunity in our model.

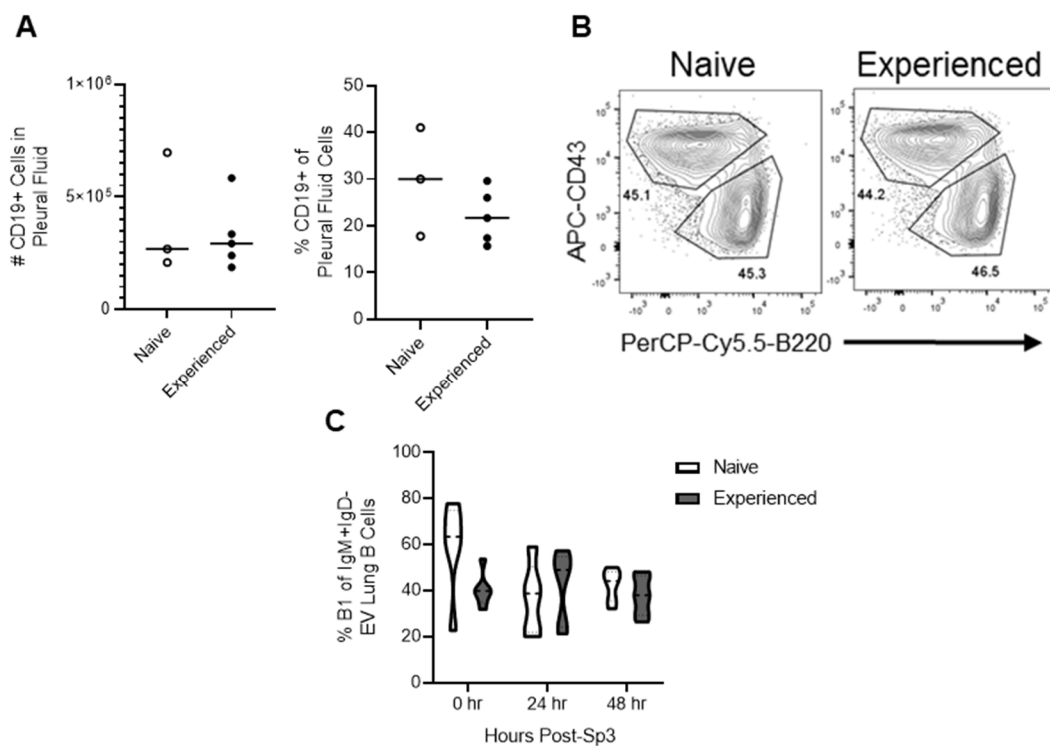


Figure 13. B1 B cells are not changed in the pleural fluid of experienced vs. naïve mice and do not infiltrate the lung upon Sp3 challenge. (A) The number (left) and percent (right) of CD19+ cells in the pleural fluid of naïve and experienced C57BL6/J mice as determined by flow cytometry. (B) Representative flow cytometry plots showing the similar distributions of B1 and B2 cells in the pleural fluid of naïve and experienced C57BL6/J mice. (C) The percent of EV lung IgM+ B cells with a B1 phenotype at baseline and after 1-2 days of Sp3 pneumonia in naïve and experienced C57BL6/J mice. N=6 mice per group (no significant differences by 2-way ANOVA).

Pneumonia protection by lung BRM cells

The above data indicate that aspects of B cell immunity, but not circulating B cells, contribute to lung defense in experienced mice. These findings also suggest that lung TRM cells (Fig. 11) and pre-existing antibodies (Fig. 12) are not sufficient for full protection, and that B1 B cells are unlikely to play a large role in our model of serotype-independent pneumococcal immunity (Fig. 13). This led us to hypothesize that the non-circulating lung MBCs play a functional role in bacterial clearance from experienced lungs. However, there are no means of selectively deleting these cells. Since more than half of the IgD⁻ lung EV B cells are PD-L2⁺ (Fig. 9C-D), we devised a strategy to deplete PD-L2⁺ B cells specifically. By crossing CD19-Cre mice into the PD-L2-ZsGreen-TdTomato-diphtheria toxin knock-in and inducible knockout (PZTD) background (159), all PD-L2⁺ and only PD-L2⁺ cells are fluorescent, with CD19-PD-L2⁺ cells in both Cre⁻ and Cre⁺ mice expressing the fluorescent ZsGreen protein, while CD19⁺PD-L2⁺ cells in Cre⁺ mice express the fluorescent TdTomato protein as well as the diphtheria toxin (DT) receptor (Fig. 14A-B). Resolution of Sp19F infections in these mice elicited PD-L2⁺ (TdTomato⁺) EV lung B cells (Fig. 14C, gating in Fig. 14B).

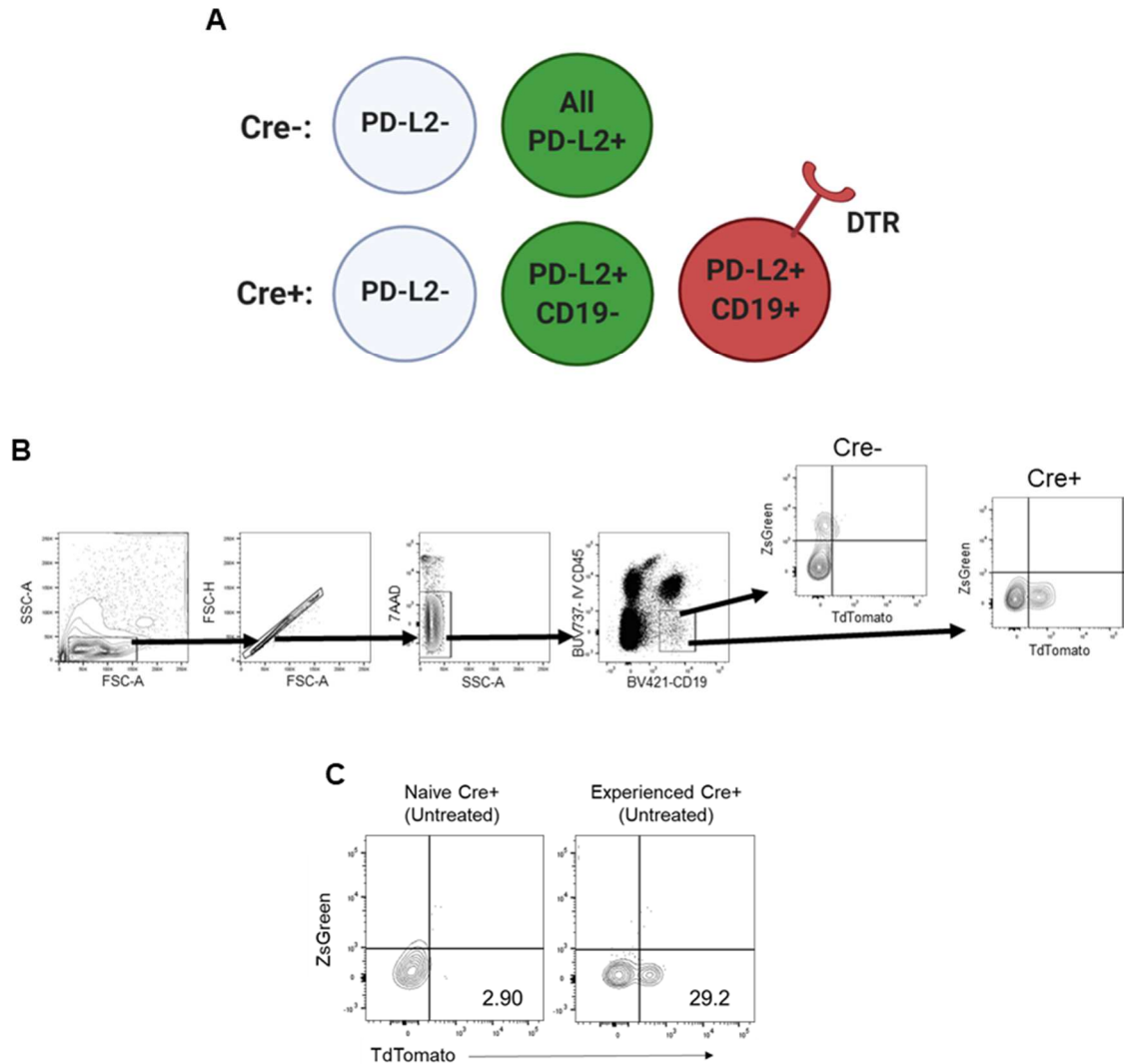


Figure 14. Lung PD-L2+ MBCs are also established by pneumococcal experience in a genetically modified mouse model. (A) Schematic depicting the cell phenotypes observed in Cre- and Cre+ offspring of PZTD mice crossed with CD19-cre mice. **(B)** Flow cytometry gating scheme used in genetically modified mouse lungs. **(C)** Representative flow plots of EV lung B cells in naïve and experienced Cre+ mice with no DT treatment.

Treating experienced Cre+ mice with DT eliminated this PD-L2+ B cell population from the lungs (Fig. 15A-B). In contrast, DT treatment of experienced Cre- mice did not significantly impact lung EV PD-L2+ B cells (Fig. 15B). DT also decreased

pleural PD-L2⁺ B cells in Cre⁺ mice, although only 53% of pleural PD-L2⁺ B cells were depleted by DT (Fig. 15C). However, as described above, pleural fluid B cells do not obviously change in response to prior pneumococcal experience (Fig. 13A-B), nor does it appear that pleural B1 cells infiltrate the lungs of naïve or experienced mice challenged with Sp3 (Fig. 13C), so these cells are unlikely to mediate improved immunity in experienced mice. Circulating Sp3-specific antibody levels did not differ between DT-treated experienced Cre⁻ and Cre⁺ mice (Fig. 15D). To determine roles of PD-L2⁺ B cells in experienced mice, we allowed resolution of Sp19F infections in Cre⁺ and Cre⁻ mice, after which DT was delivered to all mice to deplete lung PD-L2⁺ BRM cells from Cre⁺ but not Cre⁻ mice. Three weeks later, all mice were challenged with Sp3 (Fig. 15E). The Cre⁺ mice exhibited significantly more morbidity as assessed by weight loss during four days of Sp3 infection (Fig. 15F). This morbidity was likely driven by the increased bacterial burdens in the lungs of Cre⁺ mice, since the majority of Cre⁻ but not Cre⁺ mice had reduced bacteria to below the limit of detection over the 4 days of infection (Fig. 15G). We interpret these data as evidence for lung BRM cells contributing to local anti-bacterial immunity.

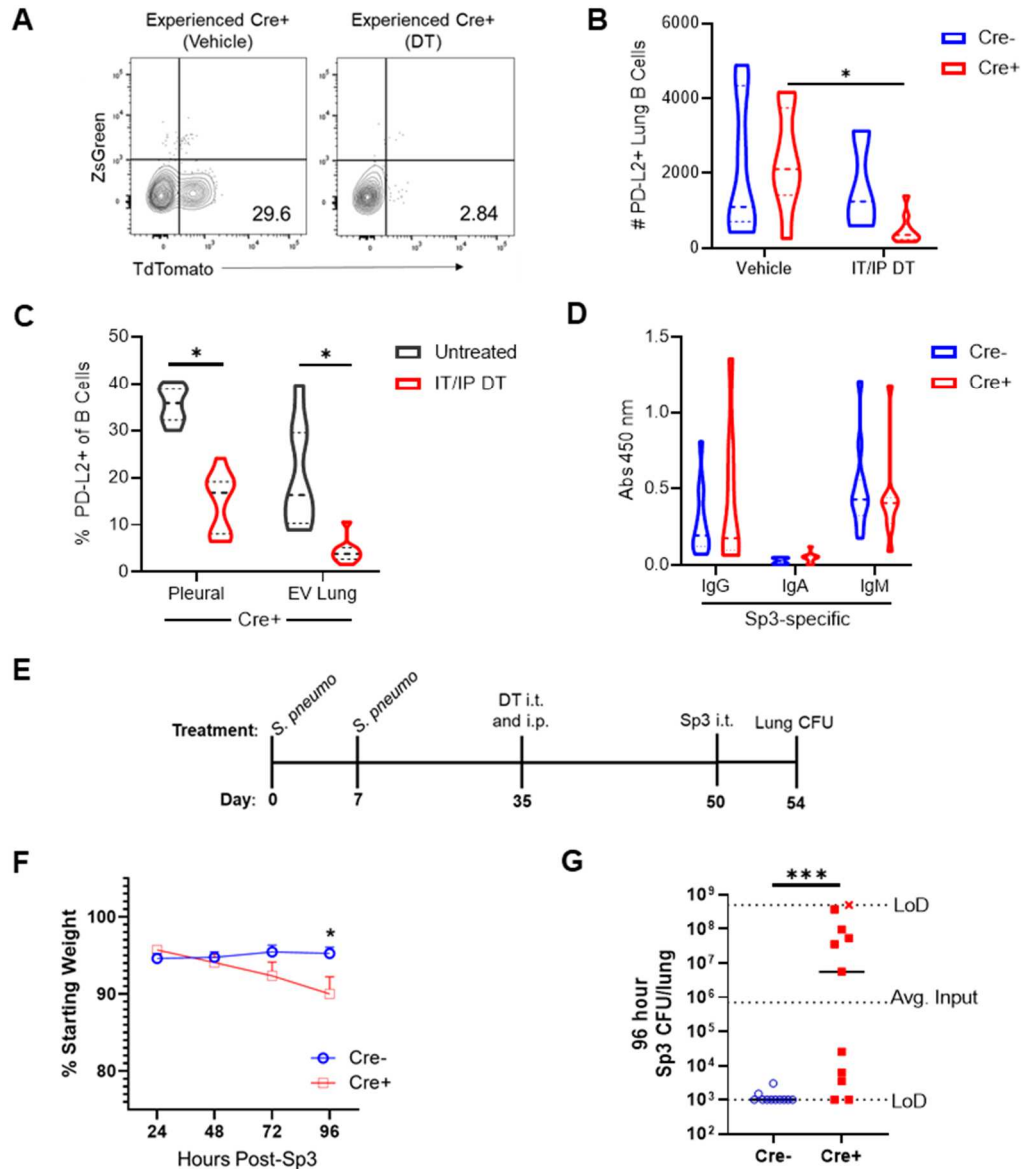


Figure 15. Lung MBCs are required for optimal serotype-independent anti-pneumococcal lung immunity. (A) Representative flow plots of EV lung B cells in experienced Cre⁺ mice with or without DT. (B) Quantification of PD-L2⁺ EV B cells in lungs of experienced Cre⁻ and Cre⁺ mice with or without DT (2-way ANOVA, N= 7 for vehicle-treated Cre⁻ mice, 3 for DT-treated Cre⁻ mice, 8 for vehicle-treated Cre⁺ mice, and 10 for DT-treated Cre⁺ mice, *P=0.029). (C) The percent of pleural fluid and EV lung B cells that are PD-L2⁺ in Cre⁺ mice with or without DT treatment (2-way ANOVA, *P<0.0001). (D) Plasma collected 96 hours after Sp3 infection from experienced DT-treated Cre⁻ and Cre⁺ mice was assessed for Sp3-reactive antibodies of the indicated isotypes via whole-cell pneumococcal ELISA. N=12 for Cre⁻ mice and 9 for Cre⁺ mice (no significant differences by Mann-Whitney test within each isotype). (E)

Timeline of infections, DT administration and Sp3 challenge in genetically modified mice. **(F)** Weight loss after Sp3 challenge in DT-treated experienced Cre- and Cre+ mice (2-way ANOVA comparing genotypes within each time point, N=11 per genotype, *P=0.0093). **(G)** 96-hour lung Sp3 burdens in DT-treated experienced Cre- and Cre+ mice (Mann-Whitney test, *P=0.0004). Square=female; circle=male for Cre+ group. One male mouse, indicated by the 'X', died shortly before lung harvest. LoD= Limit of detection.

Discussion

These studies show that mouse lungs recovered from pneumococcal infections contain BRM cells that contribute to serotype-independent anti-pneumococcal protection. In light of these results, combined with the evidence that influenza also elicits lung BRM cells (112, 139, 149) and our finding that normal human lung tissue is enriched with BRM-like cells, we propose that BRM cells are a common component of the lung adaptive immune cell repertoire.

Although we consistently observed lung B cells in small clusters near bronchovascular bundles, we did not find evidence of tertiary lymphoid tissues in these pneumococcus-recovered lungs, which lacked large lymphocyte aggregates, organized B and T cell zones, and high endothelial venules. This differs from influenza, which elicits these features in addition to lung BRM cells (139, 155). Distinct populations of lung TRM cells in influenza-recovered mouse lungs display differing tendencies to be associated with areas of iBALT (188). However, B cell studies in the context of influenza have not reported lung B cells outside of iBALT (188-190), and it is therefore unclear whether influenza-generated lung BRM cells reside exclusively in these structures. The current pneumococcus studies dissociate BRM cells from iBALT and reveal definitively that lung BRM cells can be components of histologically unremarkable lungs.

In addition to our studies of pneumococcus-experienced mice, we observed cells with a BRM phenotype in disease-free human lung tissues, which have likely been

exposed to both pneumococcus and influenza in addition to a wide variety of other respiratory pathogens. The phenotype of lung B cells observed in this study, where 50-70% of the lung B cells expressed the memory marker CD27, differs from that typically observed in blood of adult humans, where the majority of B cells are naïve (191). We conclude that the antigen-experienced lung represents a site of BRM cell accumulation across species.

We chose to give mice initial pneumococcal exposures directly in the lung, as opposed to using a colonization model. Whether the outcomes after repeat i.t. exposures in mice truly mimic the lungs of humans, who are frequently colonized and less frequently experience true pneumonia events, may be questioned. However, there is evidence that colonization alone can change BALF macrophage and T cell populations in humans, and the density of pneumococcal colonization has been shown to correlate with the amount of pneumococcal DNA found in human BALF (70, 192). These findings lead us to believe that the repeated colonization events experienced by most humans likely result in changes to the lung immune cell environment similar to those elicited by lobar exposures in mice.

Epidemiological evidence suggests that natural human exposures to pneumococcus confer serotype-independent immunity against both colonization and invasive pneumococcal disease (67, 175). The difficulties in scaling up current serotype-specific pneumococcal vaccines to cover all serotypes has led to extensive interest in understanding what immune components are required for this natural heterotypic

protection. Studies addressing this in mice have highlighted roles for lung and nasal TRM cells, remodeled alveolar macrophages, plasma antibodies, and long-lived bone marrow plasma cells (67, 177). A role for MBCs in serotype-independent immunity has not previously been investigated. The PZTD mouse model afforded us a unique opportunity to assess the effects of inducible depletion of memory marked (PD-L2+) B cells while leaving naïve B cells and pre-existing antibodies intact. Depletion of CD19+PD-L2+ B cells in pneumococcus-experienced mice led to a substantial loss of serotype-independent lung protection.

This result differs from those of a prior study in which pneumococcal colonization of mice protected against serotype-matched lung infection. In that setting, while LLPCs are crucial, MBCs are dispensable (62). These findings may reflect the particular importance of MBCs in responses to related but not identical infections. This partitioning of function has been observed for influenza and West Nile viruses, for which pre-existing antibodies protect against homologous virus rechallenge, while reactivated MBCs confer immunity against an antigenically distinct virus (149, 176). We postulate that MBCs, especially those in the lung, also play an important role in the heterotypic immune response to bacterial respiratory pathogens. This would imply that vaccines against pathogens that rapidly mutate or comprise many subtypes should be designed with a goal of eliciting B cell memory in addition to circulating antibody.

A limitation to our studies is the difficulty in distinguishing the functional contributions of BRM cells from those of other B cell subpopulations, notably LLPCs

and B1 B cells. Plasma cells have been observed within lungs recovered from viral infections (153), and although they are outside the scope of this work, it is important to consider whether such cells may have contributed to our observations. Some mature plasma cells express CD19 (193). However, the high CD38 expression on EV mouse lung CD19+IgD- B cells and lack of CD38 expression on most human lung CD19+CD27+ B cells indicates that CD19+ plasma cells were not major components recovered in uninfected collagenase digested lungs (106).

In humans, anti-CD20 depletion of B cells is a treatment for B cell malignancies. However, previous studies have noted a resistance of solid tissue B cell populations to this therapy (194), and it is possible that depletion-resistant BRM cells in the lung contribute to the fairly low rates of infection among anti-CD20-treated patients (195). A similar observation was noted in studies using Alutizimab for T cell depletion, which did not lead to the expected increases in skin infections due to the presence of protective TRM cells (196). Interestingly, there is some evidence that anti-CD20 therapy is effective against BALT lymphomas, which may imply that unlike BRM cells outside of organized lymphoid structures, lung B cells within BALT are more accessible to the circulation (197).

The COVID-19 pandemic raises new questions about lung immunology. It will be of interest to determine whether resolution of SARS-CoV-2 infection results in lung BRM cells. Relating to the evidence that lung BRM cells are essential components of immunity against heterotypic respiratory infection, it will be important to test whether

human lungs contain cross-reactive BRM cells elicited by the endemic human coronaviruses, and if so, whether those BRM cells influence the outcome of SARS-CoV-2 infection.

Many aspects of BRM cells demand further investigation, including factors leading to their recruitment and retention, mechanisms by which they provide protection, their immunoglobulin repertoire, and whether BRM cells, like TRM cells, are found across a wide range of organ systems in mice and humans. Despite these unknowns, a burgeoning body of evidence including the present study has begun to shed light on the previously unrecognized importance of BRM cells in the lung. Our findings lead to a more complete picture of the natural lung defenses that pneumococcal exposures generate and that are crucial for subsequent pneumonia protection. Defining these protective mechanisms in healthy hosts will guide studies into what aspects of this protection are lost with age or comorbidities. And as many mucosal vaccine development strategies have begun to focus on eliciting resident memory cells, this knowledge will also be crucial for future investigations into correlates of optimal mucosal immunity.

CHAPTER FOUR: THE ESTABLISHMENT OF LUNG TRM CELLS AFTER PNEUMOCOCCAL PNEUMONIA

Introduction

Often, the ultimate goal in biomedical and immunological research is the translation of basic findings into applications for human health. For example, evidence that TRM cells provide superior protection compared to circulating cells in animal models of natural infections (198-200) has led to early attempts at eliciting TRM cells with vaccination approaches. Parenteral vaccination of mice with killed pneumococci has recently been found to establish nasal CD4⁺ TRM cells that protect against pneumococcal colonization (76). Intravenous, but not intramuscular or intradermal, administration of a malaria vaccine in non-human primates generated liver CD8⁺ TRM cells that were crucial for durable sterilizing immunity (201). In many cases, this translational focus has been possible because of prior studies elucidating the signals required for TRM cell establishment, which have been carried out in a variety of organs and infection settings (202-205). The basic observation that genital HSV-2 infection-induced CXCL9 and CXCL10 are required for anti-viral CD8⁺ TRM cell recruitment has been applied to a “prime-pull” vaccination approach where parenteral vaccination is followed by topical chemokine administration. This method effectively eliminated clinical disease development in mice (206) and decreased recurrent HSV-induced disease in guinea pigs (207), highlighting its potential as a therapeutic strategy.

The kinetics of TRM cell establishment have also been characterized in various settings, providing crucial information on the optimal time after immunization to give a pull or boost to best mimic the TRM cell generation that occurs in a natural infection. In the HSV-2 studies mentioned above, appropriate timing of chemokine administration was determined by previous work demonstrating that CD4⁺ T cells are recruited to the vaginal mucosa 3-4 days post-infection, prior to CD8⁺ T cells, which enter the tissue at days 4 and 5. Interferon produced by the early recruited CD4⁺ T cells is responsible for the production of local chemokines on day 4 that subsequently drive recruitment of CD8⁺ T cells that establish tissue residency (208). In the lungs of mice following a single influenza virus infection, a rapid influx of CD4⁺ T cells protected from i.v. antibody labeling is observed as early as 3 days post-infection, and these cells peak between days 10 and 14. Contraction of this population occurs in tandem with clearance of viral antigen over a period of three weeks, at which point steady-state numbers of TRM cells are reached (169). As in the case of HSV-2, influenza-specific CD4⁺ T cells enter the lung around day 5 post-infection, a day earlier than CD8⁺ T cells, and interferon-gamma derived from lung CD4⁺ T cells is crucial for functional CD8⁺ TRM cell formation (209).

Given the newness of the BRM cell field, it is perhaps unsurprising that very little is known about the signals required for establishment of these cells in the lung or elsewhere. What we do know comes from studies in the context of murine influenza infections. The majority of lung BRM cells in this setting express the chemokine receptor CXCR3 (112, 139), which has been shown to promote CD8⁺ and CD4⁺ T cell homing to

the lung after various infections (210, 211). Establishment, but not maintenance, of influenza-specific lung BRM cells is dependent on CD40:CD40L interactions with T cells (139). Multiple groups have observed fairly consistent kinetics of lung B cell recruitment following influenza infection in mice. Initial detection of influenza-specific MBCs in the lung occurs at day 7 post-infection, followed by a peak at days 14-15 and then a steady decline over about three weeks until equilibrium numbers of lung MBCs are reached (112, 139, 148). Whether lung BRM cells outside of the context of influenza infections develop with similar kinetics may indicate if there is a conserved pattern of BRM cell establishment across infection types or if establishment dynamics are context-dependent.

As described in the previous section, one of the characteristic features of influenza infections in mice is the induction of iBALT, but to what extent influenza-specific lung BRM cells are found within iBALT is not known. These structures support persistent GC reactions within the lung beginning as early as day 10 post-infection and lasting for several weeks thereafter (139, 149, 186), and these GCs are responsible for production of influenza strain cross-reactive MBCs (149). Whether GCs within the lung are required for lung BRM cell accumulation in all infection settings has not been explored. Additionally, several distinct signaling pathways are known to be important for the recruitment of B cells into iBALT (212, 213), but it is unclear whether any of those pathways are relevant to lung BRM cells that are maintained independently of tertiary lymphoid structures.

Therefore, this study was undertaken to determine the requirements for and kinetics of lung BRM cell formation in a very different infection setting: here we studied lungs following infection with *S. pneumoniae*, which does not elicit iBALT but does generate a long-lasting and non-circulating population of MBCs within the mouse lung (Chapter 3). A better understanding of the signals and timing involved in BRM cell formation will enable future studies of tissue resident B cells to mimic the progress that has been made in the lung TRM cell field towards translational applications.

Results

CD4⁺ T cell dependence of lung BRM cell establishment

Typical MBC responses, whether of extrafollicular origin or from a GC, require the help of CD4⁺ T cells at some stage during development (86). However, quiescent antigen-specific B cells that resemble MBCs can arise from proliferating precursor cells (probably a B1 B cell subset) in T cell-independent responses to polysaccharide antigens such as the pneumococcal capsule (214). We previously showed that respiratory exposures to *S. pneumoniae* in mice generate lung BRM cells that are required for serotype-independent pneumococcal immunity (Chapter 3). The cross-reactivity of antibodies secreted by these MBCs led us to hypothesize that they were specific to pneumococcal species conserved protein antigens, as opposed to the serotype defining capsular polysaccharide. However, there are other highly conserved pneumococcal polysaccharide antigens, such as cell wall polysaccharide (215). Additionally, the expression of defining MBC markers such as PD-L2, CD73, and CD80 has not been assessed on T-independent MBCs (216), so the expression of these markers on BRM cells in pneumococcus recovered lungs does not exclude them from a T-independent origin.

We used a previously established mouse infection model in which 6-8 week old C57BL6/J mice were infected twice at a weekly interval with i.t. Sp19F, with each infection resulting in a self-limiting pneumococcal pneumonia cleared within 5 days (74, 177). This exposure model has been shown to generate lung CD4⁺ TRM cells (74) and

lung BRM cells (Chapter 3). To test whether establishment of lung BRM cells after pneumococcal exposures was dependent on CD4⁺ T cells, we administered the CD4⁺ T cell depleting antibody GK1.5 or an isotype control antibody to mice before, during, and immediately after the two exposures to i.t. Sp19 (Fig. 16A). At day 35, flow cytometry with an i.v. stain to exclude circulating leukocytes from the analysis was used to assess whether memory B and T cells accumulated in the lungs after pneumococcal exposures. As expected, total lung CD4⁺ T cells and CD4⁺ lung TRM cells (CD11a^{hi}CD69⁺), which were intact in experienced mice treated with an isotype control antibody, were nearly undetectable at day 35 in GK1.5-treated mice (Fig. 16B). GK1.5 treatment during memory establishment also significantly reduced lung BRM cells (EV CD19⁺CD69⁺ cells) in proportion and number to levels seen in naïve mice at day 35 (Fig. 16C). These findings definitively show that lung BRM cells generated by pneumococcal pneumonia in mice are T cell-dependent and therefore likely specific to a pneumococcal protein antigen.

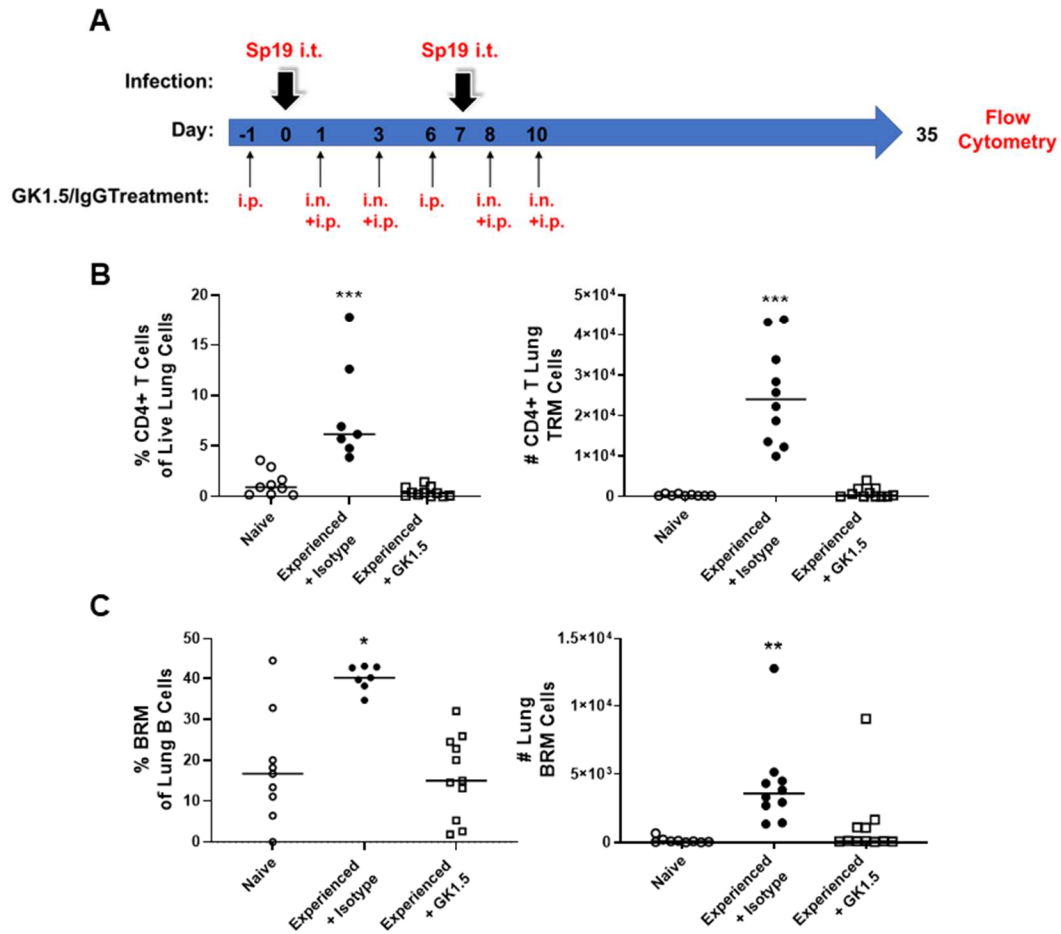


Figure 16. Lung BRM cell establishment requires the presence of CD4+ T cells during initial infections. (A) Prior to, during, and after initial Sp19 exposures, mice were treated i.p. or i.n./i.p. as indicated with the CD4+ T cell depleting antibody GK1.5 or with an isotype control antibody. Lung cell populations were assessed four weeks after the second Sp19 infection. (B) The percent (left) and number (right) of EV CD4+ T cells in lungs of naïve mice and experienced mice treated with GK1.5 or an isotype control antibody as described in (A). (C) The percent (left) and number (right) of EV CD19+CD69+ cells in lungs of naïve mice and experienced mice treated with GK1.5 or an isotype control antibody as described in (A). Comparisons all made by one-way ANOVA; *P<0.05, **P<0.01, ***P<0.001.

Kinetics of lung BRM cell recruitment after multiple pneumococcal exposures

We previously showed that initial pneumococcal infection protects mice from a subsequent serotype-mismatched challenge with an otherwise lethal strain (74). However,

one pneumococcal exposure with 1×10^6 CFU of Sp19F was not enough to provide this protection; at least two exposures at a one week interval were required. Because we had also shown that lung PD-L2+ MBCs are needed for serotype-independent lung protection (Chapter 3), we wondered whether multiple pneumococcal exposures are necessary to establish a lung B cell population. When we compared the lung B cell populations of mice given either one or two i.t. Sp19 exposures four weeks previously, we observed a statistically significant increase in total lung B2 cells and in lung BRM cells (EV CD19+CD69+) only in mice that received two prior infections (Fig. 17A-B). This observation confirmed that at least two exposures to Sp19 are required to establish a substantial lung BRM cell pool.

To gain a more thorough understanding of the kinetics of lung BRM cell establishment in our model, lungs of mice were analyzed via flow cytometry at various time points following one (Fig. 17C, “1x Sp19 group”) or two (Fig. 17D, “2x Sp19 group”) Sp19 infections. A large influx of B2 B cells was observed as early as day 1 and peaked at day 3 after the initial Sp19 infection. In 1x Sp19 mice, these infiltrated B cells began to wane in number between days 3 and 7, and by day 10 returned nearly to baseline levels (Fig. 17C). In contrast, the second Sp19 infection generated another influx of B cells into the lung, which again peaked three days later but was over twice as large in magnitude as the influx generated by the first infection. As the inflammation resolved, the number of lung B cells dropped precipitously through day 35 but then stabilized, with around 10,000 EV B cells maintained for at least 6-8 weeks (Fig. 17D). This pattern was mirrored in the kinetics of CD69+ lung B cells (Fig. 17E). Each Sp19 exposure led to an

increase in the proportion of B cells in the lung expressing CD69, which is probably a marker of activation within the first three days of infection (217). However, at time points after two infections where CD69 is more likely to represent a marker of residence, the proportion of CD69⁺ B cells remained significantly higher than at corresponding time points after one infection. These data show that the second Sp19 infection results in a larger initial B cell influx and a residual resident B cell population not elicited by a single exposure to Sp19.

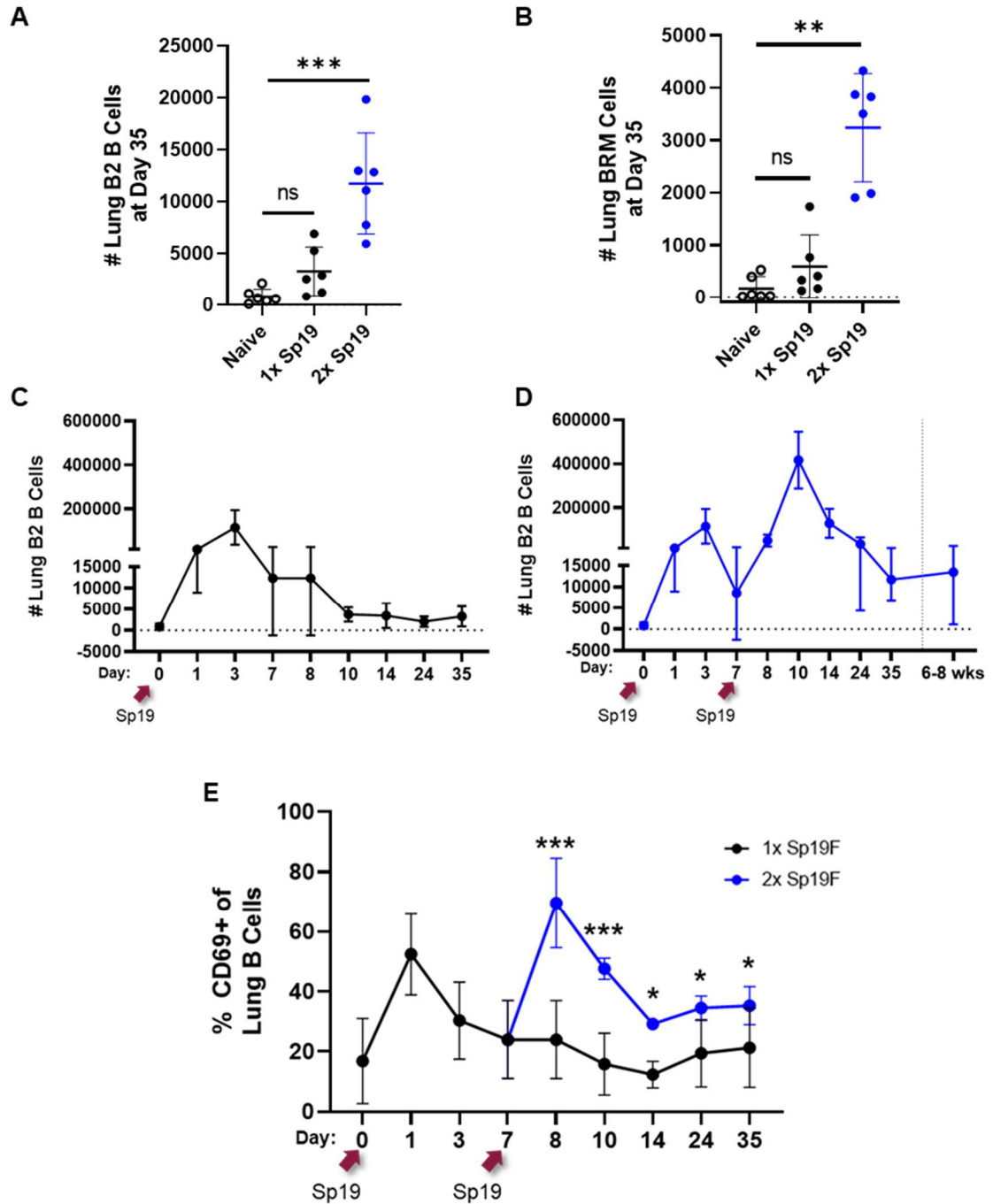


Figure 17. Two pneumococcal infections are required to generate a robust lung BRM cell population. (A-B) The number of total EV lung B2 cells (A) and EV lung CD69+ B2 cells (B) after one or two Sp19 infections four weeks prior (one-way ANOVA; ** $P < 0.01$, *** $P < 0.0001$). (C-D) The number of total EV lung B2 B cells at the indicated time points following one (C) or two (D) Sp19 infections. (E) The percent of EV lung B cells that are CD69+ at indicated time points following one (black curve) or

two (blue curve) Sp19 infections (comparisons between the 1x and 2x curves at each time point made via multiple t-tests; * $P < 0.05$, *** $P < 0.001$).

Timing and requirements for lung class-switched MBC expansion

Using the same experimental design as in Fig. 17, we also analyzed class-switched and memory marked EV lung B cells after one or two Sp19 infections. Each infection resulted in a transient increase in naïve (IgD+IgM+) B cells (Fig. 18A). In 1x Sp19 mice, the distribution of naïve, IgM+, and class-switched B cells returned to approximately baseline proportions 8 to 10 days later (Fig. 18A, top row). Interestingly, after the influx of naïve B cells generated by the second Sp19 infection, an increase in class-switched B cells in the lung was observed at day 14 (7 days after the second infection), and this increase was maintained through day 35 (Fig. 18A, bottom row). The proportion of class-switched B cells was significantly higher in the 2x Sp19 group than in the 1x Sp19 group at days 14, 24, and 35, and while the lungs of mice in the 2x group contained significantly more class-switched B cells than naïve lungs, lungs of mice after only one Sp19 infection did not (Fig. 18B).

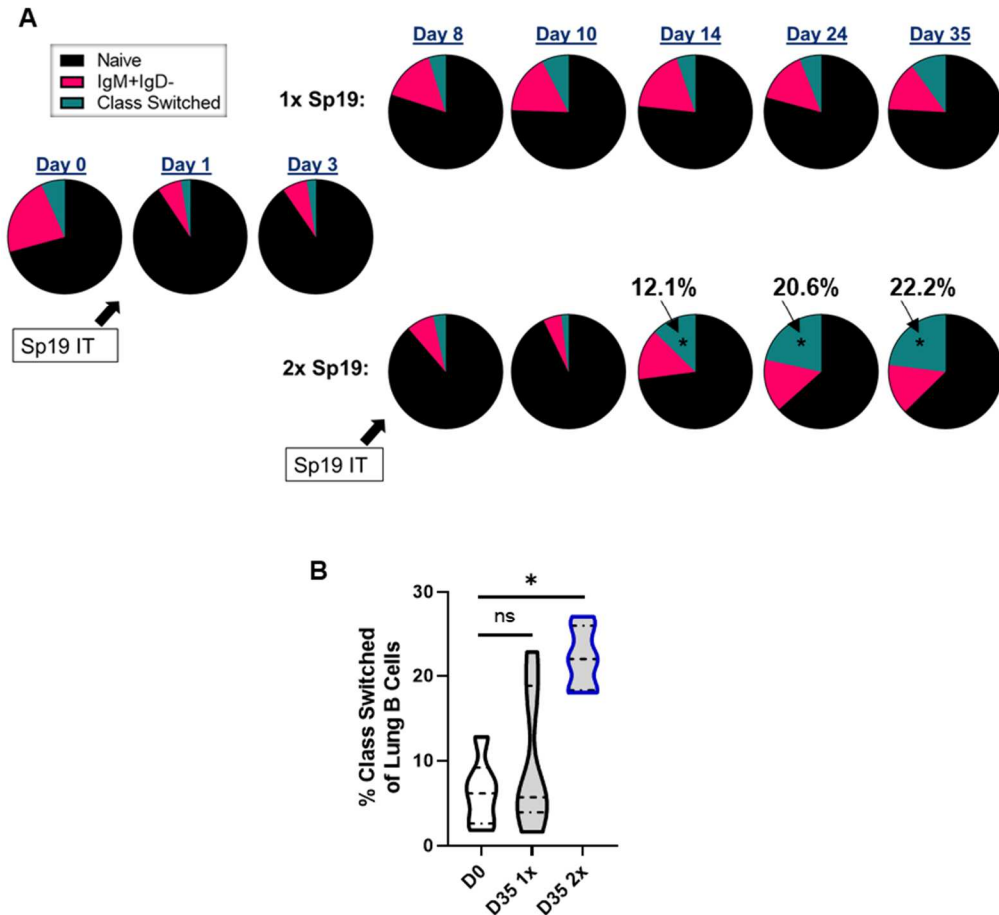


Figure 18. The proportion of class-switched lung MBCs expands one week after a second Sp19 infection. (A) The proportions of EV lung B cells that are naïve (black), IgM+IgD- (pink), or class-switched (blue) at the indicated time points after one or two Sp19 infections. Each pie slice represents the average from 6 mice at that time point, except on the graphs for day 10, where each represents the average from 3 mice (comparisons between the 1x and 2x groups at each time point from day 8 onward made via multiple t-tests; * $P < 0.05$). **(B)** The percent of EV lung B cells that are class-switched four weeks after one or two Sp19 infections (one-way ANOVA; * $P < 0.05$). ns, not significant.

In looking at the distribution of memory markers on lung B cells over time, we first looked only at 2x Sp19 mice and divided EV lung B cells into three populations. The first population consisted of all naïve (IgD+) B cells, which, as mentioned above, increased in proportion after each infection and then declined from day 10 onward (Fig.

19A). No time point significantly differed in naïve B cell content in the lung compared to baseline, likely due to the wide spread in the naïve B cell proportions in uninfected mouse lungs. The second population, termed double negative (DN) MBCs, consisted of IgD⁻ B cells that expressed CD38, and can therefore be classified as MBCs (106), but did not express either of the memory markers PD-L2 or CD73. As explained in the preceding sections, PD-L2 and CD73 are two markers of mouse MBCs that are co-expressed on B cells that tend to be class-switched and contain more BCR mutations (97). The DN MBCs did not appreciably change in proportion over the time course of the study (Fig. 19B), though there was again a wide spread in how frequent this population was in naïve lungs. The third population, double positive (DP) MBCs, were IgD⁻CD38⁺PD-L2⁺CD73⁺ B cells. Between 3 and 7 days after the second infection, this population significantly increased in the lung, indicating the MBC pool was likely becoming progressively more mutated and class-switched (Fig. 19C). The latter was confirmed by the observation that the proportion of DP MBCs that were IgM⁺ decreased significantly from day 8 to days 14-35 (Fig. 19D). Interestingly, one Sp19 exposure also elicited a small but significant increase in DP lung MBCs between 3 and 7 days post-infection (Fig. 19E). After this brief rise in number, the population stabilized right away, without the continued increase seen in the 2x Sp19 group. This increase in DP MBCs in the 1x group lungs did not appear to correlate with the expected increase in class-switched lung MBCs, as the percent IgM⁺ DP MBCs did not decrease between day 3 and day 35 (Fig. 19F).

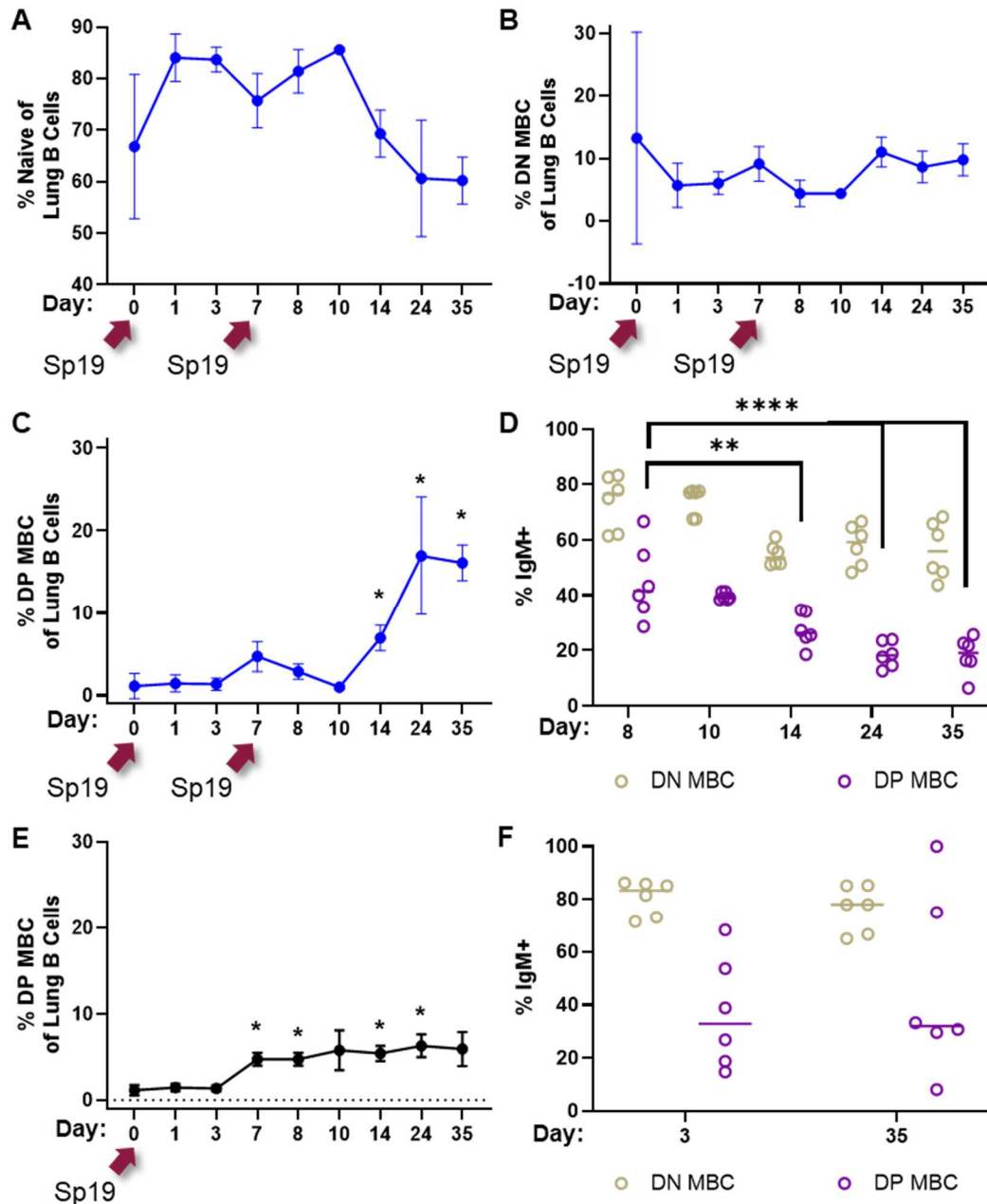


Figure 19. MBCs bearing multiple memory markers accumulate in the lungs starting one week after a second Sp19 infection. (A-C) The proportion of EV lung B cells that are naïve (A), DN MBCs (IgD-CD38+PD-L2-CD73-) (B), or DP MBCs (IgD-CD38+PD-L2+CD73+) (C) at indicated time points following two Sp19 infections (one-way ANOVA comparing each time point to the day 0 baseline group; * $P < 0.05$). (D) The proportion of DN MBCs (gray) and DP MBCs (purple) that are IgM+ at the indicated time points following two Sp19 infections (two-way ANOVA; ** $P < 0.01$, **** $P < 0.0001$). (E) The proportion of EV lung B cells that are DP MBCs at indicated time points following one Sp19 infection (one-way ANOVA comparing each time point

to the day 0 baseline group; *P<0.05). **(F)** The proportion of DN MBCs (gray) and DP MBCs (purple) that are IgM+ at the indicated time points following one Sp19 infection. DN, double negative; DP, double positive.

The preceding data showing that a second Sp19 infection results in a larger and more rapid accumulation of class-switched and likely mutated MBCs within the lung after day 10 led us to wonder whether there might be lung-localized GC reactions in the 2x Sp19 group. We examined lungs of 1x and 2x Sp19 mice at various time points for B cells bearing either a “pre-GC” phenotype (GL7+CD38^{hi}) (89, 218) or a GC B cell phenotype (GL7+CD38^{lo}) (Fig. 20A). In 1x mice, a very small number of pre-GC and GC B cells were observed in the lungs at day 3 (around 50 GC B cells in a whole lung on average). GC B cells in 1x lungs peaked at day 7 (around 450 GC B cells in a whole lung) but were not maintained through day 35 (Fig. 20C-D, black points). In contrast, a second Sp19 infection led to a significant accumulation of pre-GC (Fig. 20B) and GC (Fig. 20C) B cells in the lung, peaking at day 10 for pre-GC B cells and day 14 for GC B cells (around 5,000 GC B cells per lung). Although the number of GC B cells steeply declined after day 14, at day 35 a few hundred remained in the lungs of 2x Sp19 mice, while 1x Sp19 lungs contained essentially none (Fig. 20D-F). Because GC B cells are known to lack many homing receptors that allow for recirculation and mucosal migration (219, 220), it is likely these GC B cells are indicative of ongoing local GC reactions in the lungs, as opposed to being a recruited population from SLO GCs. Therefore, these data indicate that between 3 and 17 days after the second Sp19 infection, lungs of 2x mice contain fairly abundant GCs that largely contract by day 24 but persist at low levels

for weeks after the resolution of local inflammation. Notably, GL7+CD38^{hi} pre-GC phenotype B cells in 2x Sp19 lungs at days 10 and 14 vastly outnumber GC B cells at any point (Fig. 20 B-C). This GL7+CD38^{hi} phenotype has been shown to mark precursor B cells that can enter a GC and typically become class-switched MBCs, however, these cells also have the potential to directly differentiate into IgM+ or class-switched MBCs independently of a GC reaction (89). This GL7+CD38^{hi} population may therefore contribute to both GC B cells and GC-independent lung MBCs, a hypothesis that will require further testing.

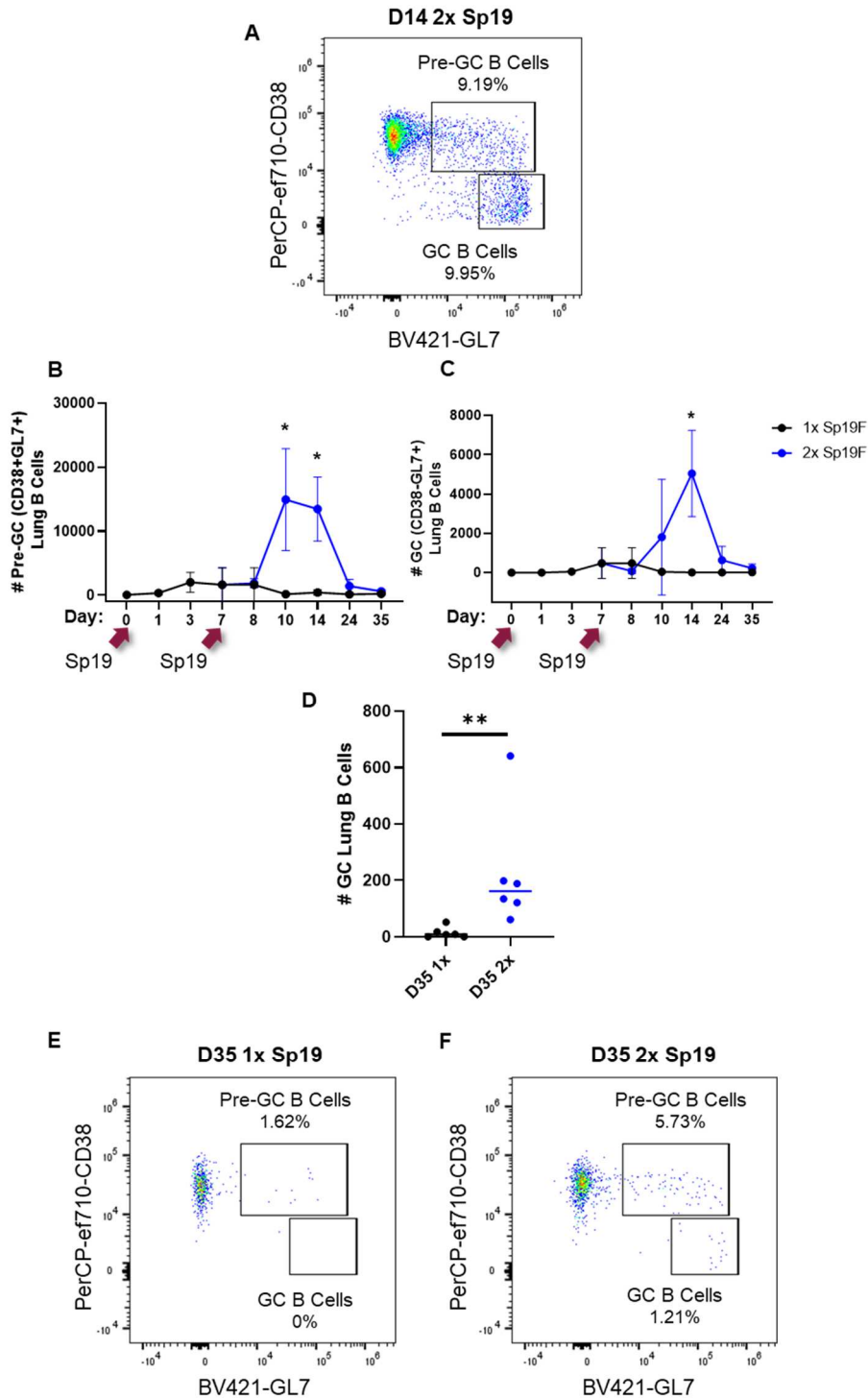


Figure 20. Pre-GC and GC B cells are observed in mouse lungs following two Sp19 infections. (A) Representative flow cytometry plot showing the gating of pre-GC B cells (EV CD19+CD38+GL7+) and GC B cells (EV CD19+CD38-GL7+) in the lung of a mouse one week following a second Sp19 infection. (B-C) The numbers of pre-GC B

cells **(B)** and GC B cells **(C)** in lungs of mice at the indicated time points following one or two Sp19 infections (comparisons between the 1x and 2x groups at each time point from day 8 onward made via multiple t-tests; * $P < 0.05$). **(D)** The number of lung GC B cells at day 35 following one or two Sp19 infections (Mann-Whitney test; ** $P < 0.01$). **(E-F)** Representative flow cytometry plots showing gating of pre-GC B cells and GC B cells in lungs of mice four weeks following one **(E)** or two **(F)** Sp19 infections.

The window between days 10 and 14 (3 and 7 days after the second infection, respectively) in the above experiments seemed to be a period of importance for the development of B cell memory in the lung. In this window, the percentage of lung B cells expressing CD69 reaches its final value, the initial accumulation of class-switched and DP MBCs in the lung is observed, and lung GC B cells reach their peak numbers. Two possible scenarios that might explain these findings are: 1) the initial Sp19 infection seeds a small number of B cells in the lung that, upon second infection, undergo a proliferative burst and form local GCs that lead to rapid class-switched and DP MBC accumulation locally, or 2) the initial Sp19 infection primes the lung in some way to enhance recruitment or retention of B cells such that after the second infection, more MBCs formed in SLOs enter the lung and stay and/or more naïve B cells are recruited to join lung GC reactions and contribute to local MBC generation. To try and distinguish between these possibilities, we treated mice recovered from an initial Sp19 infection with FTY720, an inhibitor of lymphocyte exit from SLOs and tissues (221), before, during, and after the second Sp19 infection (Fig. 21A). This protocol allows normal establishment of lung cells elicited by the first infection, but recruitment of new cells upon the second Sp19 exposure is prevented in FTY720-treated mice. In this experiment, days 13 and 17 corresponded to days 10 and 14, respectively, in the previous kinetic experiments. As expected, FTY720 treatment

resulted in a large reduction in circulating B cells at either 3 or 7 days after the second Sp19 infection (Fig. 21B). In vehicle-treated mice, an increase in non-naïve and CD69+ B cells between days 3 and 7 post-second Sp19 was seen, consistent with results from the kinetic studies in Fig. 19 (Fig. 21 C-D, black dots). However, treatment with FTY720 abrogated these increases; while vehicle and FTY720-treated mice had similar naïve and IgD-CD69+ B cell populations in the lungs three days after the second Sp19 infection, four days later neither a decrease in naïve nor an increase in IgD-CD69+ B cells in the lungs was observed in the FTY720-treated group (Fig. 21C-D, blue dots). The induction of local GCs between 3 and 7 days after the second infection was also not seen in FTY720-treated mice based on GC B cell percent and number (Fig. 21E-F). Together, these data indicate that cells established in the lung by the first Sp19 infection are not sufficient to drive the phenotypic changes in the lung B cell repertoire associated with BRM cell development upon a second pneumococcal infection.

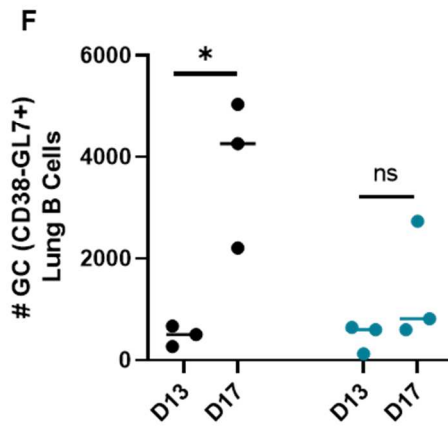
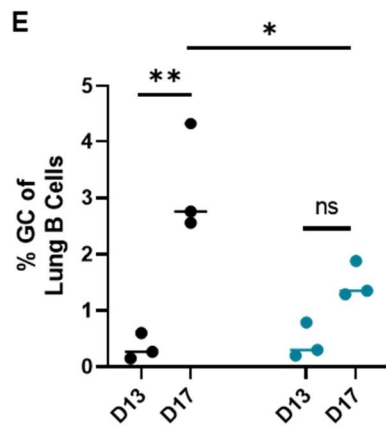
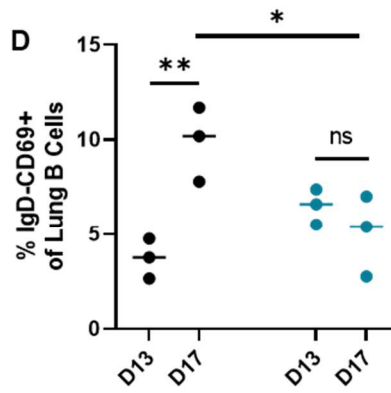
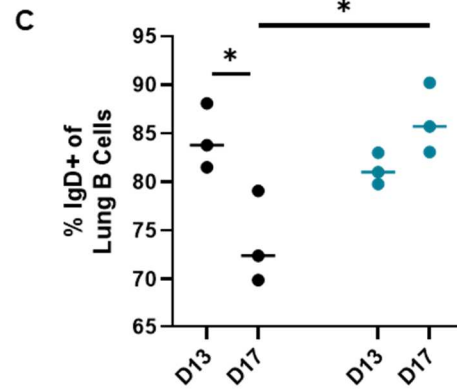
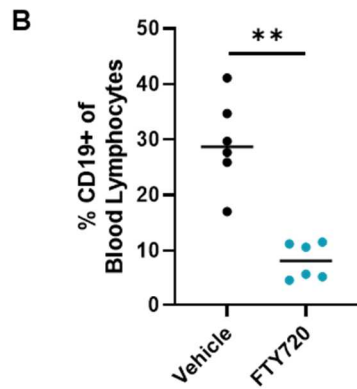
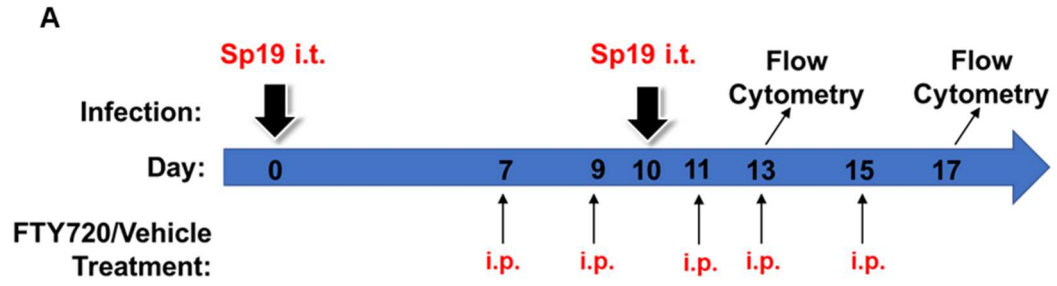


Figure 21. Continued influx of immune cells into the lung during and after the second Sp19 infection is required to generate lung GC reactions and class-switching. (A) Prior to, during, and after a second Sp19 infection, mice were treated with i.p. FTY720 or with vehicle alone. Lung cell populations were assessed three (day 13) and seven (day 17) days following the second Sp19 infection. (B) The percent of CD19+ lymphocytes in the blood of vehicle or FTY720-treated mice. Data from day 13 and day 17 shown together (Mann-Whitney test, **P<0.01). (C-E) The percent IgD+ (C), percent IgD-CD69+ (D), and percent GC B cells (E) among EV lung B cells in vehicle- (black) or FTY720- (blue) treated mice at day 13 and day 17 (two-way ANOVA; *P<0.05). (F) The number of GC lung B cells in vehicle- (black) or FTY720- (blue) treated mice at day 13 and day 17 (two-way ANOVA; *P<0.05). ns, not significant.

CXCL13 correlation with lung BRM cell recruitment

The FTY720 experiment data suggested to us that recruitment of B cells from SLOs after the second Sp19 infection played a crucial role in generating a robust lung BRM cell compartment. Therefore, we next wanted to explore what chemokine signals may be playing a role in this recruitment. Most prior studies of mechanisms by which B cells are recruited to the lungs have been in settings of iBALT.

After influenza infection in mice, induction of IL-1 or type 1 interferon can induce stromal cell production of CXCL13, which is crucial for the recruitment of naïve, CXCR5+ B cells to form lung GC reactions and establish iBALT (212, 222). This recruitment pathway occurs independently of CXCL12, chemokine (C-C Motif) ligand 19 (CCL19), CCL21, and TFH cells, and is not required for maintenance of lung GC, only establishment. In the context of sterile lung inflammation or mucosally delivered tuberculosis antigen plus adjuvant, IL-17 produced by CD4+ T cells is required to induce CXCL13 expression in the lung and establish iBALT (223, 224). Again, this IL-17 signal was required only for iBALT formation, not maintenance. A similar CXCL13-dependent

pathway of iBALT formation occurs in mice infected i.n. with a modified vaccinia virus (213). This CXCL13-dependent iBALT contains FDCs, indicating it is well-organized and mature. In contrast, lung infection of mice with *Pseudomonas aeruginosa* elicits IL-17 production from gamma-delta T cells in the lung, which leads to stromal cell-derived CXCL12 production (213). In this study, CXCL12 (and not CXCL13) was required for formation of iBALT that does not contain FDCs, and the authors propose that different pathogens lead to iBALT with varying levels of organization and varying chemokine requirements for formation.

Although we have previously shown that there are not iBALT structures in 2x pneumococcus-experienced lungs at day 35 (Chapter 3), we hypothesized that some of the same mechanisms known to be important for B cell recruitment into iBALT might also be at play in the establishment phase for BRM cells in our model. Since mechanisms of lung B cell recruitment appear to vary by type of pathogen, we set out to determine the initial signals that may be responsible for bringing B cells into the lung after pneumococcal exposures in mice.

Because the published pathways of iBALT formation rely on either CXCL13 or CXCL12, we wanted to determine whether expression of either of these chemokines was induced in lungs of mice after pneumococcal infections. Whole lung homogenates of mice were analyzed by ELISA at various time points after one or two Sp19 infections. One to 3 days after a second Sp19 infection, significantly higher levels of CXCL13 protein were observed in lung homogenates compared to baseline levels at day 0 (Fig. 22A). A small peak in CXCL13 was observed 1 day after the first Sp19 infection, but this

increase was not statistically significant and was neither as large nor as protracted as the increase induced by the second Sp19 infection one week later. In contrast to CXCL13, CXCL12 protein levels in lung homogenate did not statistically vary from baseline after one or two Sp19 infections (Fig. 22B). An important caveat in the interpretation of these results is that ELISA analysis of bulk lung homogenates does not allow for assessment of the micro-localization of these chemokines within the lung, which may be as important as total chemokine production. Follow-up studies should use microscopy to assess chemokines in the context of the lung architecture to validate these findings. However, we generally took these data to indicate that CXCL13 may play an important role in the enhanced recruitment of B cells to the lung that occurs after a second Sp19 infection. We then assessed expression of the CXCL13 receptor, CXCR5, on EV B cells in the lung at various time points and saw that both one and two Sp19 infections resulted in significant increases in CXCR5+ B cells within the lungs 1 and 2 days post-infection (Fig. 22C). However, the influx that occurred following the second infection was three times as large in magnitude and was longer lasting, with a significant increase in CXCR5+ B cells over baseline observed at one week after the second, but not the first, Sp19 exposure. The fact that CXCL13 protein presence in the lung preceded a significant influx of CXCR5+ B cells in the lung EV tissue is compelling evidence that, as in many other settings of lung infection, CXCL13 plays an important role in B cell recruitment to the lung after pneumococcal infections as well. The enhanced production of this chemokine after a second Sp19 infection suggests that remodeling of a CXCL13-producing cell population in the lung occurs following the first Sp19 exposure and enables increased production

upon reinfection. The cell types and upstream signals involved in CXCL13 production and the importance of this signaling axis for establishment of various BRM cell subsets remains to be determined.

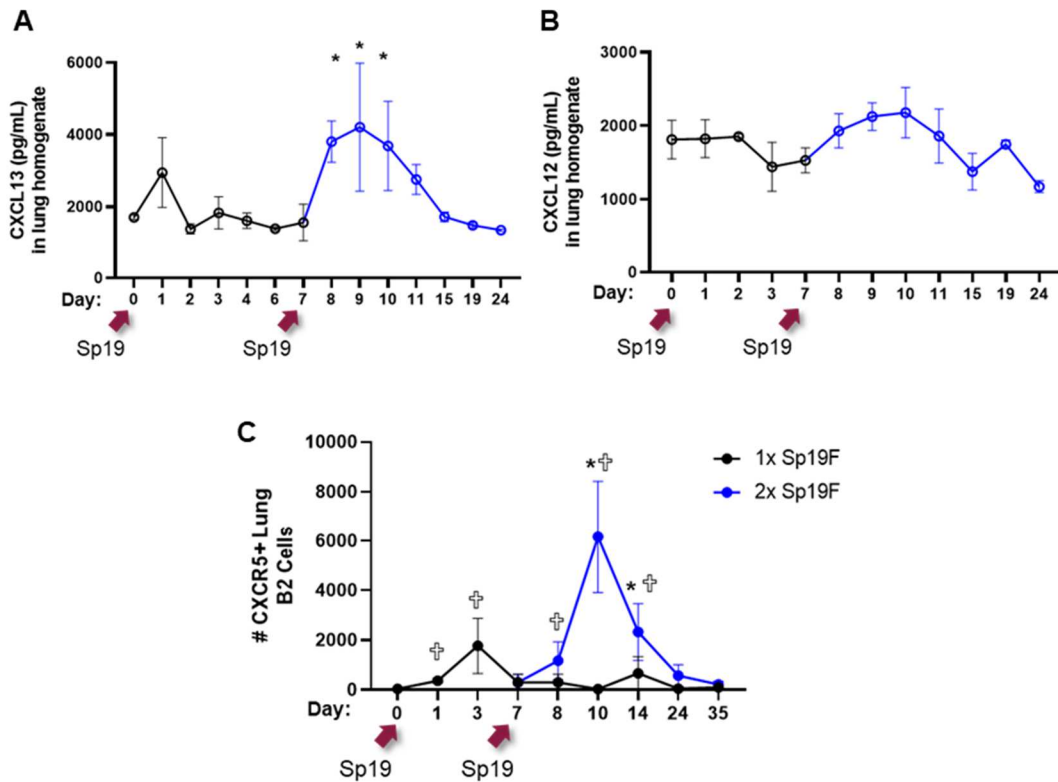


Figure 22. Lung CXCL13 levels and CXCR5+ B cells are elevated following a second Sp19 infection. (A-B) CXCL13 (A) and CXCL12 (B) protein as detected by ELISA in whole lung homogenates of mice collected at the indicated time points following one (black curve) or two (blue curve) Sp19 infections (one-way ANOVA comparing each time point to the day 0 baseline group; * $P < 0.05$). (C) The number of EV CD19+CXCR5+ B2 cells in lungs of mice at the indicated time points following one (black curve) or two (blue curve) Sp19 infections (crosses indicate significant results ($P < 0.05$) for a one-way ANOVA comparing each time point to the day 0 baseline group. Stars indicate significant results ($P < 0.05$) for multiple t-tests comparing matched time points for the 1x and 2x curves).

Discussion

The research described in this chapter is ongoing, but results obtained so far provide insight on the signals required for establishment of MBCs in the lung after pneumococcal pneumonia. We have shown that lung BRM cells are T cell-dependent and thus likely specific to a pneumococcal protein antigen as opposed to a species conserved polysaccharide. Furthermore, two Sp19 infections are necessary for the establishment of a lung BRM cell pool, while one is not sufficient. The second Sp19 infection drives an increase in class-switched and PD-L2+CD73+ MBCs within the lung, which, based on prior literature, are likely to contain affinity matured BCRs and secrete antibody upon reactivation (97). These phenotypes may result from the lung-localized GC reactions that occur around a week after the second Sp19 infection. Whatever lymphocytes are established within the lung by the initial pneumococcal exposure are not sufficient to proliferate and form a BRM cell pool locally upon second infection, since FTY720 treatment after the first Sp19 infection abrogates the increase in non-naïve B cells, CD69+ B cells, and GC B cells that normally occurs between 3 and 7 days post-second infection. This finding highlights the importance of B cell recruitment during the second Sp19 infection, which may be largely mediated by CXCL13, since this chemokine is induced within the lung at higher levels following a second Sp19 infection compared to the first, and its expression precedes an influx of CXCR5+ B cells into the lung 1-2 days later.

As mentioned above, GL7+CD38^{hi} “pre-GC” phenotype B cells can either enter a GC reaction or differentiate directly into MBCs (89). Although confirmatory experiments

must be done to test the following hypotheses, it is tempting to speculate that the relatively large number of GL7+CD38^{hi} cells at days 10 and 14 compared to the much lower number of GC B cells at day 14 indicates that only a small number of pre-GC B cells receive the appropriate signals in the lung to enter a GC reaction, and many or possibly most of the pre-GC B cells instead become extrafollicular MBCs. This would perhaps account for the large proportion of lung MBCs that are IgM⁺ (Chapter 3), since extrafollicular MBCs are often, though not always, unswitched (119). This theory may also help explain the slow accumulation of class-switched MBCs after day 14 (Figs 18A and 19D); GCs in the lung that develop at day 14 may output MBCs that are predominantly class-switched by days 24 and 35. It is also worth noting that the number of CXCR5⁺ B cells recruited at day 10 approximates the number of GC B cells in the lung 4 days later. Given that the CXCL13/CXCR5 axis is known to be important for promoting recruitment of GC-bound B cells to the lung after influenza (212), the possibility that this small subset of CXCR5⁺ B cells is responsible for seeding the lung GCs should be explored. This idea would also align with the data showing that preventing B cell recruitment to the lung during the second infection with FTY720 abrogates lung GC formation a week later. Testing whether these data-driven suggestions hold true with further experimentation is required to conclude the studies presented here.

Many of the results described here for BRM cells elicited by pneumococcus have also been explored in the context of influenza-specific lung BRM cells. Establishment of BRM cells after influenza infection in mice also depends on T cell interactions (specifically CD40:CD40L interactions) (139). The kinetics of B cell establishment in the

lung are also comparable after influenza and pneumococcal infections, with the caveat that influenza studies have described the kinetics for antigen-specific B cells, which we have not yet done. After an initial early B cell influx post-infection, lung B cells appear to take around 3 weeks to reach an equilibrium in both models (112, 139, 149).

Additionally, CXCL13, which is known to be important for lung B cell recruitment early after influenza infections, also seems to correlate with recruitment of a subset of B cells to the lung in response to pneumococcal pneumonia. Whether CXCL13 in our model acts downstream of IL-17, as observed in other non-influenza settings (223), will be important to test given the known importance of IL-17 in anti-pneumococcal lung immunity (178). Other potentially important chemokine signaling axes should be investigated in our model, including CXCR3 and its ligands, as this receptor is commonly expressed on lung MBCs (112, 139).

One obvious difference between previously described infections that elicit lung B cells and our model is the requirement for two infections to generate lung BRM cells after pneumococcal exposure. Our data indicate that a more robust CXCL13 response upon the second pneumococcal infection compared to the first may be part of the reason the first infection is not sufficient. This idea warrants a study of what cells in the lung are remodeled by the initial pneumococcal exposure to produce more CXCL13 on reinfection. An additional factor behind the two infection requirement may involve the presence of antigen during a critical time frame: for CD4⁺ T cells to transition to memory, encounter with cognate antigen is required around 7 days after initial antigen exposure and priming (225). It may be that because the initial Sp19 infection is cleared

between days 3 and 5 post-infection (177), effector CD4⁺ T cells do not encounter enough presented cognate antigen to receive survival signals and transition to memory unless the second Sp19 infection is given. Although B cells do not follow an analogous effector to memory transition, they do require T cell help and perhaps cannot survive in the lung unless there are sufficient surviving T cells there to provide it. Experiments to determine whether there is a critical window in which the second Sp19 infection must be given to generate elevated CXCL13 and/or resident memory lymphocytes would further our understanding of the two infection requirement.

A parallel idea that may explain the need for two infections in our model is that the severity of an infection is tied to the magnitude of the response seen in the lung. Evidence for this comes from a study that showed that infecting mice with a lower dose of influenza virus or using a less virulent strain leads to drastically lower lung GC responses (226). This has been confirmed in other studies; while infecting mice with the highly virulent PR8 strain of influenza results in around 30,000 GC B cells in the lung at peak (139), the less virulent X31 strain generates a peak of only around 1,000 GC B cells (149). The Sp19 infection given in our studies is a self-limiting infection that is fairly low virulence in mice. It may be that the lung resident lymphocyte responses to such a mild infection are minimal, but enough remodeling occurs that upon a second infection, the immune system is able to respond more vigorously to what it now perceives as a repetitive threat.

One other area in which the pneumococcal and influenza models differ is in the generation of iBALT, which is seen only after influenza, and in the extent of long-lasting

lung GC reactions following infection resolution. In one influenza study, for example, at day 45 post-infection, the lungs of mice still contained around 20,000 GC B cells (139). This is over 100 times more than the number of GC B cells seen in our 2x pneumococcus recovered lungs at the 35 day time point. Given that iBALT structures readily support ongoing GC reactions, it will be interesting to determine whether there are more organized lymphocytic infiltrates in the lung one week after a second Sp19 infection. What is perhaps surprising is that the iBALT-free pneumococcus recovered mouse lungs continue to contain GC B cells at all at day 35. GCs are typically thought of as well-defined microanatomical structures involving B cells, TFH cells, and FDCs. Although we have not yet formally looked for the latter two specialized cell types, CD4⁺ T cells are relatively rare within the loose B cell clusters in the lungs of pneumococcus-experienced mice at day 35 (Chapter 3). It will be interesting to determine whether the persistent lung GC B cells specifically localize near the CD4⁺ T cells within B cell clusters and whether FDCs acting as reservoirs for continued antigen presentation can also be found nearby.

The results presented here provide initial knowledge on the cells and signals required for lung BRM cell establishment after resolution of pneumococcal pneumonia in mice. A thorough understanding of the mechanism of BRM cell establishment will be crucial to optimize vaccine-elicited resident memory within the lung. This is especially true in settings free of lung tertiary lymphoid organs such as the one presented here, as these structures are atypical in adult human lungs (157).

CHAPTER FIVE: DISCUSSION

An integrated model of serotype-independent anti-pneumococcal immunity in mice

In the studies presented here, we explored the phenotypes, establishment, and importance of lung MBC populations elicited by respiratory exposures to *Streptococcus pneumoniae* in mice. A focus of Chapter 3 was how these lung MBCs contribute to serotype-independent protection against pneumococcal pneumonia. These findings can now be integrated with previous work from our lab and others to describe a more complete model of the serotype-independent immune response that occurs in experienced mice upon Sp3 challenge (Fig. 23).

Initial Sp19 pneumococcal exposures seed the lung with CD4⁺ TRM cells that can respond to mismatched pneumococcal serotypes and are crucial for controlling bacterial growth during the first 24 hours of an Sp3 challenge infection (74). The CD4⁺ TRM cells mediate this immunity through secretion of IL-17A upon reactivation, which stabilizes CXCL5 transcripts in lung epithelial cells. This allows for enhanced CXCL5 secretion, driving faster neutrophil recruitment in experienced mouse lungs compared to lungs of naïve mice, which lack this signaling axis (178). The early time points between 0 and 24 hours post-Sp3 are when peak cellular infiltration, vascular permeability, and airspace edema occur in the experienced lung (74). The increased access of blood components to the lung during this phase may mean that the pre-existing serotype cross-reactive circulating antibodies elicited by the Sp19 infections are able to enter the lung

tissue. These antibodies are predominantly of IgG isotypes, and therefore may be able to access the airspace via the neonatal Fc receptor, which is expressed on lung epithelial cells and is crucial for luminal transport of IgG (227).

Multiple lines of evidence suggest that these pre-existing anti-pneumococcal antibodies play a role in protection against Sp3 challenge but are not sufficient to mediate bacterial clearance. First, right lobes of experienced mice, which did not receive the initial Sp19 exposures and do not contain resident T or B cells, are still better protected from an i.n. Sp3 lung challenge than right lobes of naïve mice (74, 177). This finding indicates that some level of systemic immunity, most likely conferred by anti-pneumococcal antibodies, contributes to protection throughout the whole lung. However, experienced left lobes are even better protected from the i.n. Sp3 challenge than the experienced right lobes are, which shows that additional contributions from lung-localized immune components are required for optimal anti-Sp3 immunity. Additionally, plasma of experienced, but not naïve, mice is able to opsonize Sp3 and prevent bacterial growth within 24 hours when pre-opsonized Sp3 is instilled into naïve recipient lungs. However, this pre-opsonization is not sufficient to mediate the bacterial clearance observed in immune competent experienced mice at 24 hours, again highlighting that plasma antibodies alone are not sufficient for full anti-Sp3 protection. A final piece of evidence comes from the fact that experienced mice depleted of lung MBCs while leaving pre-existing antibodies and TRM cells intact are better protected from Sp3 challenge than μ MT mice, which also have TRM cells but lack lung MBCs, circulating

MBCs (which play no role in 24 hour protection against Sp3), and pre-existing antibodies.

As just mentioned, depletion of PD-L2+ lung MBCs from experienced mice renders them highly susceptible to Sp3 lung infection at 96 hours post-infection. This phenotype is observed despite TRM cells and pre-formed antibodies remaining intact in these mice. Although the mechanisms behind this loss of immunity are still under investigation, the timing is consistent with local reactivation of lung BRM cells into ASCs being required for full clearance of Sp3, which occurs in experienced mice between 48 and 96 hours post-infection. The lung BRM cells comprise a mix of IgM, IgG, and IgA isotypes, and are located within the lung parenchyma. Therefore, secreted antibodies would likely need to be transported into the airspace lumen to play a role in immunity against pneumococci there. As previously described, for secreted IgG this could be mediated by the neonatal Fc receptor on lung epithelial cells. If the reactivated IgM+ and IgA+ MBCs produce the polymeric forms of these respective antibodies, they could then be transported to the airspace lumen via the polymeric immunoglobulin receptor (pIgR). Notably, pIgR upregulation on lung epithelial cells can be mediated by CD4+ Th17 responses (228); this interesting potential connection between the lung T and B resident memory cells in our model deserves further investigation.

Interestingly, work from another group shows that nasopharyngeal exposure to pneumococcal serotype 4 generated serotype cross-reactive antibodies, and i.p. transfer of these antibodies to naïve mice conferred 70-80% protection against subsequent i.t. infection with 10^7 Sp19 (a normally lethal dose) (62). Comparing this result with our own

indicates that mechanisms of serotype-independent protection may differ depending on serotype. Sp19 has a fairly thin capsule, while the Sp3 challenge serotype used in our model has a very thick, mucoid capsule that is likely very effective at preventing antibodies from easily accessing subcapsular antigens. This may mean that for Sp3, a higher antibody titer is required for effective clearance, and MBC reactivation is required to provide those additional antibodies.

Many aspects of this model require further experimentation to confirm or expand upon. For example, a role for LLPCs within the lung has not yet been explored at all. Additionally, whether or not a subset of the lung BRM cell pool re-enters GC reactions either locally or in the lung draining lymph nodes upon reactivation is unknown, although these fates are certainly possible for reactivated MBCs. However, the data collected so far are consistent with an overall model of serotype-independent pneumococcal lung immunity involving early contributions of TRM cells (74, 178) and pre-existing antibody followed by a later, but crucial, contribution from reactivated lung BRM cells.

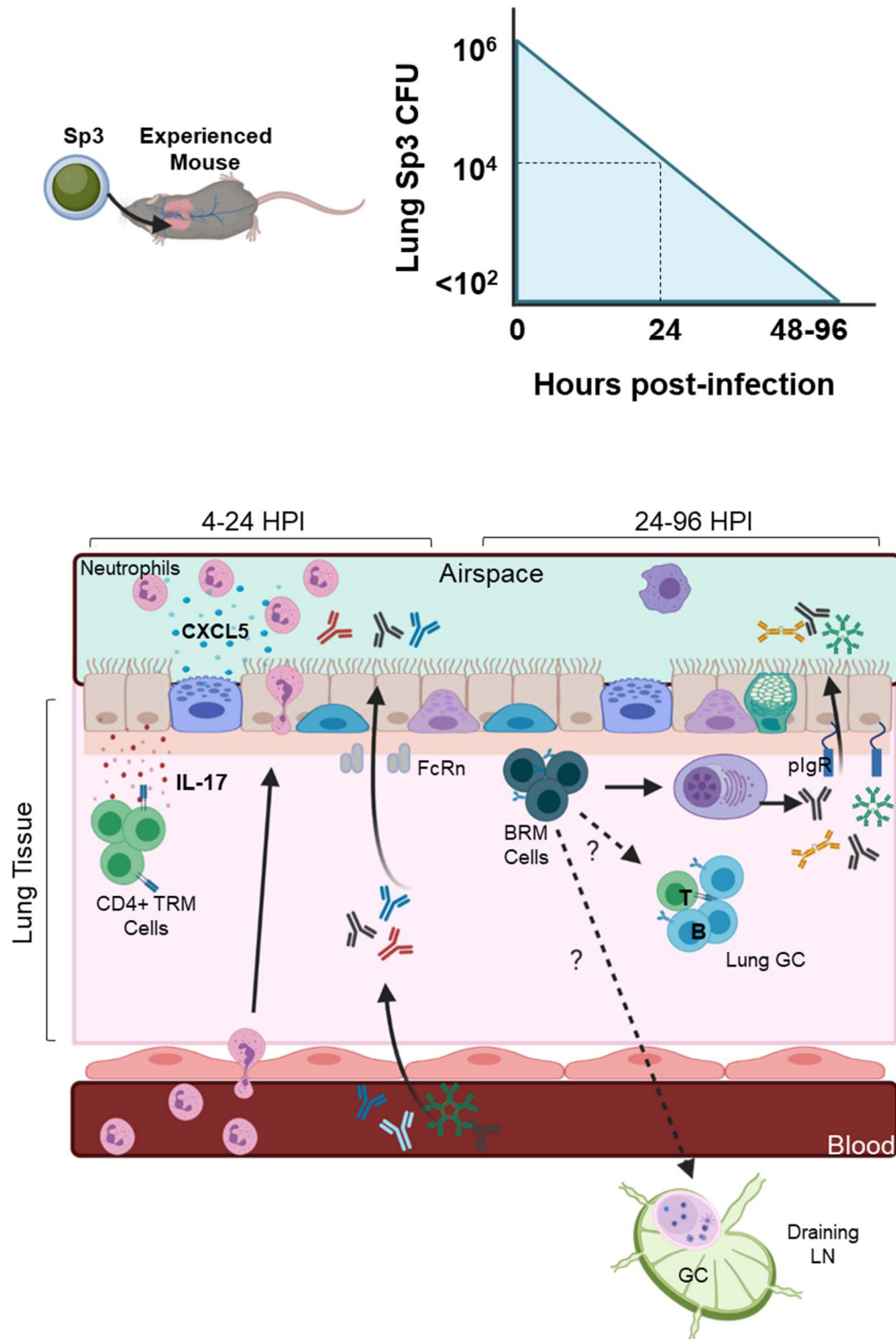


Figure 23. An integrated model of serotype-independent anti-pneumococcal immunity in mice. When Sp3 is instilled into the lungs of experienced mice that previously recovered from two Sp19 lung infections, the bacterial CFU is reduced by one

to two logs by 24 hours and is below the level of detection of CFU counts by 48-96 hours post-infection. Immune components that we have shown or that we hypothesize contribute to this early and late bacterial clearance are depicted. CD4+ lung TRM cells are reactivated to produce IL-17, which stabilizes CXCL5 transcripts in lung epithelial cells. CXCL5 production drives enhanced early recruitment of neutrophils into the lungs. Pre-existing heterotypic anti-pneumococcal IgG antibodies may also come into the increasingly permeable lung and be transported into the airspaces via the neonatal Fc receptor. Later reactivation of lung BRM cells enables them to differentiate into antibody-secreting cells secreting heterotypic anti-pneumococcal IgG, IgA, and IgM. Increased expression of the polymeric IgA receptor on lung epithelial cells may enhance transport of IgA and IgM into the airspaces as well. Whether reactivated lung BRM cells also seed new GC reactions in the lung or in draining lymph nodes is unknown. GC, germinal center; FcRn, neonatal Fc receptor; pIgR, polymeric Ig receptor. Created with Biorender.com.

A preliminary model of lung MBC recruitment following pneumococcal infections

In Chapter 4, we explored the kinetics of MBC recruitment to the lungs after pneumococcal serotype Sp19 infection and what factors were required to establish this B cell population. One possible model of recruitment that accounts for the observations made is proposed below (Fig. 24). However, follow-up experiments will be required to formally test most aspects of the hypothesized model described here. In this model, the initial Sp19 antigens are brought to the lung draining lymph node by lung DCs to initiate an adaptive immune response. A small amount of the B cell recruitment cytokine CXCL13 is produced in the lung after this initial infection, and a correspondingly small influx of B cells occurs, although this influx does not lead to BRM cell formation. Based on observations in the literature, we hypothesize that around days 5-7 after the initial Sp19 exposure, effector T cells generated by the first infection home back to the lung. If cognate antigen is present there (i.e., if a second Sp19 infection was given at day 7), these effector T cells are able to undergo a transition into memory T cells, some of which

reside long-term in the lung. Notably, our experiments in μ MT mice demonstrate that this TRM cell pool is established and can persist entirely independently of B cells, in contrast with reports of lung TRM cells dependent on B cells for maintenance in a mouse model of lymphocytic choriomeningitis virus (184).

In addition to enabling T cells to transition to a memory phenotype, the second Sp19 infection generates a larger CXCL13 response in the lung than the first infection did, which leads to a comparably larger influx of CXCR5⁺ B cells into the lung around a day later. The CXCR5⁺ B cells, however, are outnumbered by CXCR5⁻ B cells coming into the lung at day 10 as well, many of which express a pre-GC phenotype (GL7⁺CD38^{hi}). Based on prior literature, we hypothesize that many of these pre-GC phenotype B cells directly differentiate into extrafollicular MBCs of a predominantly IgM⁺ isotype. We speculate that the CXCR5⁺ B cell population may instead seed lung-localized GC reactions that peak in number at day 14 and result in more lung MBC accumulation by predominantly class-switched, PD-L2⁺CD73⁺ B cells from day 14 onward. The composite accumulation of these B cell populations leads to a lung B cell compartment at day 35 comprised of around half IgD⁺ B cells, 30% IgM⁺IgD⁻ MBCs, and 20% class-switched MBCs. These B cells do not re-enter the circulation, and around 40-60% of them express the residence marker CD69. However, the true signals required for these B cells to remain resident within the lung after pneumonia resolution have yet to be discovered. At some point during establishment, B cell interaction with CD4⁺ T cells is required for a BRM cell pool to form. However, our current results do not allow us to distinguish between a requirement for CD4⁺ help in initial priming within an SLO during

the first infection from a potential requirement for CD4⁺ T cell help within the lung after the second Sp19 infection.

Around 2% of the lung B cells at day 35 continue to express a GC phenotype, despite no evidence for ongoing iBALT reactions in pneumococcus-experienced mouse lungs. One group has reported that proliferating B cells with a GC phenotype can exist in the lung outside of typical FDC-containing GC structures, although these B cells were found nearby CD4⁺ T cells with helper capabilities (229). Follow-up experiments should assess whether FDCs are present in pneumococcus-experienced lungs, and test whether the ongoing GC reactions in resting experienced lungs are important for continued generation of local plasma cells or MBCs.

The persistence of a large number of IgD⁺IgM⁺ B cells in the lung at day 35 is an intriguing observation, as these cells would typically be classified as naïve. These IgD⁺ cells express CD69 to a comparable extent as the IgD⁻ lung B cells, and although they do not express the typical mouse MBC markers PD-L2, CD73, or CD80, they are not depleted by anti-CD20 treatment, indicating they are also part of the resident lung B cell pool (these data not shown). In humans, a population of IgD⁺IgM⁺CD27⁺ MBCs exists and is not rare in peripheral blood; these cells have the same functional capacities as typical MBCs, as they can both differentiate rapidly into plasma cells or re-enter GCs (230). Recent work in a murine malaria model also identified a population of IgD⁺ MBCs, and although no functional role for these cells was described, they were found to be the most long-lived MBC population (110). Follow-up work in our model should

explore whether IgD+PD-L2- lung B cells are also important for anti-pneumococcal lung immunity in some way.

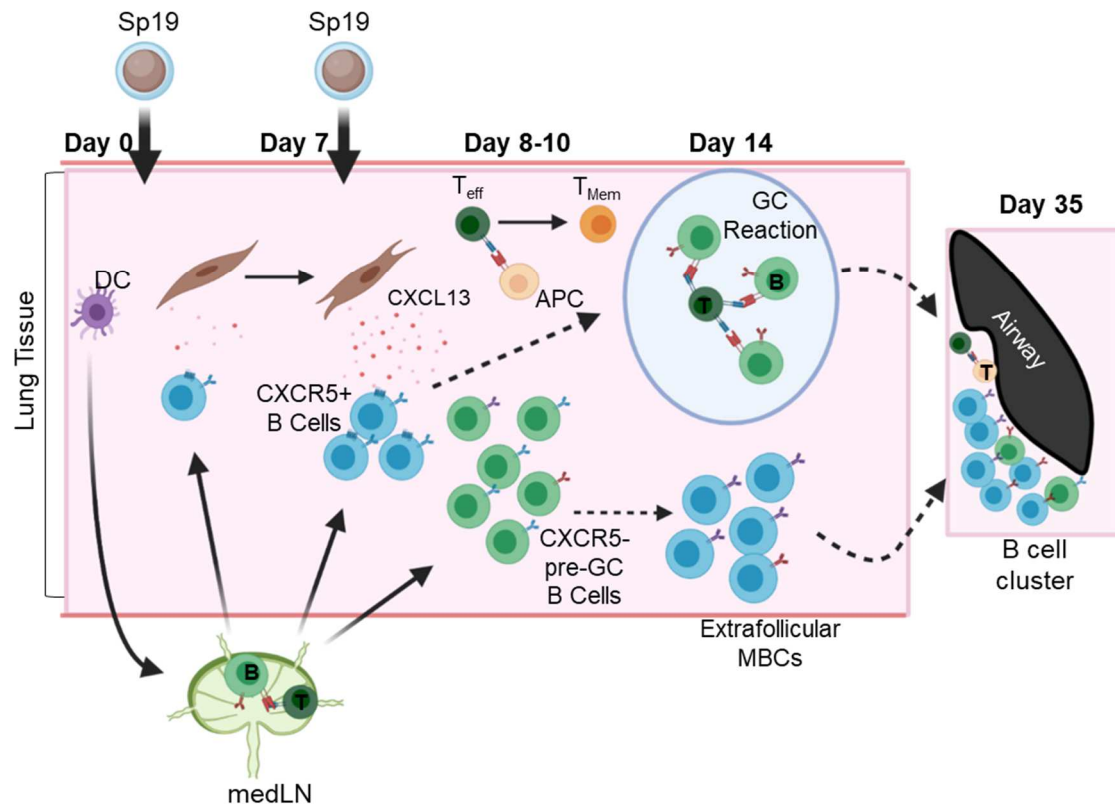


Figure 24. A preliminary model of lung MBC recruitment following two pneumococcal infections. Two Sp19 infections in mice are required to generate an appreciable lung BRM cell pool. The proposed sequence of events that lead to establishment of this B cell population are depicted here. We hypothesize that on initial Sp19 infection, lung APCs deliver pneumococcal antigens to draining lymph nodes and activate an adaptive immune response. A small population of CXCR5⁺ B cells infiltrates the lung, likely in response to the small amount of CXCL13 produced there. Effector CD4⁺ T cells are also recruited into the lung. Upon a second infection, these T cells are provided with the necessary antigen to transition into memory T cells. Additionally, increased lung CXCL13 production one to three days following the second infection drives a larger influx of CXCR5⁺ naïve B cells on the third day. Concurrently, a much larger pool of CXCR5⁻ B cells bearing a pre-GC phenotype are recruited, and comprise a mix of naïve, IgM⁺, and class-switched cells. These pre-GC B cells have the potential to directly become extrafollicular MBCs. The recruited CXCR5⁺ B cells (and perhaps a subset of cells from the pre-GC phenotype pool) may seed lung-localized GCs, which peak seven days after the second Sp19 infection and lead to an increased proportion of

lung class-switched MBCs starting one week after the second infection. By day 35, clusters of lung BRM cells are found near airways and contain rare CD4⁺ T cells that may associate with the rare remaining GC B cells in the lung. Blue B cell receptor=naïve, IgD⁺, Red B cell receptor=IgM+IgD⁻, Purple B cell receptor=IgM-IgD⁻, class-switched. APC, antigen-presenting cell; GC, germinal center; Teff, effector T cell; Tmem, memory T cell; medLN, mediastinal lymph node; DC, dendritic cell. Created with BioRender.com.

Unresolved questions in the lung BRM cell field

The intent of the research described here was to further our understanding of the contexts in which lung BRM cells occur and are important. However, many features of BRM cell biology still require investigation. Although the kinetics of BRM cell establishment appear to be consistent between studies and pathogens, one unresolved aspect of BRM cells is the length of time they persist in the lung. Generally, by 3 months after an infection, between 100 and several thousand class-switched BRM cells remain (112, 139, 148). BRM cells may be infrequent in the lung compared to TRM cells, but it has been estimated that reactivation of 10-100 MBCs is enough for production of biologically significant antibody titers in the serum (97); this effect would likely be magnified in a confined anatomical space like the lung. Therefore, detailed investigations of how long even small populations of antigen-specific BRM cells remain in the lung after infection resolution will be crucial. Whether BRM cells are maintained beyond a 6 month time point has not yet been explored in any context. Lung CD8⁺ TRM cells seem to have short-term maintenance compared to other TRM cell populations in the body, and the waning of CD8⁺ TRM cells that occurs around 6 months post-infection corresponds to a loss of heterosubtypic anti-influenza lung immunity in mice (231). Recent work

indicates that maintenance of these CD8⁺ TRM cells can be extended to at least a year in mice if persistent antigen is provided via a vaccination approach (232). Given that MBCs are another cell population that contribute to heterosubtypic protection against influenza (233, 234) and pneumococcus (Chapter 3), whether similar dynamics are at play for these cells after the 6 month time point will be critical for attempts to utilize lung BRM cells in establishing long-term mucosal protection.

Additional future studies should explore whether lung BRM cells are lost with aging, comorbidities, or upon exposure to different respiratory infections. Alternatively, whether the frequent exposures to respiratory pathogens like pneumococcus or influenza that most humans experience expand lung BRM cell populations specific to these microbes should be investigated as well.

Many questions also remain regarding the reactivation of lung BRM cells. Thus far, antibody secretion is the only effector mechanism that has been explored, yet B cells can also play important roles in antigen presentation, cytokine secretion, and even regulation of immune responses. The enhanced expression of the co-stimulatory molecule CD80 on MBCs along with the co-localization of some resident memory B and T cells in the lung makes antigen presentation to T cells an especially interesting possibility. However, some MBCs can be activated independently of T cells, and whether this is true of lung MBCs, especially those found outside of iBALT structures, must be addressed in future studies. Additionally, if lung BRM cells can be activated without T cell help, it may make sense for a subset of these cells to be positioned within the lung airways in addition to the parenchyma, as is the case for lung CD8⁺ TRM cells (235). Reactivated

airway BRM cells could secrete antibody directly into the infected space, bypassing the need for epithelial transcytosis.

MBCs and cross-reactivity

A final aspect of MBC immunity deserving of discussion is the idea that MBCs represent a pool of immune memory with a diverse repertoire that can be reactivated in response to reinfection with a related, but not identical, pathogen variant. As alluded to in the introduction, MBCs exit the GC relatively early and accumulate less mutations than GC B cells that eventually become LLPCs (236). A consequence of this early GC emergence and lack of affinity maturation is that in several infection settings, MBCs appear to recognize variants of the initially infecting pathogen that LLPC-secreted antibodies cannot bind. Following West Nile virus infection in mice, LLPCs secrete antibody that recognizes a dominant neutralizing epitope and cannot bind a variant epitope on a mutated reinfecting virus (176). Antibodies from reactivated MBCs, however, effectively neutralize both the original and variant viruses. Another group showed that MBCs specific to Zika virus in human blood exhibit more cross-reactivity between viral types than Zika-specific serum antibodies do (237). While these studies provide compelling evidence that this phenomenon extends across pathogens and species, the majority of work on cross-reactive B cell memory has been conducted in the context of influenza infections.

In mice recovered from a primary influenza infection, pre-existing antibodies from LLPCs are sufficient to protect against a homologous reinfection, but not against infection with an antigenically drifted virus. In contrast, antibodies directed against the

conserved hemagglutinin stem that were secreted by reactivated MBCs were sufficient to protect against heterologous challenge (234). Human blood also contains MBCs able to recognize hemagglutinin proteins of multiple influenza subtypes, although whether these MBCs are enriched in human lungs remains to be tested (233). Lungs of healthy adult humans and mice recovered from influenza also contain CD8⁺ TRM cells that can bind to conserved influenza antigens (135, 238). While loss of these T cells from the lung correlates with the loss of heterotypic influenza immunity in mice (231), these studies did not distinguish the protective contributions of cross-reactive memory T and B cells. It is likely that in a heterologous influenza infection that cannot be neutralized by pre-existing antibodies, both reactivated MBCs and CD8⁺ T cells contribute to optimal antiviral defense.

A dual contribution of memory T and B cells to heterotypic immunity is also what we have observed in the pneumococcal infections in mice described in this thesis. Our data further imply that pre-existing antibodies produced by LLPCs are insufficient to mediate full serotype-independent protection against pneumonia in our model. One hypothesis that may explain this observation is that the pre-existing antibody pool is primarily comprised of serotype-specific antibodies, even though it does contain some antibodies able to bind a mismatched serotype. Based on the data described above for viral immunology, this would likely contrast with the lung MBCs, which may largely be capable of recognizing multiple pneumococcal serotypes. Formally testing whether the partitioning of cross-reactivity into the MBC pool holds true for pneumococcal infections, as it does for many viral pathogens, should be the focus of future studies. Such

an observation would have important implications for the development of a pneumococcal vaccine that can protect broadly against all serotypes.

Conclusion

In conclusion, in this study we explored the lung BRM cell populations elicited by respiratory exposures to *S. pneumoniae*. We have shown that lung BRM cells are induced after respiratory pneumococcal exposures in mice and are required for optimal clearance of a subsequent serotype-mismatched pneumococcal challenge. These results represent the first evidence that lung BRM cells are elicited by and contribute to immunity against bacterial infections. We also observed B cells with a resident memory phenotype in normal human lung tissue, providing preliminary evidence that lung BRM cells may be a common feature of healthy experienced lungs across species. Finally, we explored the kinetics and signals involved in lung BRM cell formation after pneumococcal pneumonia, and discovered that repeated antigen exposures are necessary to drive seeding of lung GCs and accumulation of class-switched MBCs within the lung tissue, potentially through a signaling axis involving CXCL13. These studies provide the foundation for future BRM cell studies in many infection settings and organs, and argue that BRM cells in the lung should be considered as potentially important correlates of optimal mucosal immunity.

BIBLIOGRAPHY

1. DALYs GBD, and Collaborators H. Global, regional, and national disability-adjusted life-years (DALYs) for 359 diseases and injuries and healthy life expectancy (HALE) for 195 countries and territories, 1990-2017: a systematic analysis for the Global Burden of Disease Study 2017. *Lancet*. 2018;392(10159):1859-1922.
2. Pappas G, Kiriaze IJ, and Falagas ME. Insights into infectious disease in the era of Hippocrates. *International Journal of Infectious Diseases*. 2008;12(4):347-350.
3. Osler W, and McCrae T. *The principles and practice of medicine*. New York, London,: D. Appleton and company; 1920.
4. Witt WP, Weiss AJ, and Elixhauser A. *Healthcare Cost and Utilization Project (HCUP) Statistical Briefs*. Rockville (MD); 2006.
5. Fry AM, Shay DK, Holman RC, Curns AT, and Anderson LJ. Trends in hospitalizations for pneumonia among persons aged 65 years or older in the United States, 1988-2002. *JAMA*. 2005;294(21):2712-2719.
6. Quinton LJ, and Mizgerd JP. Dynamics of lung defense in pneumonia: resistance, resilience, and remodeling. *Annual Review of Physiology*. 2015;77:407-430.
7. Quinton LJ, Walkey AJ, and Mizgerd JP. Integrative Physiology of Pneumonia. *Physiological Reviews*. 2018;98(3):1417-1464.
8. Ablij H, and Meinders A. C-reactive protein: history and revival. *European Journal of Internal Medicine*. 2002;13(7):412.
9. Watson DA, Musher DM, Jacobson JW, and Verhoef J. A brief history of the pneumococcus in biomedical research: a panoply of scientific discovery. *Clinical Infectious Diseases*. 1993;17(5):913-924.
10. Jain S, et al. Community-Acquired Pneumonia Requiring Hospitalization among U.S. Adults. *New England Journal of Medicine*. 2015;373(5):415-427.
11. Jain S, et al. Community-acquired pneumonia requiring hospitalization among U.S. children. *New England Journal of Medicine*. 2015;372(9):835-845.
12. Henriques-Normark B, and Tuomanen EI. The pneumococcus: epidemiology, microbiology, and pathogenesis. *Cold Spring Harbor Perspectives in Medicine*. 2013;3(7).

13. Huang SS, et al. Healthcare utilization and cost of pneumococcal disease in the United States. *Vaccine*. 2011;29(18):3398-3412.
14. Ganaie F, et al. A New Pneumococcal Capsule Type, 10D, is the 100th Serotype and Has a Large cps Fragment from an Oral Streptococcus. *mBio*. 2020;11(3).
15. Gray BM, Converse GM, 3rd, and Dillon HC, Jr. Epidemiologic studies of *Streptococcus pneumoniae* in infants: acquisition, carriage, and infection during the first 24 months of life. *Journal of Infectious Diseases*. 1980;142(6):923-933.
16. Goldblatt D, et al. Antibody responses to nasopharyngeal carriage of *Streptococcus pneumoniae* in adults: a longitudinal household study. *Journal of Infectious Diseases*. 2005;192(3):387-393.
17. Bogaert D, De Groot R, and Hermans PW. *Streptococcus pneumoniae* colonisation: the key to pneumococcal disease. *Lancet Infectious Diseases*. 2004;4(3):144-154.
18. Weiser JN, Ferreira DM, and Paton JC. *Streptococcus pneumoniae*: transmission, colonization and invasion. *Nature Reviews: Microbiology*. 2018;16(6):355-367.
19. Kadioglu A, and Andrew PW. The innate immune response to pneumococcal lung infection: the untold story. *Trends in Immunology*. 2004;25(3):143-149.
20. Shenoy AT, and Orihuela CJ. Anatomical site-specific contributions of pneumococcal virulence determinants. *Pneumonia (Nathan)*. 2016;8.
21. Yamamoto K, et al. Roles of lung epithelium in neutrophil recruitment during pneumococcal pneumonia. *American Journal of Respiratory Cell and Molecular Biology*. 2014;50(2):253-262.
22. Mizgerd JP. Respiratory infection and the impact of pulmonary immunity on lung health and disease. *American Journal of Respiratory and Critical Care Medicine*. 2012;186(9):824-829.
23. Smith FL, and Baumgarth N. B-1 cell responses to infections. *Current Opinion in Immunology*. 2019;57:23-31.
24. Baumgarth N, Tung JW, and Herzenberg LA. Inherent specificities in natural antibodies: a key to immune defense against pathogen invasion. *Springer Seminars in Immunopathology*. 2005;26(4):347-362.
25. Montecino-Rodriguez E, and Dorshkind K. B-1 B cell development in the fetus and adult. *Immunity*. 2012;36(1):13-21.

26. Ansel KM, Harris RB, and Cyster JG. CXCL13 is required for B1 cell homing, natural antibody production, and body cavity immunity. *Immunity*. 2002;16(1):67-76.
27. Hooijkaas H, Bos N, Benner R, Pleasants JR, and Wostmann BS. Immunoglobulin isotypes and antibody specificity repertoire of "spontaneously" occurring ("background") immunoglobulin-secreting cells in germfree mice fed chemically defined ultrafiltered "antigen-free" diet. *Advances in Experimental Medicine and Biology*. 1985;186:131-138.
28. Briles DE, Forman C, Hudak S, and Claflin JL. Anti-phosphorylcholine antibodies of the T15 idiotype are optimally protective against *Streptococcus pneumoniae*. *Journal of Experimental Medicine*. 1982;156(4):1177-1185.
29. Haas KM, Poe JC, Steeber DA, and Tedder TF. B-1a and B-1b cells exhibit distinct developmental requirements and have unique functional roles in innate and adaptive immunity to *S. pneumoniae*. *Immunity*. 2005;23(1):7-18.
30. Rothstein TL, Griffin DO, Holodick NE, Quach TD, and Kaku H. Human B-1 cells take the stage. *Annals of the New York Academy of Sciences*. 2013;1285:97-114.
31. Tangye SG. To B1 or not to B1: that really is still the question! *Blood*. 2013;121(26):5109-5110.
32. Griffin DO, Holodick NE, and Rothstein TL. Human B1 cells in umbilical cord and adult peripheral blood express the novel phenotype CD20+ CD27+ CD43+ CD70. *Journal of Experimental Medicine*. 2011;208(1):67-80.
33. Leggat DJ, et al. Pneumococcal polysaccharide vaccination induces polysaccharide-specific B cells in adult peripheral blood expressing CD19(+)/CD20(+)/CD3(-)/CD70(-)/CD27(+)/IgM(+)/CD43(+)/CD5(+/-). *Vaccine*. 2013;31(41):4632-4640.
34. Verbinnen B, Covens K, Moens L, Meyts I, and Bossuyt X. Human CD20+CD43+CD27+CD5- B cells generate antibodies to capsular polysaccharides of *Streptococcus pneumoniae*. *Journal of Allergy and Clinical Immunology*. 2012;130(1):272-275.
35. Weill JC, Weller S, and Reynaud CA. Human marginal zone B cells. *Annual Review of Immunology*. 2009;27:267-285.
36. Martin F, Oliver AM, and Kearney JF. Marginal zone and B1 B cells unite in the early response against T-independent blood-borne particulate antigens. *Immunity*. 2001;14(5):617-629.

37. Nelson AL, Roche AM, Gould JM, Chim K, Ratner AJ, and Weiser JN. Capsule enhances pneumococcal colonization by limiting mucus-mediated clearance. *Infection and Immunity*. 2007;75(1):83-90.
38. Hyams C, Camberlein E, Cohen JM, Bax K, and Brown JS. The *Streptococcus pneumoniae* capsule inhibits complement activity and neutrophil phagocytosis by multiple mechanisms. *Infection and Immunity*. 2010;78(2):704-715.
39. Davis KM, Akinbi HT, Standish AJ, and Weiser JN. Resistance to mucosal lysozyme compensates for the fitness deficit of peptidoglycan modifications by *Streptococcus pneumoniae*. *PLoS Pathogens*. 2008;4(12):e1000241.
40. Hirst RA, Sikand KS, Rutman A, Mitchell TJ, Andrew PW, and O'Callaghan C. Relative roles of pneumolysin and hydrogen peroxide from *Streptococcus pneumoniae* in inhibition of ependymal ciliary beat frequency. *Infection and Immunity*. 2000;68(3):1557-1562.
41. Bewley MA, et al. Pneumolysin activates macrophage lysosomal membrane permeabilization and executes apoptosis by distinct mechanisms without membrane pore formation. *mBio*. 2014;5(5):e01710-01714.
42. Beiter K, Wartha F, Albiger B, Normark S, Zychlinsky A, and Henriques-Normark B. An endonuclease allows *Streptococcus pneumoniae* to escape from neutrophil extracellular traps. *Current Biology*. 2006;16(4):401-407.
43. Chien YW, Klugman KP, and Morens DM. Bacterial pathogens and death during the 1918 influenza pandemic. *New England Journal of Medicine*. 2009;361(26):2582-2583.
44. Chien YW, Klugman KP, and Morens DM. Efficacy of whole-cell killed bacterial vaccines in preventing pneumonia and death during the 1918 influenza pandemic. *Journal of Infectious Diseases*. 2010;202(11):1639-1648.
45. Macleod CM, Hodges RG, Heidelberger M, and Bernhard WG. Prevention of Pneumococcal Pneumonia by Immunization with Specific Capsular Polysaccharides. *Journal of Experimental Medicine*. 1945;82(6):445-465.
46. Daniels CC, Rogers PD, and Shelton CM. A Review of Pneumococcal Vaccines: Current Polysaccharide Vaccine Recommendations and Future Protein Antigens. *Journal of Pediatric Pharmacology and Therapeutics*. 2016;21(1):27-35.
47. Mond JJ, Lees A, and Snapper CM. T cell-independent antigens type 2. *Annual Review of Immunology*. 1995;13:655-692.

48. Pollard AJ, Perrett KP, and Beverley PC. Maintaining protection against invasive bacteria with protein-polysaccharide conjugate vaccines. *Nature Reviews: Immunology*. 2009;9(3):213-220.
49. Shapiro ED, et al. The protective efficacy of polyvalent pneumococcal polysaccharide vaccine. *New England Journal of Medicine*. 1991;325(21):1453-1460.
50. Taillardet M, et al. The thymus-independent immunity conferred by a pneumococcal polysaccharide is mediated by long-lived plasma cells. *Blood*. 2009;114(20):4432-4440.
51. Giebink GS. The prevention of pneumococcal disease in children. *New England Journal of Medicine*. 2001;345(16):1177-1183.
52. Jose RJ, and Brown JS. Adult pneumococcal vaccination: advances, impact, and unmet needs. *Current Opinion in Pulmonary Medicine*. 2017;23(3):225-230.
53. Eskola J, et al. Efficacy of a pneumococcal conjugate vaccine against acute otitis media. *New England Journal of Medicine*. 2001;344(6):403-409.
54. Kaplan SL, et al. Decrease of invasive pneumococcal infections in children among 8 children's hospitals in the United States after the introduction of the 7-valent pneumococcal conjugate vaccine. *Pediatrics*. 2004;113(3 Pt 1):443-449.
55. Casadevall A, and Scharff MD. Serum therapy revisited: animal models of infection and development of passive antibody therapy. *Antimicrobial Agents and Chemotherapy*. 1994;38(8):1695-1702.
56. Janeway CAJ, Travers P, Walport M, and Shlomchik MJ. New York: Garland Science; 2001.
57. Adler H, Ferreira DM, Gordon SB, and Rylance J. Pneumococcal Capsular Polysaccharide Immunity in the Elderly. *Clinical and Vaccine Immunology*. 2017;24(6).
58. Lipsitch M, Whitney CG, Zell E, Kaijalainen T, Dagan R, and Malley R. Are anticapsular antibodies the primary mechanism of protection against invasive pneumococcal disease? *PLoS Medicine*. 2005;2(1):e15.
59. Weinberger DM, Dagan R, Givon-Lavi N, Regev-Yochay G, Malley R, and Lipsitch M. Epidemiologic evidence for serotype-specific acquired immunity to pneumococcal carriage. *Journal of Infectious Diseases*. 2008;197(11):1511-1518.

60. Simell B, Kilpi TM, and Kayhty H. Pneumococcal carriage and otitis media induce salivary antibodies to pneumococcal capsular polysaccharides in children. *Journal of Infectious Diseases*. 2002;186(8):1106-1114.
61. McCool TL, and Weiser JN. Limited role of antibody in clearance of *Streptococcus pneumoniae* in a murine model of colonization. *Infection and Immunity*. 2004;72(10):5807-5813.
62. Bou Ghanem EN, et al. Nasopharyngeal Exposure to *Streptococcus pneumoniae* Induces Extended Age-Dependent Protection against Pulmonary Infection Mediated by Antibodies and CD138(+) Cells. *Journal of Immunology*. 2018;200(11):3739-3751.
63. Cohen JM, Khandavilli S, Camberlein E, Hyams C, Baxendale HE, and Brown JS. Protective contributions against invasive *Streptococcus pneumoniae* pneumonia of antibody and Th17-cell responses to nasopharyngeal colonisation. *PLoS One*. 2011;6(10):e25558.
64. Wilson R, Cohen JM, Jose RJ, de Vogel C, Baxendale H, and Brown JS. Protection against *Streptococcus pneumoniae* lung infection after nasopharyngeal colonization requires both humoral and cellular immune responses. *Mucosal Immunology*. 2015;8(3):627-639.
65. Wang Y, et al. Cross-protective mucosal immunity mediated by memory Th17 cells against *Streptococcus pneumoniae* lung infection. *Mucosal Immunology*. 2017;10(1):250-259.
66. Zhang Z, Clarke TB, and Weiser JN. Cellular effectors mediating Th17-dependent clearance of pneumococcal colonization in mice. *Journal of Clinical Investigation*. 2009;119(7):1899-1909.
67. Ramos-Sevillano E, Ercoli G, and Brown JS. Mechanisms of Naturally Acquired Immunity to *Streptococcus pneumoniae*. *Frontiers in Immunology*. 2019;10:358.
68. Malley R, Trzcinski K, Srivastava A, Thompson CM, Anderson PW, and Lipsitch M. CD4+ T cells mediate antibody-independent acquired immunity to pneumococcal colonization. *Proc Natl Acad Sci U S A*. 2005;102(13):4848-4853.
69. Ferreira DM, et al. Controlled human infection and rechallenge with *Streptococcus pneumoniae* reveals the protective efficacy of carriage in healthy adults. *American Journal of Respiratory and Critical Care Medicine*. 2013;187(8):855-864.
70. Wright AK, et al. Experimental human pneumococcal carriage augments IL-17A-dependent T-cell defence of the lung. *PLoS Pathogens*. 2013;9(3):e1003274.

71. Cohen JM, Wilson R, Shah P, Baxendale HE, and Brown JS. Lack of cross-protection against invasive pneumonia caused by heterologous strains following murine *Streptococcus pneumoniae* nasopharyngeal colonisation despite whole cell ELISAs showing significant cross-reactive IgG. *Vaccine*. 2013;31(19):2328-2332.
72. Richards L, Ferreira DM, Miyaji EN, Andrew PW, and Kadioglu A. The immunising effect of pneumococcal nasopharyngeal colonisation; protection against future colonisation and fatal invasive disease. *Immunobiology*. 2010;215(4):251-263.
73. Roche AM, King SJ, and Weiser JN. Live attenuated *Streptococcus pneumoniae* strains induce serotype-independent mucosal and systemic protection in mice. *Infection and Immunity*. 2007;75(5):2469-2475.
74. Smith NM, et al. Regionally compartmentalized resident memory T cells mediate naturally acquired protection against pneumococcal pneumonia. *Mucosal Immunology*. 2018;11(1):220-235.
75. Malley R, et al. Antibody-independent, interleukin-17A-mediated, cross-serotype immunity to pneumococci in mice immunized intranasally with the cell wall polysaccharide. *Infection and Immunity*. 2006;74(4):2187-2195.
76. O'Hara JM, et al. Generation of protective pneumococcal-specific nasal resident memory CD4(+) T cells via parenteral immunization. *Mucosal Immunology*. 2020;13(1):172-182.
77. Trzcinski K, Thompson CM, Srivastava A, Basset A, Malley R, and Lipsitch M. Protection against nasopharyngeal colonization by *Streptococcus pneumoniae* is mediated by antigen-specific CD4+ T cells. *Infection and Immunity*. 2008;76(6):2678-2684.
78. Lebon A, et al. Natural antibodies against several pneumococcal virulence proteins in children during the pre-pneumococcal-vaccine era: the generation R study. *Infection and Immunity*. 2011;79(4):1680-1687.
79. Malley R, et al. Serum antipneumococcal antibodies and pneumococcal colonization in adults with chronic obstructive pulmonary disease. *Journal of Infectious Diseases*. 2007;196(6):928-935.
80. Wilson R, et al. Naturally Acquired Human Immunity to *Pneumococcus* Is Dependent on Antibody to Protein Antigens. *PLoS Pathogens*. 2017;13(1):e1006137.
81. Panum PL. Observations on the Epidemic of Measles in the Faroe Isles, in 1846. *British and Foreign Medico-Chirurgical Review*. 1851;7(14):419-429.

82. Phan TG, Gray EE, and Cyster JG. The microanatomy of B cell activation. *Current Opinion in Immunology*. 2009;21(3):258-265.
83. Harwood NE, and Batista FD. Early events in B cell activation. *Annual Review of Immunology*. 2010;28:185-210.
84. Cyster JG, and Allen CDC. B Cell Responses: Cell Interaction Dynamics and Decisions. *Cell*. 2019;177(3):524-540.
85. Akkaya M, et al. Toll-like receptor 9 antagonizes antibody affinity maturation. *Nature Immunology*. 2018;19(3):255-266.
86. Akkaya M, Kwak K, and Pierce SK. B cell memory: building two walls of protection against pathogens. *Nature Reviews: Immunology*. 2020;20(4):229-238.
87. Roco JA, et al. Class-Switch Recombination Occurs Infrequently in Germinal Centers. *Immunity*. 2019;51(2):337-350 e337.
88. Nutt SL, Hodgkin PD, Tarlinton DM, and Corcoran LM. The generation of antibody-secreting plasma cells. *Nature Reviews: Immunology*. 2015;15(3):160-171.
89. Taylor JJ, Pape KA, and Jenkins MK. A germinal center-independent pathway generates unswitched memory B cells early in the primary response. *Journal of Experimental Medicine*. 2012;209(3):597-606.
90. Victora GD, and Nussenzweig MC. Germinal centers. *Annual Review of Immunology*. 2012;30:429-457.
91. Paus D, Phan TG, Chan TD, Gardam S, Basten A, and Brink R. Antigen recognition strength regulates the choice between extrafollicular plasma cell and germinal center B cell differentiation. *Journal of Experimental Medicine*. 2006;203(4):1081-1091.
92. Muramatsu M, Kinoshita K, Fagarasan S, Yamada S, Shinkai Y, and Honjo T. Class switch recombination and hypermutation require activation-induced cytidine deaminase (AID), a potential RNA editing enzyme. *Cell*. 2000;102(5):553-563.
93. Ise W, et al. T Follicular Helper Cell-Germinal Center B Cell Interaction Strength Regulates Entry into Plasma Cell or Recycling Germinal Center Cell Fate. *Immunity*. 2018;48(4):702-715 e704.
94. Liu D, et al. T-B-cell entanglement and ICOSL-driven feed-forward regulation of germinal centre reaction. *Nature*. 2015;517(7533):214-218.

95. Victora GD, et al. Germinal center dynamics revealed by multiphoton microscopy with a photoactivatable fluorescent reporter. *Cell*. 2010;143(4):592-605.
96. Sidwell T, and Kallies A. Bach2 is required for B cell and T cell memory differentiation. *Nature Immunology*. 2016;17(7):744-745.
97. Weisel F, and Shlomchik M. Memory B Cells of Mice and Humans. *Annual Review of Immunology*. 2017;35:255-284.
98. McHeyzer-Williams MG, Nossal GJ, and Lalor PA. Molecular characterization of single memory B cells. *Nature*. 1991;350(6318):502-505.
99. Dogan I, et al. Multiple layers of B cell memory with different effector functions. *Nature Immunology*. 2009;10(12):1292-1299.
100. Tangye SG, and Good KL. Human IgM+CD27+ B cells: memory B cells or "memory" B cells? *Journal of Immunology*. 2007;179(1):13-19.
101. Klein U, Rajewsky K, and Kuppers R. Human immunoglobulin (Ig)M+IgD+ peripheral blood B cells expressing the CD27 cell surface antigen carry somatically mutated variable region genes: CD27 as a general marker for somatically mutated (memory) B cells. *Journal of Experimental Medicine*. 1998;188(9):1679-1689.
102. Tangye SG, Liu YJ, Aversa G, Phillips JH, and de Vries JE. Identification of functional human splenic memory B cells by expression of CD148 and CD27. *Journal of Experimental Medicine*. 1998;188(9):1691-1703.
103. Fecteau JF, Cote G, and Neron S. A new memory CD27-IgG+ B cell population in peripheral blood expressing VH genes with low frequency of somatic mutation. *Journal of Immunology*. 2006;177(6):3728-3736.
104. Wei C, et al. A new population of cells lacking expression of CD27 represents a notable component of the B cell memory compartment in systemic lupus erythematosus. *Journal of Immunology*. 2007;178(10):6624-6633.
105. Portugal S, et al. Malaria-associated atypical memory B cells exhibit markedly reduced B cell receptor signaling and effector function. *Elife*. 2015;4.
106. Ridderstad A, and Tarlinton DM. Kinetics of establishing the memory B cell population as revealed by CD38 expression. *Journal of Immunology*. 1998;160(10):4688-4695.

107. Anderson SM, Tomayko MM, Ahuja A, Haberman AM, and Shlomchik MJ. New markers for murine memory B cells that define mutated and unmutated subsets. *Journal of Experimental Medicine*. 2007;204(9):2103-2114.
108. Good-Jacobson KL, Szumilas CG, Chen L, Sharpe AH, Tomayko MM, and Shlomchik MJ. PD-1 regulates germinal center B cell survival and the formation and affinity of long-lived plasma cells. *Nature Immunology*. 2010;11(6):535-542.
109. Tomayko MM, Steinel NC, Anderson SM, and Shlomchik MJ. Cutting edge: Hierarchy of maturity of murine memory B cell subsets. *Journal of Immunology*. 2010;185(12):7146-7150.
110. Krishnamurthy AT, et al. Somatic Hypermutated Plasmodium-Specific IgM(+) Memory B Cells Are Rapid, Plastic, Early Responders upon Malaria Rechallenge. *Immunity*. 2016;45(2):402-414.
111. Lindner C, et al. Diversification of memory B cells drives the continuous adaptation of secretory antibodies to gut microbiota. *Nature Immunology*. 2015;16(8):880-888.
112. Onodera T, et al. Memory B cells in the lung participate in protective humoral immune responses to pulmonary influenza virus reinfection. *Proceedings of the National Academy of Sciences of the United States of America*. 2012;109(7):2485-2490.
113. Good KL, Avery DT, and Tangye SG. Resting human memory B cells are intrinsically programmed for enhanced survival and responsiveness to diverse stimuli compared to naive B cells. *Journal of Immunology*. 2009;182(2):890-901.
114. Tomayko MM, et al. Systematic comparison of gene expression between murine memory and naive B cells demonstrates that memory B cells have unique signaling capabilities. *Journal of Immunology*. 2008;181(1):27-38.
115. Good KL, and Tangye SG. Decreased expression of Kruppel-like factors in memory B cells induces the rapid response typical of secondary antibody responses. *Proceedings of the National Academy of Sciences of the United States of America*. 2007;104(33):13420-13425.
116. Bhattacharya D, et al. Transcriptional profiling of antigen-dependent murine B cell differentiation and memory formation. *Journal of Immunology*. 2007;179(10):6808-6819.
117. Engels N, et al. The immunoglobulin tail tyrosine motif upgrades memory-type BCRs by incorporating a Grb2-Btk signalling module. *Nature Communications*. 2014;5:5456.

118. Moran I, et al. Memory B cells are reactivated in subcapsular proliferative foci of lymph nodes. *Nature Communications*. 2018;9(1):3372.
119. Palm AE, and Henry C. Remembrance of Things Past: Long-Term B Cell Memory After Infection and Vaccination. *Frontiers in Immunology*. 2019;10:1787.
120. Zuccarino-Catania GV, et al. CD80 and PD-L2 define functionally distinct memory B cell subsets that are independent of antibody isotype. *Nature Immunology*. 2014;15(7):631-637.
121. Mesin L, et al. Restricted Clonality and Limited Germinal Center Reentry Characterize Memory B Cell Reactivation by Boosting. *Cell*. 2020;180(1):92-106 e111.
122. Benson MJ, et al. Distinction of the memory B cell response to cognate antigen versus bystander inflammatory signals. *Journal of Experimental Medicine*. 2009;206(9):2013-2025.
123. Vieira P, and Rajewsky K. Persistence of memory B cells in mice deprived of T cell help. *International Immunology*. 1990;2(6):487-494.
124. Hebeis BJ, et al. Activation of virus-specific memory B cells in the absence of T cell help. *Journal of Experimental Medicine*. 2004;199(4):593-602.
125. Weisel FJ, et al. Unique requirements for reactivation of virus-specific memory B lymphocytes. *Journal of Immunology*. 2010;185(7):4011-4021.
126. Ochsenbein AF, Pinschewer DD, Sierro S, Horvath E, Hengartner H, and Zinkernagel RM. Protective long-term antibody memory by antigen-driven and T help-dependent differentiation of long-lived memory B cells to short-lived plasma cells independent of secondary lymphoid organs. *Proceedings of the National Academy of Sciences of the United States of America*. 2000;97(24):13263-13268.
127. Yu A, et al. Efficient induction of primary and secondary T cell-dependent immune responses in vivo in the absence of functional IL-2 and IL-15 receptors. *Journal of Immunology*. 2003;170(1):236-242.
128. Takatsuka S, et al. IL-9 receptor signaling in memory B cells regulates humoral recall responses. *Nature Immunology*. 2018;19(9):1025-1034.
129. Wang NS, McHeyzer-Williams LJ, Okitsu SL, Burris TP, Reiner SL, and McHeyzer-Williams MG. Divergent transcriptional programming of class-specific B cell memory by T-bet and ROR α . *Nature Immunology*. 2012;13(6):604-611.

130. Masopust D, Vezys V, Marzo AL, and Lefrancois L. Preferential localization of effector memory cells in nonlymphoid tissue. *Science*. 2001;291(5512):2413-2417.
131. Schenkel JM, and Masopust D. Tissue-resident memory T cells. *Immunity*. 2014;41(6):886-897.
132. Kumar BV, et al. Human Tissue-Resident Memory T Cells Are Defined by Core Transcriptional and Functional Signatures in Lymphoid and Mucosal Sites. *Cell Reports*. 2017;20(12):2921-2934.
133. Szabo PA, Miron M, and Farber DL. Location, location, location: Tissue resident memory T cells in mice and humans. *Science Immunology*. 2019;4(34).
134. Jozwik A, et al. RSV-specific airway resident memory CD8⁺ T cells and differential disease severity after experimental human infection. *Nature Communications*. 2015;6:10224.
135. Pizzolla A, et al. Influenza-specific lung-resident memory T cells are proliferative and polyfunctional and maintain diverse TCR profiles. *Journal of Clinical Investigation*. 2018;128(2):721-733.
136. Sathaliyawala T, et al. Distribution and compartmentalization of human circulating and tissue-resident memory T cell subsets. *Immunity*. 2013;38(1):187-197.
137. Beura LK, et al. T Cells in Nonlymphoid Tissues Give Rise to Lymph-Node-Resident Memory T Cells. *Immunity*. 2018;48(2):327-338 e325.
138. Aiba Y, et al. Preferential localization of IgG memory B cells adjacent to contracted germinal centers. *Proceedings of the National Academy of Sciences of the United States of America*. 2010;107(27):12192-12197.
139. Allie SR, et al. The establishment of resident memory B cells in the lung requires local antigen encounter. *Nature Immunology*. 2019;20(1):97-108.
140. Becker SC, et al. A comparative analysis of human bone marrow-resident and peripheral memory B cells. *Journal of Allergy and Clinical Immunology*. 2018;141(5):1911-1913 e1917.
141. Johnson JL, et al. The Transcription Factor T-bet Resolves Memory B Cell Subsets with Distinct Tissue Distributions and Antibody Specificities in Mice and Humans. *Immunity*. 2020;52(5):842-855 e846.

142. Bemark M, et al. Limited clonal relatedness between gut IgA plasma cells and memory B cells after oral immunization. *Nature Communications*. 2016;7:12698.
143. Quiding-Jarbrink M, Granstrom G, Nordstrom I, Holmgren J, and Czerkinsky C. Induction of compartmentalized B-cell responses in human tonsils. *Infection and Immunity*. 1995;63(3):853-857.
144. Shehata L, et al. Systematic comparison of respiratory syncytial virus-induced memory B cell responses in two anatomical compartments. *Nature Communications*. 2019;10(1):1126.
145. Saul L, et al. IgG subclass switching and clonal expansion in cutaneous melanoma and normal skin. *Scientific Reports*. 2016;6:29736.
146. Camell CD, et al. Aging Induces an Nlrp3 Inflammasome-Dependent Expansion of Adipose B Cells That Impairs Metabolic Homeostasis. *Cell Metabolism*. 2019;30(6):1024-1039 e1026.
147. Jones PD, and Ada GL. Persistence of influenza virus-specific antibody-secreting cells and B-cell memory after primary murine influenza virus infection. *Cellular Immunology*. 1987;109(1):53-64.
148. Joo HM, He Y, and Sangster MY. Broad dispersion and lung localization of virus-specific memory B cells induced by influenza pneumonia. *Proceedings of the National Academy of Sciences of the United States of America*. 2008;105(9):3485-3490.
149. Adachi Y, et al. Distinct germinal center selection at local sites shapes memory B cell response to viral escape. *Journal of Experimental Medicine*. 2015;212(10):1709-1723.
150. Koutsakos M, et al. Circulating TFH cells, serological memory, and tissue compartmentalization shape human influenza-specific B cell immunity. *Science Translational Medicine*. 2018;10(428).
151. Allie SR, and Randall TD. Resident Memory B Cells. *Viral Immunology*. 2020;33(4):282-293.
152. Takahashi Y, Onodera T, Adachi Y, and Ato M. Adaptive B Cell Responses to Influenza Virus Infection in the Lung. *Viral Immunology*. 2017;30(6):431-437.
153. Silva-Sanchez A, and Randall TD. Role of iBALT in Respiratory Immunity. *Current Topics in Microbiology and Immunology*. 2020.

154. van der Strate BW, et al. Cigarette smoke-induced emphysema: A role for the B cell? *American Journal of Respiratory and Critical Care Medicine*. 2006;173(7):751-758.
155. GeurtsvanKessel CH, et al. Dendritic cells are crucial for maintenance of tertiary lymphoid structures in the lung of influenza virus-infected mice. *Journal of Experimental Medicine*. 2009;206(11):2339-2349.
156. Takahashi Y, Onodera T, Kobayashi K, and Kurosaki T. Primary and secondary B-cell responses to pulmonary virus infection. *Infectious Disorders Drug Targets*. 2012;12(3):232-240.
157. Tschernig T, and Pabst R. Bronchus-associated lymphoid tissue (BALT) is not present in the normal adult lung but in different diseases. *Pathobiology*. 2000;68(1):1-8.
158. Kitamura D, Roes J, Kuhn R, and Rajewsky K. A B cell-deficient mouse by targeted disruption of the membrane exon of the immunoglobulin mu chain gene. *Nature*. 1991;350(6317):423-426.
159. Lee RA, Mao C, Vo H, Gao W, and Zhong X. Fluorescence tagging and inducible depletion of PD-L2-expressing B-1 B cells in vivo. *Annals of the New York Academy of Sciences*. 2015;1362:77-85.
160. Moffitt KL, Yadav P, Weinberger DM, Anderson PW, and Malley R. Broad antibody and T cell reactivity induced by a pneumococcal whole-cell vaccine. *Vaccine*. 2012;30(29):4316-4322.
161. Bolger AM, Lohse M, and Usadel B. Trimmomatic: a flexible trimmer for Illumina sequence data. *Bioinformatics*. 2014;30(15):2114-2120.
162. Dobin A, et al. STAR: ultrafast universal RNA-seq aligner. *Bioinformatics*. 2013;29(1):15-21.
163. Anders S, Pyl PT, and Huber W. HTSeq--a Python framework to work with high-throughput sequencing data. *Bioinformatics*. 2015;31(2):166-169.
164. Love MI, Huber W, and Anders S. Moderated estimation of fold change and dispersion for RNA-seq data with DESeq2. *Genome Biology*. 2014;15(12):550.
165. Barron AMS, et al. Perivascular Adventitial Fibroblast Specialization Accompanies T Cell Retention in the Inflamed Human Dermis. *Journal of Immunology*. 2019;202(1):56-68.

166. Nazari B, et al. Altered Dermal Fibroblasts in Systemic Sclerosis Display Podoplanin and CD90. *American Journal of Pathology*. 2016;186(10):2650-2664.
167. Beura LK, et al. Normalizing the environment recapitulates adult human immune traits in laboratory mice. *Nature*. 2016;532(7600):512-516.
168. Masopust D, and Soerens AG. Tissue-Resident T Cells and Other Resident Leukocytes. *Annual Review of Immunology*. 2019;37:521-546.
169. Turner DL, et al. Lung niches for the generation and maintenance of tissue-resident memory T cells. *Mucosal Immunology*. 2014;7(3):501-510.
170. Reboldi A, and Cyster JG. Peyer's patches: organizing B-cell responses at the intestinal frontier. *Immunological Reviews*. 2016;271(1):230-245.
171. Mahallawi WH, et al. Infection with 2009 H1N1 influenza virus primes for immunological memory in human nose-associated lymphoid tissue, offering cross-reactive immunity to H1N1 and avian H5N1 viruses. *Journal of Virology*. 2013;87(10):5331-5339.
172. Oh JE, et al. Migrant memory B cells secrete luminal antibody in the vagina. *Nature*. 2019;571(7763):122-126.
173. Pichyangkul S, et al. Tissue Distribution of Memory T and B Cells in Rhesus Monkeys following Influenza A Infection. *Journal of Immunology*. 2015;195(9):4378-4386.
174. Zuccotti G, et al. Serotype distribution and antimicrobial susceptibilities of nasopharyngeal isolates of *Streptococcus pneumoniae* from healthy children in the 13-valent pneumococcal conjugate vaccine era. *Vaccine*. 2014;32(5):527-534.
175. Granat SM, Ollgren J, Herva E, Mia Z, Auranen K, and Makela PH. Epidemiological evidence for serotype-independent acquired immunity to pneumococcal carriage. *Journal of Infectious Diseases*. 2009;200(1):99-106.
176. Purtha WE, Tedder TF, Johnson S, Bhattacharya D, and Diamond MS. Memory B cells, but not long-lived plasma cells, possess antigen specificities for viral escape mutants. *Journal of Experimental Medicine*. 2011;208(13):2599-2606.
177. Guillon A, et al. Pneumonia recovery reprograms the alveolar macrophage pool. *JCI Insight*. 2020;5(4).
178. Shenoy AT, et al. Lung CD4(+) resident memory T cells remodel epithelial responses to accelerate neutrophil recruitment during pneumonia. *Mucosal Immunology*. 2020;13(2):334-343.

179. Montalvao F, et al. The mechanism of anti-CD20-mediated B cell depletion revealed by intravital imaging. *Journal of Clinical Investigation*. 2013;123(12):5098-5103.
180. Purwar R, Campbell J, Murphy G, Richards WG, Clark RA, and Kupper TS. Resident memory T cells (T(RM)) are abundant in human lung: diversity, function, and antigen specificity. *PLoS One*. 2011;6(1):e16245.
181. Arpin C, et al. Generation of memory B cells and plasma cells in vitro. *Science*. 1995;268(5211):720-722.
182. Li Z, et al. CD83: Activation Marker for Antigen Presenting Cells and Its Therapeutic Potential. *Frontiers in Immunology*. 2019;10:1312.
183. Weber GF, et al. Pleural innate response activator B cells protect against pneumonia via a GM-CSF-IgM axis. *Journal of Experimental Medicine*. 2014;211(6):1243-1256.
184. Hondowicz BD, Kim KS, Ruterbusch MJ, Keitany GJ, and Pepper M. IL-2 is required for the generation of viral-specific CD4(+) Th1 tissue-resident memory cells and B cells are essential for maintenance in the lung. *European Journal of Immunology*. 2018;48(1):80-86.
185. DiLillo DJ, et al. Maintenance of long-lived plasma cells and serological memory despite mature and memory B cell depletion during CD20 immunotherapy in mice. *Journal of Immunology*. 2008;180(1):361-371.
186. Boyden AW, Legge KL, and Waldschmidt TJ. Pulmonary infection with influenza A virus induces site-specific germinal center and T follicular helper cell responses. *PLoS One*. 2012;7(7):e40733.
187. Mansouri S, et al. Immature lung TNFR2(-) conventional DC 2 subpopulation activates moDCs to promote cyclic di-GMP mucosal adjuvant responses in vivo. *Mucosal Immunology*. 2019;12(1):277-289.
188. Swarnalekha N, et al. Redefining CD4 T cell residency: Helper T cells orchestrate protective humoral immunity in the lung. *bioRxiv*. 2020.
189. Tan HX, Esterbauer R, Vanderven HA, Juno JA, Kent SJ, and Wheatley AK. Inducible Bronchus-Associated Lymphoid Tissues (iBALT) Serve as Sites of B Cell Selection and Maturation Following Influenza Infection in Mice. *Frontiers in Immunology*. 2019;10:611.
190. Son YM, et al. Tissue-resident CD4+ T helper cells assist protective respiratory mucosal B and CD8+ T cell memory responses. *bioRxiv*. 2020.

191. Morbach H, Eichhorn EM, Liese JG, and Girschick HJ. Reference values for B cell subpopulations from infancy to adulthood. *Clinical and Experimental Immunology*. 2010;162(2):271-279.
192. Mitsi E, et al. Nasal Pneumococcal Density Is Associated with Microaspiration and Heightened Human Alveolar Macrophage Responsiveness to Bacterial Pathogens. *American Journal of Respiratory and Critical Care Medicine*. 2020;201(3):335-347.
193. Chernova I, et al. Lasting antibody responses are mediated by a combination of newly formed and established bone marrow plasma cells drawn from clonally distinct precursors. *Journal of Immunology*. 2014;193(10):4971-4979.
194. Leandro MJ. B-cell subpopulations in humans and their differential susceptibility to depletion with anti-CD20 monoclonal antibodies. *Arthritis Research & Therapy*. 2013;15 Suppl 1:S3.
195. Gea-Banacloche JC. Rituximab-associated infections. *Seminars in Hematology*. 2010;47(2):187-198.
196. Clark RA, et al. Skin effector memory T cells do not recirculate and provide immune protection in alemtuzumab-treated CTCL patients. *Science Translational Medicine*. 2012;4(117):117ra117.
197. Wei Z, Li J, Cheng Z, Yuan L, and Liu P. A single center experience: rituximab plus cladribine is an effective and safe first-line therapy for unresectable bronchial-associated lymphoid tissue lymphoma. *Journal of Thoracic Disease*. 2017;9(4):1081-1092.
198. Gebhardt T, Wakim LM, Eidsmo L, Reading PC, Heath WR, and Carbone FR. Memory T cells in nonlymphoid tissue that provide enhanced local immunity during infection with herpes simplex virus. *Nature Immunology*. 2009;10(5):524-530.
199. Teijaro JR, Turner D, Pham Q, Wherry EJ, Lefrancois L, and Farber DL. Cutting edge: Tissue-retentive lung memory CD4 T cells mediate optimal protection to respiratory virus infection. *Journal of Immunology*. 2011;187(11):5510-5514.
200. Wu T, et al. Lung-resident memory CD8 T cells (TRM) are indispensable for optimal cross-protection against pulmonary virus infection. *Journal of Leukocyte Biology*. 2014;95(2):215-224.
201. Ishizuka AS, et al. Protection against malaria at 1 year and immune correlates following PfSPZ vaccination. *Nature Medicine*. 2016;22(6):614-623.

202. Bergsbaken T, Bevan MJ, and Fink PJ. Local Inflammatory Cues Regulate Differentiation and Persistence of CD8(+) Tissue-Resident Memory T Cells. *Cell Reports*. 2017;19(1):114-124.
203. Iijima N, and Iwasaki A. T cell memory. A local macrophage chemokine network sustains protective tissue-resident memory CD4 T cells. *Science*. 2014;346(6205):93-98.
204. Tse SW, Radtke AJ, Espinosa DA, Cockburn IA, and Zavala F. The chemokine receptor CXCR6 is required for the maintenance of liver memory CD8(+) T cells specific for infectious pathogens. *Journal of Infectious Diseases*. 2014;210(9):1508-1516.
205. Zaid A, et al. Chemokine Receptor-Dependent Control of Skin Tissue-Resident Memory T Cell Formation. *Journal of Immunology*. 2017;199(7):2451-2459.
206. Shin H, and Iwasaki A. A vaccine strategy that protects against genital herpes by establishing local memory T cells. *Nature*. 2012;491(7424):463-467.
207. Bernstein DI, et al. Successful application of prime and pull strategy for a therapeutic HSV vaccine. *NPJ Vaccines*. 2019;4:33.
208. Nakanishi Y, Lu B, Gerard C, and Iwasaki A. CD8(+) T lymphocyte mobilization to virus-infected tissue requires CD4(+) T-cell help. *Nature*. 2009;462(7272):510-513.
209. Laidlaw BJ, et al. CD4+ T cell help guides formation of CD103+ lung-resident memory CD8+ T cells during influenza viral infection. *Immunity*. 2014;41(4):633-645.
210. Jeyanathan M, et al. CXCR3 Signaling Is Required for Restricted Homing of Parenteral Tuberculosis Vaccine-Induced T Cells to Both the Lung Parenchyma and Airway. *Journal of Immunology*. 2017;199(7):2555-2569.
211. Kohlmeier JE, et al. CXCR3 directs antigen-specific effector CD4+ T cell migration to the lung during parainfluenza virus infection. *Journal of Immunology*. 2009;183(7):4378-4384.
212. Denton AE, et al. Type I interferon induces CXCL13 to support ectopic germinal center formation. *Journal of Experimental Medicine*. 2019;216(3):621-637.
213. Fleige H, et al. IL-17-induced CXCL12 recruits B cells and induces follicle formation in BALT in the absence of differentiated FDCs. *Journal of Experimental Medicine*. 2014;211(4):643-651.

214. Obukhanych TV, and Nussenzweig MC. T-independent type II immune responses generate memory B cells. *Journal of Experimental Medicine*. 2006;203(2):305-310.
215. Faden H, Heimerl M, Varma C, Goodman G, and Winkelstein P. Urinary excretion of pneumococcal cell wall polysaccharide in children. *Pediatric Infectious Disease Journal*. 2002;21(8):791-793.
216. Defrance T, Taillardet M, and Genestier L. T cell-independent B cell memory. *Current Opinion in Immunology*. 2011;23(3):330-336.
217. Swan DJ, Kirby JA, and Ali S. Post-transplant immunosuppression: regulation of the efflux of allospecific effector T cells from lymphoid tissues. *PLoS One*. 2012;7(9):e45548.
218. Shinall SM, Gonzalez-Fernandez M, Noelle RJ, and Waldschmidt TJ. Identification of murine germinal center B cell subsets defined by the expression of surface isotypes and differentiation antigens. *Journal of Immunology*. 2000;164(11):5729-5738.
219. Reichert RA, Gallatin WM, Weissman IL, and Butcher EC. Germinal center B cells lack homing receptors necessary for normal lymphocyte recirculation. *Journal of Experimental Medicine*. 1983;157(3):813-827.
220. Roy MP, Kim CH, and Butcher EC. Cytokine control of memory B cell homing machinery. *Journal of Immunology*. 2002;169(4):1676-1682.
221. Chiba K, et al. FTY720, a novel immunosuppressant, induces sequestration of circulating mature lymphocytes by acceleration of lymphocyte homing in rats. I. FTY720 selectively decreases the number of circulating mature lymphocytes by acceleration of lymphocyte homing. *Journal of Immunology*. 1998;160(10):5037-5044.
222. Neyt K, GeurtsvanKessel CH, Deswarte K, Hammad H, and Lambrecht BN. Early IL-1 Signaling Promotes iBALT Induction after Influenza Virus Infection. *Frontiers in Immunology*. 2016;7:312.
223. Gopal R, et al. Interleukin-17-dependent CXCL13 mediates mucosal vaccine-induced immunity against tuberculosis. *Mucosal Immunology*. 2013;6(5):972-984.
224. Rangel-Moreno J, et al. The development of inducible bronchus-associated lymphoid tissue depends on IL-17. *Nature Immunology*. 2011;12(7):639-646.
225. McKinstry KK, et al. Effector CD4 T-cell transition to memory requires late cognate interactions that induce autocrine IL-2. *Nature Commun*. 2014;5:5377.

226. Boyden AW, Frickman AM, Legge KL, and Waldschmidt TJ. Primary and long-term B-cell responses in the upper airway and lung after influenza A virus infection. *Immunologic Research*. 2014;59(1-3):73-80.
227. Vogelzang A, et al. Neonatal Fc Receptor Regulation of Lung Immunoglobulin and CD103+ Dendritic Cells Confers Transient Susceptibility to Tuberculosis. *Infection and Immunity*. 2016;84(10):2914-2921.
228. Jaffar Z, Ferrini ME, Herritt LA, and Roberts K. Cutting edge: lung mucosal Th17-mediated responses induce polymeric Ig receptor expression by the airway epithelium and elevate secretory IgA levels. *Journal of Immunology*. 2009;182(8):4507-4511.
229. Vu Van D, et al. Local T/B cooperation in inflamed tissues is supported by T follicular helper-like cells. *Nature Communications*. 2016;7:10875.
230. Seifert M, et al. Functional capacities of human IgM memory B cells in early inflammatory responses and secondary germinal center reactions. *Proceedings of the National Academy of Sciences of the United States of America*. 2015;112(6):E546-555.
231. Slutter B, Van Braeckel-Budimir N, Abboud G, Varga SM, Salek-Ardakani S, and Harty JT. Dynamics of influenza-induced lung-resident memory T cells underlie waning heterosubtypic immunity. *Science Immunology*. 2017;2(7).
232. Uddback I, et al. Long-term maintenance of lung resident memory T cells is mediated by persistent antigen. *Mucosal Immunology*. 2020.
233. McCarthy KR, et al. Memory B Cells that Cross-React with Group 1 and Group 2 Influenza A Viruses Are Abundant in Adult Human Repertoires. *Immunity*. 2018;48(1):174-184 e179.
234. Leach S, et al. Requirement for memory B-cell activation in protection from heterologous influenza virus reinfection. *International Immunology*. 2019;31(12):771-779.
235. McMaster SR, et al. Pulmonary antigen encounter regulates the establishment of tissue-resident CD8 memory T cells in the lung airways and parenchyma. *Mucosal Immunology*. 2018;11(4):1071-1078.
236. Weisel FJ, Zuccarino-Catania GV, Chikina M, and Shlomchik MJ. A Temporal Switch in the Germinal Center Determines Differential Output of Memory B and Plasma Cells. *Immunity*. 2016;44(1):116-130.

237. Andrade P, et al. Impact of pre-existing dengue immunity on human antibody and memory B cell responses to Zika. *Nature Communications*. 2019;10(1):938.
238. Zens KD, Chen JK, and Farber DL. Vaccine-generated lung tissue-resident memory T cells provide heterosubtypic protection to influenza infection. *JCI Insight*. 2016;1(10).

CURRICULUM VITAE

